MULTIDISCIPLINARY DESIGN OPTIMIZATION OF COMPLEX ENGINEERING SYSTEMS FOR COST ASSESSMENT UNDER UNCERTAINTY

by

Christopher Gregory Hart

A dissertation submitted in partial fulfillment
of the requirements for the degree of
Doctor of Philosophy
(Naval Architecture and Marine Engineering)
in The University of Michigan
2010

Doctoral Committee:

Professor Nickolas Vlahopoulos, Chair
Professor Gautam Kaul
Professor Jun Ni
Professor Armin W. Troesch
Assistant Research Scientist and Lecturer David J. Singer

DEDICATION

Sergeant JT Sanborn: I'm ready to die, James.
Staff Sergeant William James: Well, you're not gonna die out here, bro.
Sergeant JT Sanborn: Another two inches, shrapnel zings by; slices my throat- I bleed out like a pig in the sand. Nobody'll give a sh**. I mean my parents- they care- but they don't count, man. Who else? I don't even have a son.
Staff Sergeant William James: Well, you're gonna have plenty of time for that, amigo.
Sergeant JT Sanborn: Naw, man. I'm done. I want a son. I want a little boy, Will. I mean, how do you do it, you know? Take the risk?
Staff Sergeant William James: I don't know. I guess I don't think about it…

To:

my amazing wife, Robyn,
and our children, Tennille, Aden, Mariana, Orin, Holden and Kai.

In memory of:

Adam McSween, Kevin Bewley and Jeff Chaney.

ACKNOWLEDGEMENTS

Thank you:

Nick, for your guidance, patience, flexibility, focus and balance;
Robyn, if I acknowledge everything you do for us, it will fill another 149 pages… at least;
Tennille, Aden, Mariana, Orin, Holden and Kai, for keeping my priorities straight;
Zhijiang, Geng, Jim, Piotr, Ellie, cdwoz, Nabanita, Wei Wei, Ricardo, Steve, Oscar, Wei, MH, Greg, Bill, and Chuck/Charlie/Henry for smoothing the bumps in the road;
Mom and Dad, for your support;
Ben and Jake, for brotherhood and comic relief;
Jim and Bernetta, for being there when we needed you the most;
Armin, for thinking of me when you needed someone to do something;
Patrick, for listening;
Dave, for being Dave;
JCB, for inspiring and pushing.

TABLE OF CONTENTS

LIST OF FIGURES

LIST OF TABLES

ABSTRACT

MULTIDISCIPLINARY DESIGN OPTIMIZATION OF COMPLEX
ENGINEERING SYSTEMS FOR COST ASSESSMENT UNDER UNCERTAINTY
by
Christopher Gregory Hart

Chair: Nickolas Vlahopoulos

First, research is performed for investigating the performance of a Multidisciplinary Design Optimization (MDO) algorithm by integrating a particle swarm optimization (PSO) solver in both the system and discipline levels. The PSO solver is developed based on theoretical information available from the literature and the MDO framework is based on the Target Cascading (TC) method. The integrated MDO/PSO algorithm is employed for analyzing a conceptual ship design problem from the literature. Next, performance models are developed and employed within a gradient-based MDO framework for conducting a conceptual submarine design analysis. Four discipline level performances—internal deck area, powering, maneuvering, and structural analysis—are optimized simultaneously. The four discipline level optimizations are driven by a system level optimization which minimizes the manufacturing cost while at the same time coordinates the exchange of information and the interaction among the discipline level optimizations. The results from this coordinated MDO capture the interaction among disciplines and demonstrate the value

that the MDO solution offers in consolidating the results to a single design which improves the discipline level objective functions while at the same time produces the highest possible improvement at the system level. Thirdly, a general method for improving the fidelity of cost estimation in the design of complex engineering systems is proposed. In this method, principal component analysis (PCA) and an adaptive Kriging method are used to increase the level of sophistication and predictive capability of existing cost assessment methodologies. Finally, an evidence theory-based uncertainty estimation algorithm is created and integrated into the cost assessment model developed earlier in order to capture the uncertainty surrounding the relationship between the system design variables and cost. The general cost assessment under uncertainty model is utilized as the system-level driver in the representative MDO study of a conceptual submarine design. A set of several MDO analyses which highlight the effects of different levels of uncertainty is also performed. The theoretical developments and the results from all four interrelated areas of research are summarized and discussed.

CHAPTER 1:
INTRODUCTION

As the systems used to facilitate mankind's existence on this planet increase in complexity, the resources available to create them are dwindling. At the forefront are dwindling financial resources, as manifested both in the raising costs of labor and a need to do more with less capital. The work summarized in this dissertation strives toward a better understanding of how the process of creating these complex systems should change in the face of dwindling financial resources. A more detailed discussion of additional objectives and motivation for the research is presented in the next section.

1.1: Research Objectives and Motivation

There are four distinct phases to this work. The main objective of the first phase is to document the integration of a particle swarm optimization (PSO) algorithm into the top and discipline levels of a multidisciplinary design optimization framework in an effort to improve the optimization capability of the framework. Secondary objectives include creating a PSO algorithm and comparing it against a gradient based algorithm, previously published results, and a simple Monte Carlo model as an optimization driver for single and multicriterion optimization.

The main objective of the second phase of the work is to use multidisciplinary design optimization to systematically build a foundation for increasing the

understanding of the multifaceted relationship between affordability and performance in the conceptual design of a complex engineering system. Secondary objectives include creating a sophisticated, automated affordability model based on the manufacturing costs associated with a component of such a system, and creating automated first-order models for four engineering disciplines that are typical of those encountered in conceptual design. Finally, results from the single-discipline optimization of these disciplines will be discussed and compared to the results obtained from optimizing all disciplines in a coordinated effort governed by the response of a system-level objective.

The third phase's goal is the creation of a higher fidelity cost model for the manufacture of a complex engineering system, thus extending the goal of the second phase of the work. Secondary objectives include: 1.) the application of methodologies from datamining in order to learn more about a set of cost data and 2.) an investigation of various regression-type methods with the goal of allowing the lessons from the datamining analysis to be used to improve the predictive capability of a cost estimation model.

The fourth, and final, phase of this research works to create an evidence theory-based algorithm for quantifying uncertainty, integrating the algorithm into an improved methodology for cost assessment and then utilizing this cost assessment under uncertainty model in an MDO framework. Demonstrating the impact of considering cost uncertainties in the MDO decision-making process is the secondary objective.

A detailed review of the current literature that discusses each of these objectives is presented in the next section.

1.2: Literature Review

First introduced in 1995 by social psychologist James Kennedy and electrical engineer Russ Eberhart, PSO served two purposes in its original form. The first purpose was to model human social behavior in abstract n-dimensional psychological space. The second purpose was the optimization of continuous nonlinear multivariate functions [1]. In the early years of the algorithm's existence, there were several studies [2 - 4] investigating improvements to the original algorithm through the creation of new parameters and the permutation of their values.

PSO, along with evolutionary algorithms [5], genetic algorithms, and other biology-mimicking algorithms [6 - 8], has been gaining in popularity in the literature as a method of solving large-scale problems in several different engineering disciplines [9 - 12]. Of particular note to this work is that PSO has been given special attention recently in the naval architecture literature [13, 14].

PSO has been employed in many different forms; including a ranking selection-based PSO [15], asynchronous and synchronous parallel applications of PSO [16 - 18], and hybrid PSO/GA [19, 20]; in a multidisciplinary design optimization (MDO) environment. In addition to these different "flavors" of PSO, its basic form has also been applied in several different disciplines, including the design of an aircraft wing [21]. An editorial on the subject [22] brings the interested researcher up-to-date on the current state of the theory and entreats scholars to continue to explore novel uses and formulations of the algorithm.

Even though there are many success stories of PSO and its use, the same characteristics which give PSO its strength, that is the pseudo-random nature of the algorithm, have also caused trouble for certain applications such as the MDO-governed shape optimization of a fan blade [23]. The work summarized here is motivated by the author's desire to introduce a simple PSO algorithm into the system and discipline levels of a Target Cascading- based MDO formulation in order to use the strengths of PSO, as outlined in the literature selections above, to search for a "better" answer to a typical conceptual ship design problem.

The literature covering engineering design optimization is extensive, to say the least. The interested researcher can start very general [24 - 28] in order to establish a firm foundation before delving deeper into a particular engineering discipline. Optimal ship design has been a topic of academic interest in naval architecture for decades [29, 30]. As in other fields in which complex engineering systems are designed, such as aerospace [31 - 33], automotive [34, 35], mechanical [36 - 38] and even biomedical engineering [39], naval architecture has seen a growing research and development trend towards discovering methods for automatically synthesizing the conflicting outputs from several disciplines into the search for one globally optimum design. Topics of study in naval architecture along the design optimization lines include specific topics such as high speed vessels [40, 41], sloshing and impact in containers being transported at sea [42], computational fluid dynamics (CFD) and its use in design optimization [43, 44], the use of a hybrid agent approach to design and numerical optimization methods

[45, 46], and simulation-based design [47]. Topics of a more general ship design interest have also found space in the literature [48 - 51].

Of the design optimization methods considered and proposed in the literature, multidisciplinary design optimization (MDO) was widely recognized at an early stage by many on the cutting edge of engineering design as the key to the future [52, 53]. This recognition stems from MDO's robust ability to synthesize several complex and computationally intensive disciplines simultaneously into a single resultant design that is the optimum from the perspective of an equally complex top level objective function [54]. For guidance in using MDO, there are papers outlining the steps in creating an MDO framework [55], discussing the characteristics of existing frameworks [56], and applying MDO in various disciplines [57]. The discussions of MDO in naval architecture have become especially numerous in recent years [58 - 61].

The MDO method used in this work is based upon the target cascading (TC) method [62 - 69]. The TC method is a way of mathematically organizing an MDO analysis that facilitates the interaction between disciplines and the coordination of the decision-making process. In the past a MDO framework has been developed based on the TC method and used for MDO analysis of a thermal protection system, aircraft, and undersea vehicle [70 - 73]. The existing MDO framework utilizes a gradient based solver as an optimization driver for all the disciplines and for the top level. In this work, the PSO algorithm is chosen to replace the gradient based optimizer in all discipline levels and in the top level. This choice was made due to the documented [10 – 18, 74] improvement in results and performance that non-gradient-based algorithms have seen.

It is realized that there is a computational burden associated with using a metaheuristic such as PSO. It is hypothesized that the change in optimizers will produce an improvement in the results of the optimization that outweighs the increase in computational cost.

Another objective of this work, in addition to the exploration of PSO in the system- and discipline-levels of an MDO framework, is the study of a submarine conceptual design using MDO. Before creating models to represent the different disciplines of interest in the integrated, multidisciplinary conceptual design of a submarine, the author turned to the literature to create a basis for understanding submarine design. Classical texts on the topic [75 - 81] were the first consulted, followed by treatises on similar work in various countries around the world [82 - 86], and even the work presented by [87]. There have been several worthwhile books written on the subject [88 - 90], and many of the chapters contained therein proved very helpful in setting the stage for this work. Additionally, the topic has been studied at other academic institutions [91], and has been the subject of recent attempts at a higher fidelity treatment [92]. Lastly, several articles providing discourse on current policy issues surrounding the topic [93, 94] were also found to provide an interesting backdrop. Once sufficient knowledge was gleaned concerning submarine design in general, attention was turned to the specific disciplines of internal deck area, resistance, structures, and maneuvering.

The first model created in this work calculates the internal deck area of a submarine defined by a set of design variables. These design variables—length of

parallel midbody (Lpmb), maximum diameter (D), aft form factor (na), and forward form factor (nf)—have been used for decades in the literature to represent a submarine hullform in the conceptual design phase [95, 96]. The deck area discipline also uses parameters such as clearance between the hydrodynamic and pressure hulls, between deck height, and bilge height to build the pressure hull inside the hydrodynamic hull and assign the number and location of decks within this pressure hull. The model then references simplified geometric relationships governing the shape of the cylindrical pressure hull and its hemispherical endcaps to calculate the area of each of these decks. The goal of the optimization of this discipline is to maximize the calculated deck area subject to a pseudo-arbitrary displacement constraint.

Several sources were consulted in the search for an ideal resistance model that combined simplicity and ease of use with acceptable accuracy [97, 98]. The decision was eventually made to use Jackson's interpretation of the classic formulation [95, 96] because it meets the above criteria and integrates seamlessly with the deck area discipline. The same displacement requirement that was imposed for the deck area discipline is used to constrain the minimization of the resistance.

The structural discipline minimizes the buoyancy factor, defined as the hull weight to displaced water weight ratio [99], with frame spacing (Lf), plate thickness (tp), flange thickness (tf), flange width(wf), web thickness(tw), and web height (Hw) as the design variables. The structural discipline adds constraints in five failure modes; i.e. shell and frame yielding, general and frame instability, and lobar buckling [91, 100, 101] to the constraints from the previous two disciplines.

Preliminary research in the maneuvering discipline began with the classics [102 - 109]. After reading through these works, it was apparent that a method for automatically calculating the hydrodynamic derivatives at each iteration of the design process would be necessary. The concepts discussed in the literature covering the calculation of hydrodynamic coefficients [110 - 116] did not prove readily applicable to this particular problem formulation. There was a wealth of literature treating various specifics in the subject of submarine maneuverability [117 - 125], but none that directly applied to the task at hand, that is the highly iterative multi-level design optimization techniques used in MDO. There were also several general publications on the topic [126 - 132] that relied on model testing for the determination of the hydrodynamic derivatives and did not provide a succinct model for repetitive engagement by an automated optimizer.

The publication by [133] is very promising but requires the use of restricted software for evaluating the hydrodynamic derivatives. At this point in the process, the author selects a suitable maneuvering model introduced in the first section of Tsamilis' thesis [134]. The maneuvering discipline is constrained in the same manner as both the deck area and effective power disciplines.

A major effort of this work was spent on researching the creation of a from-scratch affordability model for the lifecycle of a vessel-of-the-sea. The author started with the fundamentals in this research in an effort to create something novel. In the early stages, it was realized that several macroeconomic issues—such as foreign exchange rates, commodities prices, international labor policies, etc.—play a major role

in these lifecycle costs. As such, the author scoured general texts and articles on macroeconomics [135 - 142] in search of helpful ideas for the creation of the affordability model. The commentary contained in these original sources pointed towards econometrics [143 - 146], engineering economy/economics [147 - 152], cost engineering [153, 154], logistics engineering [155], parametric costs analysis [156, 157], economic decision analysis [158], activity-based costing (ABC) [159], and multiple regression [160] as possible next steps to increase understanding of affordability in complex engineering systems. The author looked at each of these methods in turn and determined that no single one of them was appropriate for this model due to lack of translation from the current or original application, complexity of implementation, or a requirement for detailed historical data which was not available to the author. If any of these methods were to be incorporated, it would need to be done in a blended, or hybrid manner.

With this in mind, the author spent a considerable amount of time examining treatments of affordability and costing in several different engineering systems, including aircraft [161 - 164], spacecraft [165, 166], commercial ships [167 - 184], warships [185 - 195], and finally, submarines [185, 196]. Several of these existing costing methods were weight-based or regression-based methods. Examination of these sources provided the author with an excellent idea of what is in the marketplace, and how the system developed for this work must improve upon this selection. Of all these sources, the best two candidates for modeling the affordability were determined to be: 1.) a commercially available software package entitled SEER, offered by Galorath,

which automatically incorporates many of the macro and microeconomic issues revealed to be important from the research above, and 2.) a framework called "Business Dynamics" [197] which had already produced a lifecycle costing model for the industry [198]. Due to the proprietary nature of the Business Dynamics framework, SEER was chosen as the method to create the affordability model for integration into the MDO analysis of the conceptual submarine design, thus building upon the work in [199 – 202].

In the third phase of the work, an effort is undertaken to add further fidelity to the cost assessment methodologies currently available in the literature. A key element in addressing the shortcomings in current cost estimation involves improving the accuracy of parametric models by looking at historical cost data in a novel, more sophisticated way. In this vein, the author concentrates first on examining the literature on datamining, and the related knowledge discovery from databases (KDD) [203]. Recently-published general overviews were identified as an introduction to the world of datamining and KDD [204 - 208]. The information contained in these chapters, and several of their references [209 - 221], provided an excellent understanding of the current state of the art and a broad foundation upon which to build. Of particular interest for potential adaptation and application in this problem were datamining methods broadly identified as classification [204] and association analysis [208] methods. Specifically, the classification and regression trees (CART) [213] approach was very interesting in its broad application in the literature [204] as well as its fairly logical and straight-forward theoretical base.

It was also discovered during this initial research that there exists a large body of research which introduces and examines several methods, each based on the founding principles of linear and matrix algebra, for analyzing data held in matrix form [222]. Familiar with some of these methods, due to exposure to their usage in various aspects of multidisciplinary design [223, 224], the author began an inquiry into this space by investigating how some of these methods could be applied in developing an improved cost model. It was quickly discovered that methods such as singular value decomposition (SVD), data envelope analysis (DEA), and especially principal component analysis (PCA) were not only used in structural design, but also to analyze gene expression data in bioinformatics [225, 226], the effects of deregulation on the airline industry [227], and several other types of relationships, including those in finance [228, 229]. Interesting papers highlighting modifications to PCA [230] in order to facilitate its application in a nonlinear space were also discovered.

In addition to following the leads generated by the general papers listed above, the review of the literature on the topic of datamining also examined several other related areas. Since the problem at hand deals with cost estimation, papers on general business applications of datamining [231, 232], and more specifically, datamining in customer relationship management (CRM) [233] also proved enlightening. This path led to a brief examination of a growing area in computer science, called quantum computing, in which principles from the physical world are mapped to the world of designing and creating the computer hardware and software of the future [234 - 237].

As this area of research expands, it could have a very meaningful impact on problems such as those addressed in this dissertation.

After examining the datamining and knowledge discovery from database literature, it was determined that the best candidate for application in this problem was PCA. This decision was based on the breadth of problems that had already seen success using PCA, as well as the author's familiarity with the technology. The details of this method will be covered later in this work.

Once a candidate for executing a more sophisticated examination of historical cost data had been identified, attention turned to determining the best method of engaging the lessons learned from this examination into a better regression model. Certain aspirants identified during the datamining exploration mentioned earlier were natural fits into this phase of the work. CART and PCA are two prime examples. It was quickly determined that PCR (principal component regression) would not perform as well as desired, but another method which is a close relative to PCA and PCR, but that produces a better match to the training data, was chosen instead. This method is called Partial Least Squares (PLS) [228]. PLS was abandoned however, in the face of much better methods, known broadly as "metamodels", which are described in the next two paragraphs.

An investigation of the world of metamodels led to some promising directions regarding regression. A metamodel is a mathematically sophisticated interpolation framework which is generated from a limited number of time consuming simulations (or a set of real-world data that is difficult to recreate) and are utilized subsequently as a

replacement for the time consuming simulations (or real-world data). In other work in multidisciplinary design optimization with uncertainty (MDO-U), the author has had exposure to the idea of metamodels. Due to the large number of iterations required during a MDO process, and in an effort to include high fidelity physical simulations (which require a significant computational time even for a single analysis) in that process, theories for developing metamodels have been established. After careful consideration, it was determined that these more sophisticated models could see a worthy application in addressing the problem in the present work.

Polynomials, interpolating and smoothing splines [238], neural networks [239 - 242], radial basis functions [243], and wavelets [244] have been investigated in the past. References [245 - 247] introduce the concept of the Kriging method. The Kriging method provides an efficient predictor for a given set of data and constitutes a Gaussian process type of metamodel since it utilizes Gaussian kernels for expressing the spatial correlation functions. It treats the deterministic output as the realization of a stochastic process and provides a statistical basis for efficient prediction [248 - 251]. Kriging (i.e. Gaussian process metamodels) have been utilized in variable fidelity optimization strategies [252]; for managing system level uncertainty during conceptual design [253]; for approximating deterministic computer models [254]; and for design optimization [255]. An adaptive feature has been added to the Kriging capability employed in this work. This adaptive feature will be described in the "Adaptive Kriging Method" section of Chapter 5. To summarize, metamodels are employed in this chapter for creating a

high fidelity regression model that relates the predictor variables (physical and component-influenced parameters) to the response variables (cost parameters).

The final phase of this work integrates concepts from evidence theory with the cost assessment methodology developed in the third phase and then uses this new cost under uncertainty model as the driver in the MDO conceptual submarine design study. There have been several formal, mathematical methods proposed for quantifying uncertainty, or assessing risk. The one most often used is probability theory. Probability theory works well if enough is known about the event in question that an appropriate distribution can be assigned to that event. In the absence of this knowledge, probability often creates a level of comfort with the estimation that does not match the actual uncertainty associated with the event in question. Additional formal mathematical methods proposed to handle information that cannot be defined using the probability distributions necessary to apply probability theory include evidence theory [256], possibility theory [257], and interval analysis [258].

Evidence theory has been applied in engineering optimization [259] and shows a high level of promise for application to cost assessment due to its ability to quantify both aleatoric uncertainty (from the Latin word alea, or dice, also known as variability, irreducible uncertainty, inherent uncertainty, stochastic uncertainty, and uncertainty due to chance) and epistemic uncertainty (from the Greek word epist, or knowledge, also known as reducible uncertainty, subjective uncertainty and uncertainty due to lack of knowledge, ignorance or stupidity). Epistemic uncertainty is prevalent in any activity where subjective human error is present, such as cost estimation and assessment.

Evidence theory is built around two measures, known as belief and plausibility measures, which are analogous to the upper and lower bounds of probability. These measures are used to determine the likelihood that the event to be predicted will actually occur and signify the concept that, due to the broad range of data available, a precise probability of a certain event occurring cannot be determined. Probability theory can actually be thought of as a subset of evidence theory, since it applies when the belief and plausibility measures are equal. A very thorough background on the topic of evidence theory can be found at [260]. The algorithm presented in this paper for introducing uncertainty in the cost estimation process is utilized within a MDO analysis of a representative conceptual submarine design when defining the system level objective function. The MDO algorithm discussed throughout this dissertation is utilized for carrying out the optimization analysis. The same conceptual submarine design study is also employed in this phase's work.

1.3: Dissertation Contributions

The contributions of this work to the existing body of knowledge are summarized in the following paragraphs. In the first part of this research, an effort is undertaken to investigate the performance of a Multidisciplinary Design Optimization algorithm by integrating a non-gradient based optimizer at the top and discipline levels. A particle swarm optimization (PSO) solver is developed based on theoretical information available from the literature. The implementation is validated by utilizing the PSO optimizer as a driver for a single discipline optimization and for a multicriterion optimization and comparing the results to a commercially available gradient based

optimization algorithm, previously published results, and a simple sequential Monte Carlo model. A typical conceptual ship design statement from the literature is employed for developing the single discipline and the multicriterion benchmark optimization statements. In the first new effort presented in this dissertation, an approach is developed for integrating the PSO algorithm as a driver at both the top and the discipline levels of a multidisciplinary design optimization (MDO) framework which is based on the Target Cascading (TC) method. The integrated MDO/PSO algorithm is employed for analyzing a multidiscipline optimization statement reflecting the conceptual ship design problem from the literature. Results are compared to MDO analyses performed when a gradient based optimizer comprised the optimization driver at all levels. The results, the strengths, and the weaknesses of the integrated MDO/PSO algorithm, are discussed as related to conceptual ship design.

Performance assessment models are developed and utilized in a gradient-based MDO analysis of a conceptual submarine design. In the second part of this research, a step is taken towards relating cost and performance in a more meaningful manner. Four discipline level performances—internal deck area, powering, maneuvering, and structural analysis—are optimized simultaneously. The four discipline level optimizations are driven by a system level optimization which minimizes the manufacturing cost while at the same time coordinates the exchange of information and the interaction among the discipline level optimizations. Thus, the interaction among individual optimizations is captured along with the impact of the physical characteristics of the design on the manufacturing cost. A geometric model for the internal deck area

of a submarine is created, and resistance, structural design, and maneuvering models are adapted from theoretical information available in the literature. These models are employed as simulation drivers in the discipline level optimizations. Commercial cost estimating software is leveraged to create an automated affordability model for the fabrication of a submarine pressure hull at the system level. First, each one of the four discipline optimizations and also the cost related top level optimization are performed independently. As expected five different design configurations result, one from each analysis. These results represent the "best" solution from each individual discipline optimization and they are used as reference for comparison with the MDO solution. The deck area, resistance, structural, maneuvering, and affordability models are then synthesized into a multidisciplinary optimization statement reflecting a conceptual submarine design problem. The results from this coordinated MDO capture the interaction among disciplines and demonstrate the value that the MDO system offers in consolidating the results to a single design which improves the discipline level objective functions while at the same time produces the highest possible improvement at the system level.

In the third section of this research, a general method for improving the fidelity of cost estimation in the design of complex engineering systems is proposed. In this method, physical parameters and historical cost records are gathered for a given complex engineering system and combined into an original data set. An engineering build-up cost model is created from this original data set. An expanded data set is generated using this engineering build-up cost model. The expanded data set is then

analyzed using principal component analysis (PCA) in order to identify which original physical parameters, and resulting principal components (PCs) account for the greatest amount of variation in the design. Each high-variation PC is composed of values that are treated as weights. These weights are used to create one component-influenced parameter, or a weighted sum of the original design variables, for each PC. A set of predictor variables, composed of the high-variation physical parameters and component-influenced parameters from the original data set, is then developed. This new set of predictor variables is regressed, using the sophisticated adaptive Kriging method, on the historical cost values (response variables), thus creating a cost estimation model with a high level of predictive capability and fidelity. The same case study addressing the fabrication of a submarine pressure hull that was developed for the previous section is engaged in order to illustrate this method. The results from the final regression model are presented and compared to results from the original data set. The differences and overall benefits of the novel general method are presented and discussed.

The last section ties together the previous sections. An evidence theory-based uncertainty estimation algorithm is integrated into the cost assessment model for capturing the uncertainty surrounding the relationship between the system design variables and cost. The general cost assessment under uncertainty model is utilized as the system-level driver in the same representative multidisciplinary design optimization (MDO) study of a conceptual submarine design that was developed in the second phase of this research. The results from this coordinated MDO capture the interaction among

disciplines and demonstrate the value that the MDO solution offers in consolidating the results to a single design which improves the discipline level objective functions while at the same time produces the highest possible improvement at the system level. A set of several MDO analyses which highlight the effects of different levels of uncertainty is performed in this work. The results of these MDO analyses are presented and discussed.

1.4: Dissertation Overview

The body of this dissertation, that is Chapters 2 through 5, are organized to follow the phases of the research as discussed above. As such, the next Chapter highlights the PSO algorithm used, how it is integrated into the basic MDO framework, the case study that is explored by the integrated MDO/PSO algorithm, and the results from this case study. The third Chapter introduces the conceptual submarine design case study that was created for this work and the results from the MDO analysis of this case study. The creation of an improved cost assessment methodology, integration of evidence theory uncertainty estimation, and application of this cost under uncertainty model as the driver of an MDO analysis of the conceptual submarine design are the topics of Chapters 4 and 5. The author concludes the dissertation and recommends future work in Chapter 6.

CHAPTER 2:
AN INTEGRATED MULTIDISCIPLINARY PARTICLE SWARM OPTIMIZATION APPROACH TO CONCEPTUAL SHIP DESIGN

The main objective of this chapter is to document the integration of a particle swarm optimization (PSO) algorithm into the top and discipline levels of a multidisciplinary design optimization framework. As was outlined in the literature review, the praises of PSO, and other non-gradient-based optimizers have been sung in the engineering design optimization literature. The motivation of this work is to see if PSO can be used, along with multidisciplinary optimization, to provide better results to an engineering problem from the literature. This chapter focuses on applications related to conceptual ship design when discussing the results obtained by this integrated approach, and a conceptual ship design case study from the literature is employed for developing all optimization examples. Secondary objectives include creating a PSO algorithm and comparing it against a gradient based algorithm, previously published results, and a simple Monte Carlo model as a driver for single and multicriterion optimization.

The primary contribution of this chapter is the integration of a PSO optimization driver within a MDO framework and the evaluation of the strengths and weaknesses of the integrated MDO/PSO algorithm as related to conceptual ship design. New developments are necessary for linking the evolutionary nature of the PSO optimizer

with the mathematical structure of the TC method. A PSO solver is developed first based on information from the literature and its implementation is validated by engaging it in solving a single discipline and a multicriterion optimization related to conceptual ship design. The results are compared to previously published data, a commercially available gradient based algorithm, and a simple sequential Monte Carlo solution. The developed PSO solver is integrated with an available TC implementation. The newly integrated MDO/PSO algorithm is employed in conceptual ship design, the results are compared to MDO analysis performed when the gradient based optimizer comprises the optimization driver at all levels. The strengths and the weakness of the integrated MDO/PSO algorithm are discussed as related to conceptual ship design.

2.1: Particle Swarm Optimization (PSO)

A thorough introduction to PSO is given in many sources. The author found the information given on this topic in [14] to be most instructive. The development of the basic algorithm presented here draws heavily from this work. For completeness, several ideas from their paper are included here.

The original PSO was created to solve a single-objective unconstrained optimization problem. Since most ship design problems are heavily, and even over-, constrained the formulation used in this work is modified to solve the following general constrained optimization problem wherein the objective function $f(\mathbf{x})$ is minimized subject to the inequality constraints $\mathbf{g}(\mathbf{x})$.

$$\min_{\mathbf{x}} f(\mathbf{x}) \text{ subject to: } \mathbf{g}(\mathbf{x}) \leq 0 \qquad (1)$$

where $\mathbf{x} = [x_1, x_2, ..., x_N]$

The fundamental steps in the creation of the algorithm are summarized:

Step 0. (Initialization) An initial particle swarm is randomly distributed inside the design space and assigned an initial set of random "velocities". The number of iterations (n) is equal to 0.

Step 1. (Analysis) In the first step of the first iteration (n = 1), the objective function is evaluated for each particle of the swarm. The values of the design variables (x vector) which yield the minimum value in the swarm are recorded as p_b^n . Those that result in the minimum value encountered by each particle over all iterations are dubbed p_i^n .

Step 2. (Velocity vector updating) A new velocity vector is calculated using Equation (2).

$$v_i^{n+1} = K\left[w^n v_i^n + c_1 r_1^n \frac{\left(p_i^n - x_i^n\right)}{\Delta t} + c_2 r_2^n \frac{\left(p_b^n - x_i^n\right)}{\Delta t} \right] \qquad (2)$$

In this Equation the subscript "i" signifies the particle, and the superscript "n" signifies the iteration. There are three terms in this equation. The first term, known as the inertia term, will be discussed in greater depth later in the chapter. The second term, or the cognitive term, uses the particle's "memory" in order to influence its new position. The final term is known as the social term. This term uses the best location that any member of the swarm has seen to influence the trajectory of each

particle of the swarm. Table 1 outlines the definitions of each of the parameters contained in Equation (2).

Table 1: PSO Parameter Definition

Parameter	Definition	Value
v_i^{n+1}	Particle velocity for next iteration.	varies
K	Constriction factor. Limits the particle velocity at each iteration.	0.1
w^n	Weight function. Determines the "inertia" of the particle. Decreases with each iteration. Set to 0 if constraints are violated.	varies
v_i^n	Particle velocity for current iteration.	varies
c_1 and c_2	Cognitive and social parameters.	1.4
r_1^n and r_2^n	Randomly generated constants, uniformly distributed [0,1].	varies
x_i^n	Particle position (design variable vector) for current iteration.	varies
Δt	Time step.	1
$w_{\max}$	Maximum weight allowed.	0.9
$w_{\min}$	Minimum weight allowed.	0.1
$n_{\max}$	Maximum iterations allowed.	1000
n	Current iteration	varies

Step 3. (Updating) The position of the particle is updated using Equation (3).

$$x_i^{n+1} = x_i^n + v_i^{n+1}\Delta t \qquad (3)$$

Step 4. (Check convergence) Return to Step 1 and repeat until user defined convergence criteria are met.

The original PSO algorithm was created to solve unconstrained optimization problems. The basic algorithm can be modified to handle constraints using the weighting function in the inertia term of the PSO equation. The weighting function in this work is calculated as follows.

$$w^n = w_{\max} - \left(\frac{w_{\max} - w_{\min}}{n_{\max}} n \right) \tag{4}$$

Equation (4) introduces four new parameters, all of which are defined in the last four rows of Table 1.

When a constraint is violated, the modified PSO algorithm creates a deviation from this method of calculating w^n and sets its value to 0. This effectively causes the particle to rely solely on its cognitive and social influences to bring it back into the feasible realm.

Much work has been done in the literature concerning adjustments to the parameters in the PSO algorithm. The values used in this work are contained in the third column of Table 1. There is very minor deviation from these values as gross manipulation of the algorithm itself was beyond the scope of this work.

One of the modifications suggested in the literature is to suppress the generation of the random coefficients at each iteration [16, 17]. This approach was attempted in the early stages of this work. The results of this so-called deterministic particle swarm optimization (DPSO) did not compare favorably with those obtained with the pure PSO, and the approach was summarily abandoned.

There was no convergence criterion enumerated in the original formulation of PSO. In this work, a simple criterion of a comparison between each function value in the swarm and the minimum value that the swarm has seen to that point serves as the convergence criterion.

$$f_i^n(\mathbf{x}) - C \le K_{cc} C \tag{5}$$

In Equation (5), K_{cc} is a user-defined convergence criterion constant (set as 0.01 for this work) and C is the minimum $f(\mathbf{x})$ value attained by the algorithm to that point.

2.2: Multicriterion Design Optimization

Many of the equations and ideas for this section covering multicriterion design optimization originate from [46]. They are included here to ensure a complete statement of the problem at hand and an accurate comparison between optimization methods.

A multicriterion optimization problem is defined in the following way.

$$\min_{\mathbf{x}} \mathbf{f}(\mathbf{x}) \quad \text{where} \qquad (6)$$

$$\mathbf{f}(\mathbf{x}) = \left[f_1(\mathbf{x}), f_2(\mathbf{x}), ..., f_K(\mathbf{x}) \right]$$

$$\text{subject to} \quad \begin{matrix} \mathbf{h}(\mathbf{x}) = 0 \\ \mathbf{g}(\mathbf{x}) \geq 0 \end{matrix}$$

This problem is similar to the single criterion optimization, except the objective function is now a vector instead of a scalar. The approach chosen for the comparison in this chapter is the normed weighted sum method [46].

The normed weighted sum method is the first method developed for solving problems of this type and it is also the simplest to employ. In effect, the multicriterion optimization problem is turned into a single objective optimization problem by performing three operations on each function value. First, a base value is calculated for each of the functions. This value, termed $f_k^0(\mathbf{x})$, where $k = 1, ..., K$, is used to

normalize each of the resulting function values. If this action is not completed, the method will attempt to minimize the largest value of the functions in the objective function vector. As is the case with this chapter's case study, the values of the objective functions are often several orders of magnitude different.

After the function values are normalized, a multiplicative weighting factor is applied to each and their products are summed. It is customary in this method for the chosen weights to sum to unity. The resulting objective function is often termed the scalar preference function, P.

$$P\left[f_k(\mathbf{x}) \right] = \sum_{k=1}^{K} \left[w_k \frac{f_k(\mathbf{x})}{f_k^0} \right] \qquad (7)$$

where $\sum_{k=1}^{K} w_k = 1$

The choice of the weights is left to the user and their values represent the relative importance of each objective function to the designer. In the work presented here, equal weights were chosen for simplicity in the comparison of the results from the different optimization methods.

2.3: Background on Multidisciplinary Design Optimization (MDO)

In this work the PSO optimizer is integrated as the optimization driver in a MDO framework that is based on the target cascading (TC) method [62 - 69]. In the past a MDO framework has been developed based on the TC method and used for MDO analysis of a thermal protection system design, for aircraft design, and for undersea

vehicle design [70 - 73]; brief technical information is presented here for the TC method since it comprises a foundation for the new developments.

The TC method provides the ability to coordinate an optimization among multiple disciplines through a top level optimization statement. Typically, the top level optimization addresses a global, overall system metric (such as cost, weight, etc.), while the discipline level optimizations target improvement in different performance attributes of a system. Each discipline has its own objective function and design variables.

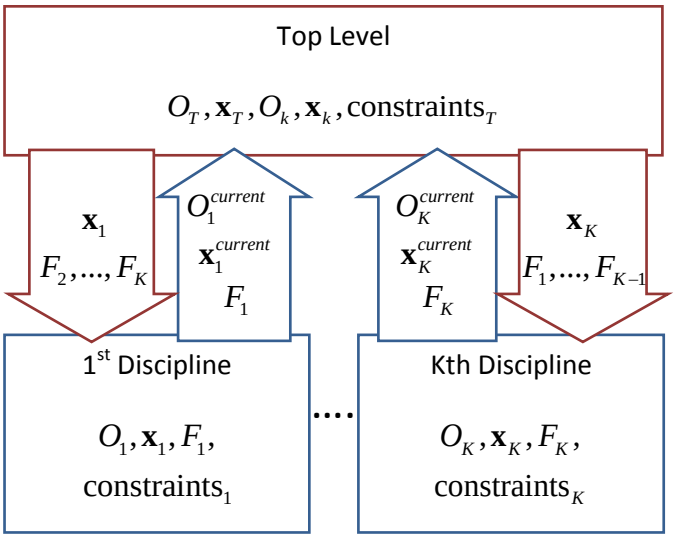

Figure 1: Flow chart of the MDO approach

Different disciplines can share common design variables and the communication of the information among all the disciplines is coordinated through the top level optimization. Figure 1 depicts the flow chart of the MDO framework.

The essence of this approach is based on tracking the values of the objective function O_k and the values of all the "$_j$" design variables x_{jk} from each discipline "$_k$"

during the iterations of the top level optimization statement. At the top level optimization extra constraints are introduced limiting the amount of change allowed in each discipline level objective function and design variables. The extra constraints are expressed as:

$$\left\| O_k^{previous} - O_k^{current} \right\| - \varepsilon_k^O \le 0 \qquad (8)$$
$$\sum_{k=1}^{K} \left\| x_{jk}^{previous} - x_{jk}^{current} \right\| - \varepsilon_j^{\mathbf{x}} \le 0$$

In Equation (8) the superscripts " ^{previous} " and " ^{current} " indicate the values for the objective functions and the design variables originating from the previous and the current step of the top level optimization; the summation $\sum_{k=1}^{K}$ represents a summation over the disciplines that a particular design variable may share. The limits ε_k^O and $\varepsilon_j^{\mathbf{x}}$ are not user prescribed limits, but instead are treated as design variables for the top level optimization that augment the top level objective function. Therefore, the overall top level objective function can be stated as:

$$F\left(\mathbf{x}_T\right) = O_T + \sum_{k=1}^{K} \varepsilon_k^O + \sum_{j=1}^{J_k} \varepsilon_j^{\mathbf{x}} \qquad (9)$$

where J_k is the total number of design variables in the kth discipline; and the overall top level optimization statement becomes:

$$\min_{\mathbf{x}_T, \mathbf{x}_k} F\left(\mathbf{x}_T\right) \tag{10}$$

$$\begin{aligned} & \mathbf{g}_T\left(O_k, \mathbf{x}_T, \mathbf{x}_k, F_k\right) \le 0 \\ & \mathbf{h}_T\left(O_k, \mathbf{x}_T, \mathbf{x}_k, F_k\right) = 0 \\ \text{subject to } & \left\| O_k^{previous} - O_k^{current} \right\| - \varepsilon_k^O \le 0 \\ & \sum_{k=1}^{K} \left\| x_{jk}^{previous} - x_{jk}^{current} \right\| - \varepsilon_j^{\mathbf{x}} \le 0 \end{aligned}$$

where $\mathbf{g}$ and $\mathbf{h}$ represent inequality and equality constraints of the top level optimization; and F_k represents a functional that is evaluated at the kth discipline that influences the constraints of the top level optimization. In order to simplify notation, the constraints can be written as follows:

$$\begin{aligned} & \mathbf{g}_T\left(O_k, \mathbf{x}_T, x_{jk}, F_k, \varepsilon_k^O, \varepsilon_j^{\mathbf{x}}\right) \le 0 \\ & \mathbf{h}_T\left(O_k, \mathbf{x}_T, x_{jk}, F_k\right) = 0 \end{aligned} \tag{11}$$

where the $\mathbf{g}_T$ includes all inequality constraints listed in Equation (10).

Through the constraints articulated by Equation (11), the top level optimization limits the amount of change introduced to the discipline level objective functions by the discipline level optimizations within each top level iteration. In addition, the changes introduced in the discipline level design variables are also limited within each top level iteration. This process allows coordination of the multiple discipline optimizations by the top level and facilitates the flow of information among disciplines.

The existing MDO framework utilizes a gradient based solver as an optimization driver for all the disciplines and for the top level. In this chapter the PSO algorithm discussed in Section 2 is chosen to replace the gradient based optimizer in all discipline levels and in the top level. This choice was made due to the documented [10 – 18, 74]

improvement in results and performance that non-gradient-based algorithms have seen. It is realized that there is a computational burden associated with using a metaheuristic such as PSO. It is hypothesized that the change in optimizers will produce an improvement in the results of the optimization that outweighs the increase in computational cost.

Due to the nature of the PSO method, multiple particles are activated during each optimization iteration, thus a separate interaction between the top level optimization and the discipline level optimizations is required for each particle of the top level optimization during each top level iteration. In addition, multiple particles are activated within each discipline level optimization. Thus, substantial new developments were required for integrating the PSO optimizer within the MDO framework as explained in the next Section. It is recognized that the implementation of a PSO algorithm at both levels of the MDO framework will be very expensive.

2.4: Integration of PSO into MDO Framework

One of the main contributions of this research is the integration of the PSO algorithm into both the top and discipline levels of an MDO framework and the presentation of the results that this integrated approach produces when applied to a conceptual ship design problem. Efforts to integrate the PSO into the discipline level optimizations alone were abandoned after these efforts did not produce appreciable improvements in the results. The integration into the top and discipline levels is discussed here and the results are presented later in the chapter.

The first step in the MDO algorithm used for this research is to call a top-level optimization routine. The inputs to this optimization routine are an initial design variable vector and a vector of maxima and minima for these design variables. As mentioned earlier, the vector of design variables at the top level includes the additional variables that define the TC method, namely, the ε_k^O and $\varepsilon_j^{\mathbf{x}}$.

$$\mathbf{x}_T^{n_T} = \left[x_j^{n_T}, \varepsilon_j^{\mathbf{x},n_T}, \varepsilon_k^{O,n_T} \right] \qquad (12)$$

where $\begin{matrix} j = 1,\ldots,J \\ k = 1,\ldots,K \end{matrix}$

In Equation (12), "^{n_T}" is the top level iteration number, "$_T$" denotes that the value is part of the top level optimization, "J" is the number of design variables, and "K" is the number of disciplines in the optimization problem.

In the MDO method, there are no explicitly defined bounds for the ε_k^O and $\varepsilon_j^{\mathbf{x}}$ parameters, thus technically they can acquire values between zero and infinity. In practice the objective function expressed by Equation (10) tries to reduce their values as much as possible as the MDO solution progresses.

$$\mathbf{x}_T^{\max} = \left[x_j^{\max}, \varepsilon_j^{\mathbf{x},\max}, \varepsilon_k^{O,\max} \right] \qquad (13)$$
$$\mathbf{x}_T^{\min} = \left[x_j^{\min}, \varepsilon_j^{\mathbf{x},\min}, \varepsilon_k^{O,\min} \right]$$

where $\begin{matrix} \varepsilon_j^{\mathbf{x},\max} = \varepsilon_k^{O,\max} = \infty \\ \varepsilon_j^{\mathbf{x},\min} = \varepsilon_k^{O,\min} = 0 \end{matrix}$

In the second major step of the MDO algorithm, the objective function for the top level optimization is evaluated. Following this step, the constraints for the top level optimization are called. Part of the calculation of these top level constraints is a call to

the discipline level optimizations. When the discipline level optimizations are called, they are provided with the current set of top level design variables, which then become $\mathbf{x}_k$. The discipline level optimizer then creates a set of upper and lower bounds, $\mathbf{x}_k^{\max}$ and $\mathbf{x}_k^{\min}$. The lower and upper bounds for the discipline level optimizations are calculated as a predetermined percent deviation, indicated in Equation (14) as "d", on the actual design variables (not the epsilon values) that are passed to the discipline level.

$$\begin{aligned} \mathbf{x}_k^0 &= \left[x_j^{n_T} \right] \\ \mathbf{x}_k^{n_k,\max} &= (1-d)\left[\mathbf{x}_k^{n_k} \right] \\ \mathbf{x}_k^{n_k,\min} &= (1+d)\left[\mathbf{x}_k^{n_k} \right] \end{aligned} \qquad (14)$$

The "n_k" in this Equation is the number of discipline level iterations. When $n_k = 0$ as in the first line of Equation (14), then the discipline level x vector, $\mathbf{x}_k^0$, is equal to the current top level x vector. For each subsequent discipline level iteration, $\mathbf{x}_k^{n_k}$ is determined internally by the optimizer. The index "$_k$" in Equation (14) signifies that the quantity is a discipline level quantity.

Once the discipline level optimizations have completed their operation, including the evaluation of their constraints, $\mathbf{g}_k$ and $\mathbf{h}_k$, they pass their optimum function value, O_k^*, and the corresponding set of design variables, $\mathbf{x}_k^*$, back to the top level constraint function. The top level constraint function then uses these values to calculate its constraint values, $\mathbf{g}_T$ and $\mathbf{h}_T$, as shown in Equation (11). Once this action has been completed, the next iteration of the top level optimization begins. When the algorithm

satisfies a predetermined convergence criterion, it returns the optimum top level objective function value and the corresponding design variable vector, O_T^* and $\mathbf{x}_T^*$ respectfully. Figure 2 gives a flow chart for the steps performed in the existing MDO algorithm.

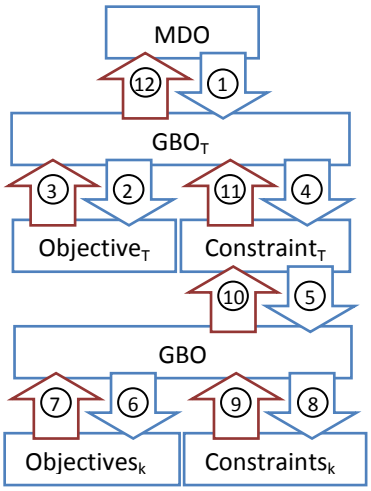

step	Quantities passed
1	$\mathbf{x}_T^{n_T}, \mathbf{x}_T^{\max}, \mathbf{x}_T^{\min}$
2	$\mathbf{x}_T^{n_T}$
3	$F\left(\mathbf{x}_T^{n_T}\right)$
4	$\mathbf{x}_T^{n_T}, \mathbf{x}_T^{\max}, \mathbf{x}_T^{\min}$
5	$\mathbf{x}_k^{n_k}, \mathbf{x}_k^{n_k,\max}, \mathbf{x}_k^{n_k,\min}$
6	$\mathbf{x}_k^{n_k}$
7	O_k
8	$\mathbf{x}_k^{n_k}$
9	$\mathbf{g}_k, \mathbf{h}_k$
10	$O_k^*, \mathbf{x}_k^*$
11	$\mathbf{g}_T, \mathbf{h}_T$
12	$O_T^*, \mathbf{x}_T^*$

Figure 2: Gradient based MDO algorithm

The initial steps in the PSO algorithm require a new development effort for integrating it as an optimization driver in the TC based MDO framework. When the PSO is initiated, it is provided only the lower and upper bounds on the design variables, the objective function and the constraint function. It generates its own initial values in the form of a matrix defining the location of a swarm of points or particles, $\mathbf{x}_T^{n_T}$, rather than a vector defining a single point.

$$\mathbf{x}_T^{n_T} = \left[x_{ij}^{n_T}, \varepsilon_{ij}^{\mathbf{x},n_T}, \varepsilon_{ik}^{O,n_T} \right] \tag{15}$$

where $i = 1,\ldots, I$

The "I" in this Equation is the number of particles in a swarm.

The actual calculation of the initial value, $\mathbf{x}_T^0$, as expressed in Equation (15) when $n_T = 0$, is calculated using the following equations for the initial iteration.

$$\begin{aligned} x_{ij}^0 &= x_j^{\max} - \left(x_{ij}^{rand} \left(x_j^{\max} - x_j^{\min} \right) \right) \\ \varepsilon_{ij}^{x,0} &= \varepsilon_j^{\max} - \left(\varepsilon_{ij}^{rand} \left(\varepsilon_j^{\max} - \varepsilon_j^{\min} \right) \right) \\ \varepsilon_{ik}^{O,0} &= \varepsilon_k^{\max} - \left(\varepsilon_{ik}^{rand} \left(\varepsilon_k^{\max} - \varepsilon_k^{\min} \right) \right) \end{aligned} \tag{16}$$

If the $\boldsymbol{\varepsilon}^{\mathbf{x},\max}$ and $\boldsymbol{\varepsilon}^{O,\max}$ values, which are part of $\mathbf{x}_T^{\max}$, remain unbounded, Equation (16) cannot determine a starting value. Thus, $\boldsymbol{\varepsilon}^{\mathbf{x},\max}$ and $\boldsymbol{\varepsilon}^{O,\max}$ must be set at a low enough value, i.e. within a reasonable order of magnitude of the objective function, that the algorithm is forced to change the actual design variables, and sequentially the objective function values, rather than just trying to lower the epsilon values. Figure 3 illustrates the entire integrated MDO/PSO process.

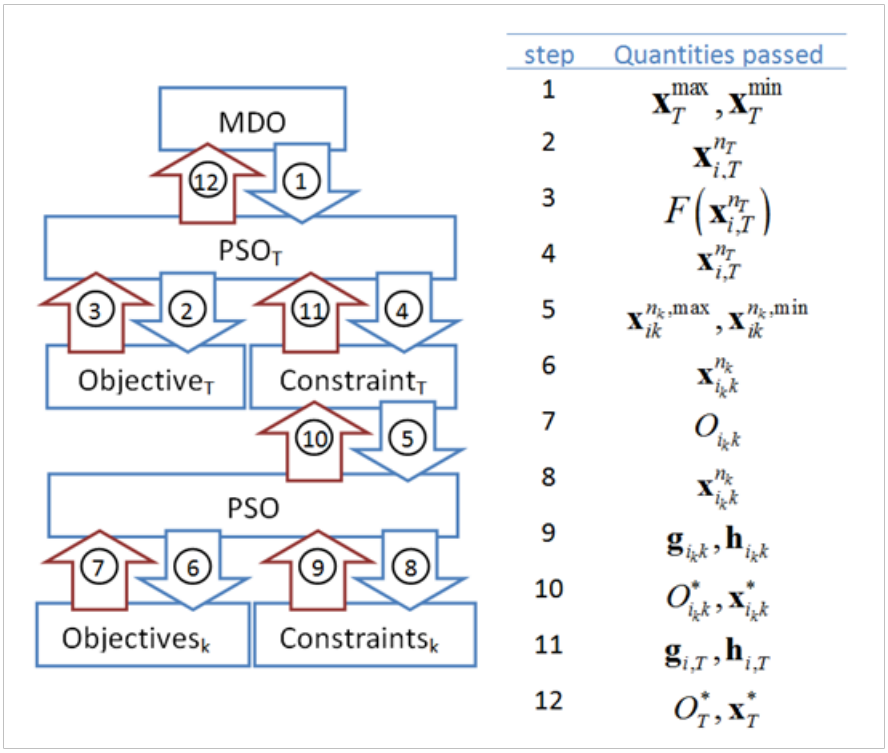

step	Quantities passed
1	$\mathbf{x}_T^{\max}, \mathbf{x}_T^{\min}$
2	$\mathbf{x}_{i,T}^{n_T}$
3	$F\left(\mathbf{x}_{i,T}^{n_T}\right)$
4	$\mathbf{x}_{i,T}^{n_T}$
5	$\mathbf{x}_{ik}^{n_k,\max}, \mathbf{x}_{ik}^{n_k,\min}$
6	$\mathbf{x}_{i_k k}^{n_k}$
7	$O_{i_k k}$
8	$\mathbf{x}_{i_k k}^{n_k}$
9	$\mathbf{g}_{i_k k}, \mathbf{h}_{i_k k}$
10	$O_{i_k k}^*, \mathbf{x}_{i_k k}^*$
11	$\mathbf{g}_{i,T}, \mathbf{h}_{i,T}$
12	$O_T^*, \mathbf{x}_T^*$

Fig. 3 PSO based MDO algorithm

In the MDO/PSO, a single particle from the swarm, $\mathbf{x}_{i,T}^{n_T}$, is passed to each discipline level, one at a time. The discipline level PSO then creates a percent boundary band, signified by $\mathbf{x}_{ik}^{n_k,\max}$ and $\mathbf{x}_{ik}^{n_k,\min}$, which are calculated using an equation similar to Equation (14), and an equation similar to (16) in order to generate its own initial swarm.

A full PSO is then executed at each discipline level, and the optimum point and corresponding design variables for that top level particle, O_{ik}^* and $\mathbf{x}_{ik}^*$, are passed back to the top level constraint function. This process is continued for every particle in the top level swarm. Once the entire top level swarm has been treated, the next top level iteration can proceed. In this manner an extra loop of swarm iterations is introduced by the top level optimization.

Figure 3 presents a flow chart of the MDO/PSO process. In this figure, "i" is defined as previously, however $i_k = 1,\ldots,I_k$ where "I_k" is the number of particles in the discipline level swarm.

2.5: Case Study Definition

The optimization statements solved in this chapter are based on a conceptual ship design application originally presented in [26] and adapted in [46]. The problem here is adapted further from Parsons and Scott's work for this chapter and is presented here as a six design variable, three objective, 21-constraint design optimization problem which uses regression data to model a family of bulk carriers.

The design variables used in the model are length (L), beam (B), depth (D), draft (T), block coefficient (C_B) and speed in knots (V_k). The three objective functions are $\min f_1(\mathbf{x}) =$ Transportation Cost (£/t), $\max f_2(\mathbf{x}) =$ Annual Cargo (t/yr), and $\min f_3(\mathbf{x}) =$ Lightship Weight (t). Table 2 summarizes the complete model.

The constraints that are employed in the various optimization statements of this chapter are summarized in Table 3. Nine of the constraints in Table 3 are physical constraints on the design itself. The remaining 12 are upper and lower bounds on the six design variables.

Table 2: Model Definition

Parameter	Equation/Definition	Parameter	Equation/Definition
Steel weight (W_s)	$0.034L^{1.7}B^{0.7}D^{0.4}C_B^{0.5}$	Fuel price (FP)	100 (£/t)
Outfit weight (W_o)	$1.0L^{0.8}B^{0.6}D^{0.3}C_B^{0.5}$	Fuel costs (C_F)	$1.05(DC)(D_S)(FP)$
A	$4977.06C_B^2 - 8105.61C_B + 4456.51$	Port cost (C_P)	$6.3DWT^{0.8}$
B	$-10847.2C_B^2 + 12817C_B - 6960.32$	Fuel carried (FC)	$DC(D_S + 5)$
Displacement (Δ)	$1.025LBTC_B$	Misc. deadweight (DWT_M)	$2.0DWT^{0.5}$
Froude number (F_n)	$\frac{V}{\sqrt{gL}}$ where $V = 0.5144V_k$ and $g = 9.8065$	Cargo deadweight (DWT_C)	$DWT - FC - DWT_M$
Power (P)	$\frac{\sqrt[3]{\Delta^2}V_k^3}{(a + bF_n)}$	Handling rate (HR)	8000 (t/day)
Machinery weight (W_m)	$0.17P^{0.9}$	Port days (D_P)	$2\left[\left(\frac{DWT_C}{HR}\right) + 0.5\right]$
Ship cost (C_S)	$1.3\left(2000W_s^{0.85} + 3500W_o + 2400P^{0.8}\right)$	Round trips per year ($RTPA$)	$\frac{350}{(D_S + D_P)}$
Capital costs (C_C)	$0.2C_S$	Voyage costs (C_V)	$(C_F + C_P)(RTPA)$
Lightship weight (W_{LS})	$C_C + C_R + C_V$	Annual cost (C_A)	$(DWT_C)(RTPA)$
Deadweight (DWT)	$\Delta - W_{LS}$	Annual cargo (AC)	$W_s + W_o + W_m$
Running cost (C_R)	$40000DWT^{0.3}$	Transportation cost (C_T)	$\frac{C_A}{AC}$
Daily consumption (DC)	$\frac{(0.19)(24)P}{1000} + 0.2$	KB	$0.53T$

Table 2: Model Definition

Parameter	Equation/Definition	Parameter	Equation/Definition
Round trip miles (RTM)	5000 (nm)	BM_T	$\frac{(0.085C_B - 0.002)B^2}{TC_B}$
Sea days (D_S)	$\frac{RTM}{24V_k}$	KG	$1.0 + 0.52D$

Table 3: Constraint Definition

Const.	Equation/Definition	Explanation	Const.	Equation/Definition	Explanation
c(1)	$6 - \frac{L}{B} \le 0$	Constraint on the length-to-beam ratio.	c(9)	$0.07B - KB - BM_T + KG \le 0$	Empirical constraint on relationship between symbols
c(2)	$\frac{L}{D} - 15 \le 0$	Constraint on length-to-depth ratio.	c(10,11)	$150 \le L \le 274.32$	Upper and lower bounds of ship length.
c(3)	$\frac{L}{T} - 19 \le 0$	Constraint on length-to-draft ratio.	c(12,13)	$20 \le B \le 32.31$	Upper and lower bounds of beam.
c(4)	$T - 0.45DWT^{0.31} \le 0$	Empirical constraint on the relationship between	c(14,15)	$13 \le D \le 25$	Upper and lower bounds of depth.
c(5)	$T - 0.7D + 0.7 \le 0$	Empirical constraint on relationship between	c(16,17)	$10 \le T \le 11.71$	Upper and lower bounds of draft.
c(6)	$DWT - 500000 \le 0$	Upper constraint on	c(18,19)	$0.63 \le C_B \le 0.75$	Upper and lower bounds of
c(7)	$25000 - DWT \le 0$	Lower constraint on	c(20,21)	$11 \le V_k \le 20$	Upper and lower bounds of
c(8)	$F_n - 0.32 \le 0$	Upper constraint on			

2.6: Comparison of PSO and a Gradient-Based Optimization Method for Single and Multicriterion Optimization

In order to demonstrate proper implementation of the PSO algorithm, a single discipline and a multicriterion conceptual ship design problem is solved and results are compared to data reported in Parsons and Scott's paper and with results from a commercial gradient based optimization driver (fmincon, which is available in MATLAB).

2.6.1: Single Criterion Optimization and Results

Results from the single objective optimization comparison are contained in Table 4. The candidates provided by each optimization algorithm for Minimum Transportation Cost, Minimum Light Ship Cost, and Maximum Annual Cargo Design are bolded. All PSO results presented therein were obtained after executing 12 runs of 1000 particles. It was found through trial and error experimentation with the algorithms that this combination of runs and particles provided an acceptable balance between computation time and results. Minimum values from these 12 runs (mean in parentheses) are presented for comparison.

One interesting note that came out of running each optimization concerns maximization of a function using PSO. There are normally two ways of doing this. The first is to minimize the negative of the function, and the second is to minimize the reciprocal of the function. The PSO algorithm does not behave well when dealing with the negative of the function for reasons unknown to the author. Because of this fact, the reciprocal of the annual cost objective function was used in all PSO iterations.

Table 4: Single Objective Results

Parameters	Min Transportation Cost Design			Min Light Ship Design			Max Annual Cargo Design		
	Excel	PSO (mean)	fmincon	Excel	PSO (mean)	fmincon	Excel	PSO (mean)	fmincon
Transport Cost (£/t)	8.377	8.213 (8.355)	8.401	9.474	9.374	9.002	10.294	10.884	12.185
Light ship (t)	9,029.0	8,444.3	9,565.2	5,240.3	5,043.2 (5,622.3)	4,983.8	12,436	12,617	13,095
Annual cargo (t/yr)	551,265	507,940	558,490	386,500	353,670	328,680	700,553	684,310 (656,510)	724,560
Length (m)	193.86	187.63	194.85	150.73	155.32	150.09	222.49	221.86	222.49
Beam (m)	32.31	30.89	32.31	25.12	23.36	25.01	32.31	31.50	32.31
Depth (m)	15.73	15.54	15.73	13.84	14.43	13.84	15.73	17.60	15.73
Draft (m)	11.71	11.58	11.71	10.39	10.76	10.39	11.71	11.68	11.71
Block Coefficient	0.681	0.730	0.750	0.750	0.693	0.750	0.750	0.730	0.750
Speed (knots)	14.00	12.25	14.00	14.00	13.62	11.00	18.00	18.69	20.00
Deadweight (t)	42,160	41,787	47,107	25,000	22,678	25,000	52,277	48,402	51,618
Power (kW)	5,358	3,604	6,651	5,018	3,613	1,923	19,060	20,459	30,906

A gradient based algorithm handles both the negative and the reciprocal methods of maximization equally well. It does provide different final answers depending on which method is used. The reciprocal method was also used with all gradient based calculations in order to preserve the comparison between the results it generated and those generated by the PSO algorithm.

Another interesting point with the PSO algorithm is that it periodically returns optima which violate one of the constraints by more than an acceptable amount. This is caused by the manner in which the PSO algorithm allows each particle to explore outside the bounds of the design space in order to ensure that they travel on a smooth trajectory. In the later stages of this work, an additional optimization was performed on any results that were found to violate the constraints. The design variables in this additional optimization were constrained to keep them within an acceptable range of their values that produced the PSO "optimum". An example of this phenomenon is contained in the PSO "Min Light Ship Design" value. This design violates one constraint by more than an acceptable amount. The results are presented here to highlight this characteristic of the PSO algorithm employed in this work.

All gradient based optimizations started from point (195; 32.31; 20; 10.5; 0.7; 16). This point was chosen because it serves as a "good" design that satisfies all constraints. It is customary for such a "good" design to serve as a starting point for a design optimization that will work to improve this design. This initial set of design variables produced initial, normalizing values of 9.9264 £/t, 547,680 t/yr, and 10,304 t for the objectives.

Parsons and Scott used the Solver tool in Microsoft Excel (8.0) to perform their optimizations. The Solver was set to use the gradient algorithm with a 100 second time limit, maximum iterations of 600, precision of 1e10-9, a convergence criterion of 1e10-7, tangent initial estimates for the one-dimensional searches, and forward difference partial derivative option. Finally, independent variables were designated as nonnegative in their method.

The conclusion that should be drawn from the data contained in Table 4 is that different optimizers provide different results on different objective functions. This is not a new discovery. When the actual practical or physical gains or losses realized by these differences are calculated (an 8.3% transportation cost savings between the Excel design and the PSO design) it becomes valuable to investigate these differences further.

Another conclusion that began to become apparent in these preliminary experiments is that there is a considerable expense, regarding computation time, associated with using an algorithm like PSO. Each iteration of the algorithm, with 1000 particles, took approximately 2 minutes to complete. Again, this is not new knowledge. The question remains: Will this increased computation burden be outweighed by an improvement in the overall value of the optimum objective function? The answer to this question will be given in the conclusion of this chapter.

2.6.2: Multicriterion Optimization and Results

Results from the multicriterion optimization are presented in Table 5. Values for the multicriterion preference function are bolded. As in the single criterion results, a series of 12 PSOs of 1000 particles each were run in order to find the best value. The

minimum value found in the 12 runs is included in the table with the mean value in parentheses.

Table 5: Multicriterion Optimization Results

Parameters	Excel	fmincon	PSO (mean)	MC	MC	SMC
$P\left[f_k(\vec{x}) \right]$ =	0.960	0.885	0.893 (0.898)	0.895	0.892	0.885
Transport Cost	9.474	8.573	8.722	8.692	8.778	8.584
Light ship (t)	5,240	7,473	7,578	7,480	7,945	7,473
Annual cargo (t/yr)	386,500	514,080	514,480	505,560	536,040	514,260
Length (m)	150.73	173.72	176.41	175.12	178.82	173.72
Beam (m)	25.12	28.95	29.34	28.85	29.73	28.95
Depth (m)	13.84	15.73	15.45	15.45	15.82	15.72
Draft (m)	10.39	11.71	11.51	11.41	11.65	11.70
Block Coefficient	0.750	0.750	0.725	0.747	0.731	0.750
Speed (knots)	14.00	14.00	14.48	14.08	14.77	14.03
Deadweight (t)	25,000	37,804	36,707	36,639	38,513	37,752
Power (kW)	5,018	6,061	6,427	6,033	7,234	6,103
CPU time (s)	UNK	2.3	1,093.7	71.3	388.7	3,026.7
Function	UNK	168	542,413	542,413	5.05x106	2.13x107

A fourth and fifth algorithm were introduced at this stage of the experimentation. After noticing the computation cost that was paid in order to use the PSO algorithm in the previous step, the author began to wonder how a simple Monte Carlo (MC) method and a sequential Monte Carlo (SMC) method would perform on this problem. The SMC method also served as a verification of the actual minimum of the function.

The MC method used in this chapter was a completely random, uniform seeding of points in the feasible design space. The method was executed with two stopping points. First, the MC method was allowed to run until it had evaluated the function the

same number of times as the PSO. Secondly, the MC method was run until it returned a value that was better than the PSO value. The results from the MC method are in columns four and five in Table 5.

The SMC method is only slightly more complex than the MC method. Due to its ability to "drill down" towards a specific minimum, it reaches a minimum more quickly than a pure MC method. The SMC method is initiated when a sequence of random points, $\mathbf{x}_0$, is distributed throughout the design space, using the inequality constraints, the upper and lower limits on the design variables, and a minimum function value as bounds. This initial distribution creates a set of points which satisfy all constraints and whose output function values are below the minimum.

The method continues with the newly created set of points, $\mathbf{x}_i$, the maximum and minimum values of each design variable in the set, $\mathbf{x}_{\max,i}$ and $\mathbf{x}_{\min,i}$, and the mean function value that is produced by the set of points. In each successive iteration, the $\mathbf{x}_{\max,i}$ and $\mathbf{x}_{\min,i}$ become the new bounds on the design variables, and the mean function value becomes the new minimum function value accepted. The method continues until a convergence criteria is met.

The SMC results are summarized in the sixth column of Table 5. Notice that the SMC algorithm took over 21 million function evaluations to reach a value close to the fmincon value. The SMC was manually stopped at this point. For comparison, a simple, that is, completely random, MC algorithm reached a value below the PSO value in just over 5 million function evaluations.

In addition to a fourth, fifth, and sixth column, two rows were added to the bottom of Table 5 for this phase of experimentation. As attention shifts from the actual values of the objective functions, it becomes necessary to track the CPU time and the number of function evaluations performed. For the PSO CPU time results, the time taken for all 12 runs is documented. Table 5 begins to document the computational expense associated with using the non-gradient-based algorithms.

Again, the same conclusions can be drawn from this data as could be drawn from the previous tables: different optimizers provide different results. Of particular note is the value that fmincon attained for this particular objective function. This is the lowest value that the author have seen for this particular objective function using any optimizer. Also of particular interest is the exceptional performance by all measurements of the fmincon optimizer. The strong performance in this example by fmincon could lead one to believe that this optimizer is the strongest presented here. It does have several positive qualities. The minimum transportation cost results in Table 4 show that it is not perfect however-- depending on the function being evaluated and the starting point for the optimizer, fmincon can be outperformed by other algorithms.

2.7: MDO Using Gradient-Based and PSO Algorithms

The multidisciplinary design optimization formulation of the conceptual ship design problem is stated as follows.

$\min f_T(\mathbf{x}) =$ Transportation Cost (£/t) (17)
$\max f_1(\mathbf{x}) =$ Annual Cargo (t/yr)
$\min f_2(\mathbf{x}) =$ Lightship Weight (t)

In Equation (17), the subscripts "$_T$", "$_1$", and "$_2$" denote the top level objective function, the first discipline level objective function, and the second discipline level objective function, respectively. This formulation was chosen because the author are interested more in cost than annual cargo carrying capacity or lightship weight as a system-level attribute. Table 6 contains the complete results from the MDO run of the bulk carrier design problem with a gradient based and PSO algorithms. The results are compared to the "best" multicriterion optimization design. In the MDO columns, a value is included in the preference function row only to serve as a comparison between the multicriterion optimization and the MDO results. The goal of the MDO was to minimize the top level objective function, which is the transportation cost. The goal of the multicriterion optimization was to minimize the preference function. Of particular interest here is the tradeoff that the MDO algorithm's structure makes between each of the disciplines. Even though it performs worse if measured by the multicriterion preference function, it produces a far better transportation cost value, the objective that was identified at the system level as the most important. It also ensures that the chosen set of design variables produces respectable values for the other disciplines.

Table 6: MDO results

Parameter	Units	Multi-criterion	MDO	MDPSO	Parameter	Units	Multi-criterion	MDO	MDPSO
$P\left[f_k(\vec{x}) \right]$=	none	0.8848	0.8996	0.9464	Running cost	£	944,700	1.00M	1.01M
Length	m	173.72	193.38	221.77	Daily consumption	t	27.84	29.83	33.48
Beam	m	28.95	32.23	31.17	Sea days	Days	14.88	14.88	14.16
Depth	m	15.73	15.72	14.38	Fuel costs	£	43,496	46,602	49,789
Draft	m	11.71	11.71	11.29	Port cost	£	28,929	33,962	34,407
Block Coef.	none	0.750	0.743	0.723	Fuel carried	t	553.44	592.96	641.59
Speed	kts	14.00	14.00	14.71	Misc. deadweight	t	388.84	429.84	433.36
Steel weight	t	6,006.2	7,731.0	9,072.9	Cargo deadweight	t	36,857	45,167	45,875
Outfit weight	t	1,036.1	1,202.6	1276.9	Port days	Days	10.21	12.29	12.47
Displacement	m3	45,273	55,583	57,810	Round trips per year	None	13.95	12.88	13.14
Froude number	None	0.17	0.17	0.16	Voyage costs	£	1.01M	1.04M	1.11M
Power	KW	6,061	6,497	7,298.4	Annual cost	£	4.41M	4.89M	5.25M
Machinery wt	t	431.25	459.07	509.75	Annual cargo	t/yr	514,080	581,660	602,900
Ship cost	£	12.3M	14.2M	15.7M	Transportation cost	£/t	8.573	8.397	8.705 (9.722)
Capital costs	£	2.45M	2.84M	3.13M	CPU time (s)	S	2.3	53.0	7894.6
Light ship wt	t	7,473.5	9,390.2	10,860	Function evals	None	168	28,630	3x107
Deadweight	t	37,800	46,174	46,950					

The MDO/PSO results in Table 6 are based on 12 initial runs with 100 particles in the top level and 10 in each discipline level. The average value of the 12 runs for the transportation cost is included in parentheses.

The results from the initial set of 12 MDO/PSO produces results inferior to the MDO results as it can be observed in Table 6. The original MDO/PSO results violated constraints and were modified using an additional optimization, as described in section 7.1. Additional efforts to obtain satisfactory results from the MDO/PSO algorithm by increasing the number of particles at the discipline level were not successful. It was quickly discovered just how costly an increase in particles was. It is projected that it would take several months to run the MDO/PSO analysis with the same fidelity as was used to obtain the results shown in Table 5. For the sake of comparison, results from additional runs of the MDO/PSO are presented in Table 7.

Table 7: MDPSO Results

		# of particles (top/discipline)			
Parameter	Units	500/100 (fixed)	100/100	100/50	100/20 (fixed)
Transport Cost	£/t	8.882 (9.962)	9.404 (10.248)	9.612 (10.148)	9.022(11.385)
Light ship	t	8,681.4	8,042.3	12,289.0	9,205.5
Annual cargo	t	514,410	488,140	586,360	549,070
Length	m	196.59	188.68	242.27	207.09
Beam	m	32.31	27.91	29.09	29.37
Depth	m	13.94	15.54	16.49	15.78
Draft	m	10.46	10.65	10.88	11.71
Block Coef.	None	0.652	0.704	0.687	0.630
Speed	kts	14.88	15.20	15.93	16.192
CPU time	s	621,073.7	110,883.8	46,351.1	14,717.2

It can be seen from the data in Table 7 that the result did improve as more particles were added to the PSO algorithm. The trend of the results violating constraints can also be seen in the 500/100 trial and the 100/20 results, as both were "fixed" using the method described. It can also be seen that the CPU time increased dramatically. At a time of over 1 week, the 500/100 particle combination, which still does not provide as good of results as the gradient based MDO method, is just too long.

CHAPTER 3:
A MULTIDISCIPLINARY DESIGN OPTIMIZATION APPROACH TO RELATING AFFORDABILITY AND PERFORMANCE IN A CONCEPTUAL SUBMARINE DESIGN

The main objective of this chapter is to document the use of multidisciplinary design optimization to systematically build a foundation for increasing the understanding of the multifaceted relationship between affordability and performance in the conceptual design of a complex engineering system. Secondary objectives include creating a sophisticated, automated affordability model based on the manufacturing costs associated with a component of such a system, and creating automated first-order models for four engineering disciplines that are typical of those encountered in conceptual design. Finally, results from the single-discipline optimization of these disciplines will be discussed and compared to the results obtained from optimizing all disciplines in a coordinated effort governed by the response of a system-level objective.

A comprehensive literature review on the topics related to this work is presented in Chapter 1. It should be noted that, although the open literature does not accurately reflect practical aspects of submarine design due to the sensitive nature of the topic, the work summarized in this chapter draws heavily from the established body of literature for the development of the discipline-level objective functions and constraints. This is deemed acceptable since the work presented in this chapter is not meant to be an accurate representation of current practice in the world of conceptual

submarine design. Rather, this chapter aims to introduce the capabilities of a very powerful tool for MDO analysis with the understanding that the technology is modular enough to accept practical models for the various submarine performance disciplines in a setting where such models are available. Figure 4 presents a schematic of the conceptual submarine design study conducted in this work.

This chapter demonstrates how affordability can be linked to the physical design characteristics of a system and how, in submarine design, MDO analysis can simultaneously coordinate multiple optimizations while optimizing at the same time the overall system objective. The value of the MDO analysis is demonstrated by comparing the MDO results with individual discipline-level optimizations. Each single-discipline optimization method creates a different optimum configuration for the system, each in respect to its own discipline. These results are compared to the MDO optimum and the benefits of a coordinated and organized MDO analysis are discussed.

3.1: Creation of the Discipline-Level Objective and Constraint Functions

In the conceptual submarine application presented in this chapter, the technical disciplines considered are: deck area, resistance (or actually the effective power necessary to overcome this resistance), structures, and maneuvering (or dynamic stability). Low-fidelity, first-order representations were chosen to model the four engineering performance disciplines. Examining each of these disciplines in the manner suggested in this work is not the way in which submarines are actually designed today since this chapter demonstrates the MDO process using models that are available in the open literature.

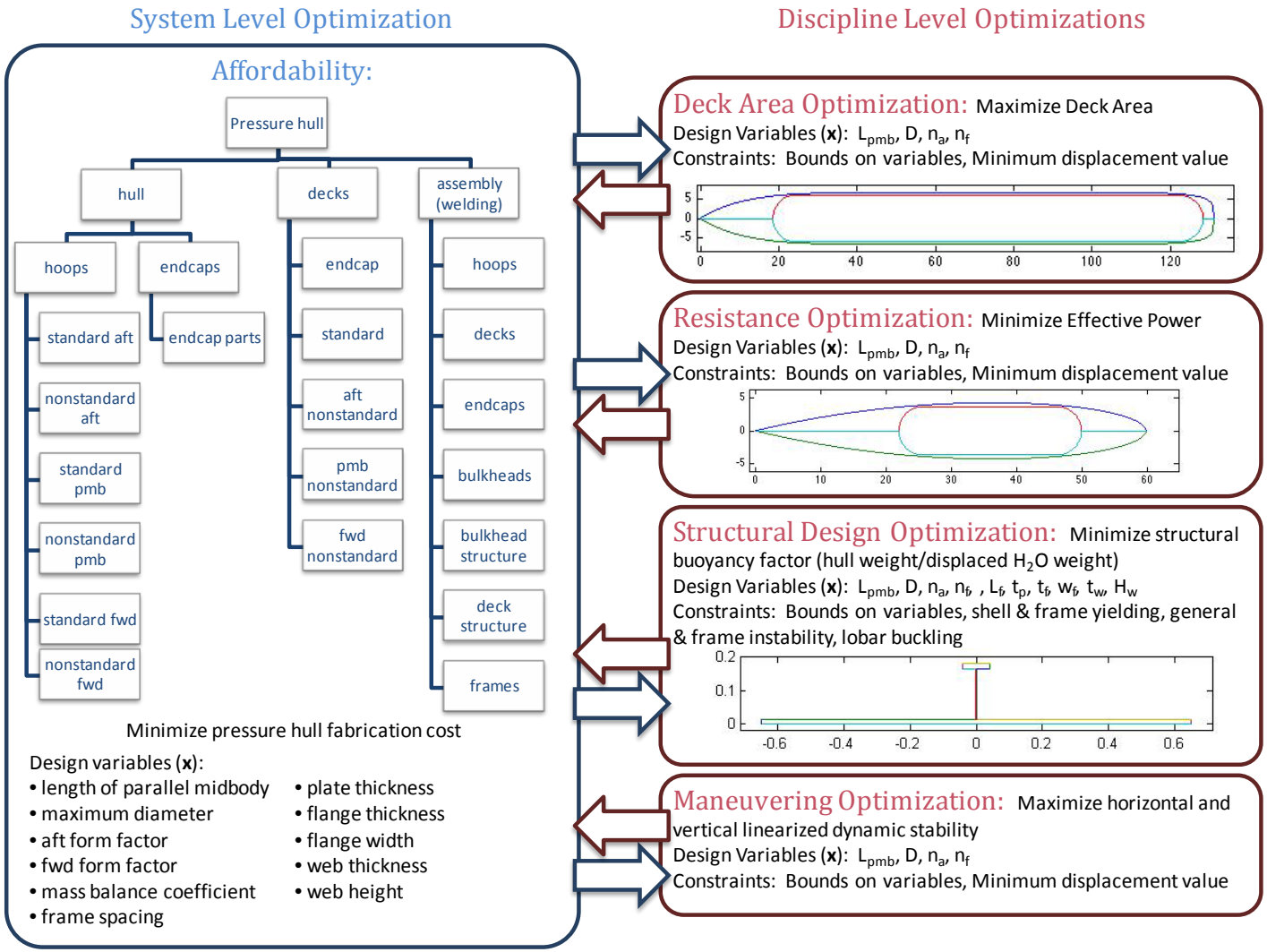

Figure 4: Schematic of conceptual submarine design MDO process for affordability

Due to the modularity of the MDO system, disciplines that are more representative of practice, such as arrangements, volumetrics, weights, and ship balance, can be considered instead if representative models are available for each discipline.

3.1.1: Deck Area

The first engineering performance discipline created was the deck area discipline. As mentioned in Chapter 1, the design variables used to approximate the shape of the hydrodynamic hull of a submarine in the conceptual design phase are those prescribed by Jackson [95, 96]. Additionally, since Jackson's treatment allows only for the creation of the hydrodynamic hull, the deck area model created here used these initial design variables, along with several parameters. Descriptions of the parameters and design variables, and nominal values for the parameters are contained in Table 8. The deck area discipline is constrained by a semi-arbitrary minimum displacement value.

The hydrodynamic hull is broken up into three sections: the aft section, the forward section and the parallel midbody. According to Jackson and many others, the ideal shape for the bare submarine hull from a purely hydrodynamic standpoint would be one in which there was no parallel midbody and in which the sum of the aft and forward lengths was six times the maximum diameter. It is understood that the required operational capabilities and potential operating environment required by today's submarine requires more volume than is available in a hull without parallel midbody, and so the hull is stretched accordingly by increasing this value. It is also understood that adding appendages to a hull increases the optimum length to diameter

ratio considerably and that the constraints on draft often outweigh desires to design a submarine at the optimum ratio.

Table 8: Deck Area Discipline Parameter and Design Variable Definitions

Parameter Definitions			Design Variable Definitions			
Param	Definition	Value	Var.	Definition	Max	Min
H_{td}	'tween deck height	2.286 m	L_{pmb}	Length of the parallel midbody	40 m	1 m
H_b	Bilge height	2.438 m	D	Maximum hull diam.	13 m	8.4 m
H_s	standard separation between hydrodynamic pressure hulls	0.607 m	n_a	Aft form factor	5	2
$H_{s,\min}$	minimum separation between hydrodynamic pressure hulls	0.25 m	n_f	Forward form factor	5	2
$n_{d,\max}$	Maximum number of decks	4				
n	Discretizations of hull	1000				

There is some disagreement in the literature about this "ideal" length-to-beam ratio because the resistance vs. L/B curve for a "clean" (that is, without appendages) hull is relatively flat in this region, and, using this curve as a judge, a ratio of six or seven would provide very nearly the same resistance. This work uses a L/B ratio of seven but maintains the same percent relationship between the aft and forward lengths that Jackson specifies, giving the length relationships summarized in Equation (18) below.

$$L_a = 4.3D \qquad (18)$$
$$L_f = 2.7D$$
$$L_{tot} = L_a + L_f + L_{pmb}$$

In Equation (18), L_a is the aft length, L_f is the forward length, and L_{tot} is the total length of the hydrodynamic hull. The remaining variables in Equation (18) are defined in Table 8.

In the deck area model, it is necessary to calculate the actual location of each point on the hydrodynamic hull. Equation (19) outlines the first step in determining this location

$$\delta x = \frac{L_{tot}}{n} \qquad (19)$$
$$i = 1...n+1$$
$$x_i = i(\delta x)$$

where δx is the change in the longitudinal direction along the submarine, and x_i is the actual longitudinal location. The next step in the process of determining the actual location of each point on the hydrodynamic hull is summarized in Equation (20).

$$y_{hh,i} = \frac{D}{2}\left(1 - \frac{x_i}{L_a}\right)^{n_a} \qquad (20)$$
$$y_{hh,i} = \frac{D}{2}$$
$$y_{hh,i} = \frac{D}{2}\left(1 - \frac{x_i - \left(L_a + L_{pmb}\right)}{L_f}\right)^{n_f}$$

Here $y_{hh,i}$ is the ith transverse location of the hydrodynamic hull. The first line of Equation (20) is used to calculate the aft portion of the hydrodynamic hull when $i(\delta x) \le L_a$, the second line when $i(\delta x) \le L_a + L_{pmb}$, and the third for all other values of i. The resulting values for $y_{hh,i}$ construct a halfplan of the hydrodynamic hull. All that is left is for the halfplan to be rotated one full rotation about the longitudinal axis of the

submarine, and the full hydrodynamic hull is now represented. Once the hydrodynamic hull has been built, the next step is to create a representation of the pressure hull.

The diameter of the pressure hull, D_{ph}, is simply the outer hull diameter, D, less twice the standard separation between the outer and pressure hulls. In determining the length of the pressure hull, it is instructive to divide it into the aft, parallel midbody, and forward section in a similar manner to the hydrodynamic hull. The parallel midbody section of the pressure hull will be the same length as the parallel midbody section of the hydrodynamic hull. The lengths of the fore and aft sections of the pressure hull are composed of two parts. The first part is the radius or depth of the hemispherical endcap, which is the same as the radius of the pressure hull itself. This part is the same for both the forward and the aft sections of the pressure hull. The second, and more difficult to calculate, part of the forward and aft length is the part of these sections that extend into the fore and aft sections of the hydrodynamic hull, but at the same diameter as the actual pressure vessel. The minimum separation between the outer and pressure hulls is used in the manner shown in Equation (21) to determine these two lengths.

$$y_{ph} = \min\left(\left| y_{hh,i} - \frac{D_{ph}}{2} + H_{s,\min} \right|\right) \tag{21}$$

Equation (21) is used to generate two y_{ph} values, one for the aft section of the hydrodynamic hull, when $i(\delta x) \le L_a$, and one for the forward section of the hull, when $i(\delta x) \ge L_a + L_{pmb}$. These y_{ph} values have a corresponding x value, and this value aids in determining the two lengths in question.

After the hydrodynamic and pressure hulls have been modeled, the decks within the pressure hull must be created. Since the pressure hull is a cylinder with hemispherical endcaps of the same diameter as the cylinder, simple geometric relationships can help to determine the required location and dimensions of these decks, and their resulting area. There is another measurement that can be taken from the dimensions of these decks, and that is the weld length needed to attach them to the hull. This weld length will be used in the affordability model.

The size of the first deck, that immediately above the bilge, is calculated in the same manner for every iteration of the deck area code. Equation (22) outlines this calculation.

$$r_1 = \sqrt{\left(\frac{D_{ph}}{2}\right)^2 - \left(\frac{D_{ph}}{2} - H_b\right)^2} \tag{22}$$

$$A_1 = 2r_1 L_{ph} + 2\pi r_1^2$$

$$L_{w,1} = 2\pi r_1 + 4L_{ph}$$

where r_1 is the half-width of the first deck in the parallel midbody, and the radius of the deck in the two hemispherical endcaps, A_{af} is the area of the deck in the two endcaps, A_1 is the total area of the first deck, $L_{w,1}$ is the weld length of the first deck, and L_{ph} is the length of the pressure hull.

As mentioned, the first deck will always be calculated in the same manner, regardless of the values of the design variables. The additional decks however, will not only vary in their size and location as the design variables change, but also in their number. The maximum number of decks in a submarine, as constrained by the depth

needed to enter some ports and the 'tween deck height required by the crew, has traditionally been four. Most submarines today are built with three decks. These decks do not span the length of the submarine, but are rather limited to the operations spaces, where the crew live and fight the ship. For the first-order model summarized here, if the pressure hull diameter is greater than the sum of four times the 'tween deck height and the bilge height, then the size of the remaining decks, which traverse the entire length of the hull in this model, is calculated in the following manner:

$$r_2 = \sqrt{\left(\frac{D_{ph}}{2}\right)^2 - \left(\frac{D_{ph}}{2} - \left(H_b + H_{td}\right)\right)^2} \qquad (23)$$

$$r_i = \sqrt{\left(\frac{D_{ph}}{2}\right)^2 - \left(\left(H_b + \left(i-1\right)H_{td}\right) - \frac{D_{ph}}{2}\right)^2}$$

Here, r_2 is the halfwidth/radius of the second deck. The second calculation determines r_i, the halfwidth/radius of the ith deck as $i = 3...n_{d,\max}$. After these r values are calculated, the areas and weld lengths for each deck are computed in much the same manner as outlined in Equation (22). Once the deck areas and weld lengths are determined for each of the decks, these values are summed to provide the values for the entire submarine. If the diameter of the pressure hull is less than the sum of four times the 'tween deck height and the bilge height, there are similar calculations for determining the deck area. These calculations are mere extensions of those summarized above and will not be covered here.

3.1.2: Resistance/ Effective Power

The effective power model adapted for this work is very familiar to Naval Architects and hydrodynamicists the world over. It is a first-order model that is used as the basic foundation for the study of the subject [75, 95, 96]. As such, only a summary of how the method was applied in this work will be discussed here for the purposes of clarity and identification.

Table 9 lists the parameters used in this discipline, their definitions, and their values. The design variables used in this discipline are the same as those listed and defined in Table 8.

Table 9: Effective Power Discipline Parameter Definitions

Parameter Definitions		
Parameter	Definition	Value
ρ	Seawater Density	1025 kg/m3
υ	Kinematic viscosity	1.05e-6 m2/s
$U_{\max}$	Maximimum speed	12.35 m/s
H_s	Sail Height	5.5 m
W_s	Sail width	2 m
L_{Sf}	Length of sail, forward	3 m
L_{Sa}	Length of sail, aft	4 m
n_{Sf}	Sail form factor, forward	2.5
n_{Sa}	Sail form factor, aft	2.5
δC_{fH}	Hull roughness coefficient	0.0004
δC_{fS}	Sail roughness coefficient	0.0004
C_{rS}	Sail residuary resistance coefficient	0.005

Using the design variables and the parameters defined above, the calculation of the effective power needed by the submarine progressed in the classic manner. First, the wetted surface of the aft, forward, and parallel midbody sections of the hull and the

Reynold's number for the hull were calculated. The frictional and residuary resistances for the hull are then calculated using the familiar expressions summarized in Equation (24).

$$C_{fH} = \frac{0.075}{\left(\log_{10}\left(Re_H\right) - 2\right)^2} \qquad (24)$$

$$C_{rH} = \frac{0.00789}{\frac{L_{tot}}{D} - K2}$$

In Equation (24), C_{fH} is the frictional resistance coefficient for the hull, Re_H is the Reynold's number for the hull, C_{rH} is the residuary resistance coefficient for the hull, L_{tot} and D are the same as identified in the previous section, that is, the total length of the hydrodynamic hull and the maximum diameter of the hydrodynamic hull, and $K2$ is calculated as illustrated in Jackson's work.

Similar calculations as those outlined above are performed for the sail. A value for the appendage resistance of 1/1000 of the product of the total length and diameter of the hull is assumed. These values are then used to calculate the effective power needed to propel the hull, and that needed to propel the sail using Equation (25)

$$P_{eH} = \frac{1}{2}\rho U_{\max}^3 \left(WS_H \left(C_{fH} + \delta C_{fH} + C_{rH}\right)\right) \qquad (25)$$

$$P_{eS} = \frac{1}{2}\rho U_{\max}^3 \left(WS_S \left(C_{fS} + \delta C_{fS} + C_{rS}\right) + R_{app}\right)$$

where P_{eH} is the effective power for the hull, P_{eS} is the effective power for the sail, there is a wetted surface, or WS for the hull and the sail, and R_{app} is the assumed value for the resistance of the appendages. Naturally, the P_{eH} and P_{eS} are then summed to

obtain a first-order estimate of the effective power necessary to propel the submarine at the given speed.

The effective power discipline is constrained by the same minimum displacement value, corresponding to the displacement when the design variables are at the midpoint of their normalized range, that constrains the optimization of the deck area discipline.

3.1.3: Structures

The model used in this work for the structures discipline was adapted from two seminal Society of Naval Architects and Marine Engineers publications [99, 100]. Several new design variables and parameters are introduced in this discipline. They are summarized in Table 10.

Upon introduction to the figures in Table 10, one may immediately recognize that there are mixed units. The units issue is due to the fact that the model adapted from the literature is an empirical model with all calculations based upon the English units whereas the work summarized in this chapter is executed in the Metric units system. Therefore all metric input units were converted to the English system before being applied to the structures discipline model.

The values in Table 10 were used to calculate the buoyancy factor for external framing, defined as the hull weight to displaced water weight ratio, for the assigned structural values, as well as the associated thickness of the endplates, bulkheads, and decks.

Table 10: Structures Discipline Parameter and Design Variable Definitions

Parameter Definitions			
Param.	Definition	Value	
g	Gravity	9.81 m/s2	
$D_{\max}$	Maximum Depth	47.2 m	
σ_y	Yield stress for steel	1.0e5 psi	
ρ_s	Density of steel	7.87e3 kg/m3	
SF_{gi}	Safety factor in general instability	3.75	
Design Variable Definitions			
Variable	Definition	Max	Min
L_f	Frame spacing	0.75 m	1.5 m
t_p	Plate thickness	0.0127 m	0.0191 m
t_f	Flange thickness	0.0127 m	0.0254 m
w_f	Flange width	0.0762 m	0.1143 m
t_w	Web thickness	0.0051 m	0.0111 m
h_w	Web height	0.127 m	0.203 m

$$W_H = 2\rho_s\left(\left(R-\frac{t_p}{2}\right)L_f t_p+\left(R+\frac{h_w}{2}\right)t_w h_w+\left(R+h_w+\frac{t_f}{2}\right)w_f t_f\right) \quad (26)$$

$$W_w = \rho\left(R^2 L_f+2\left(\left(R+\frac{h_w}{2}\right)t_w h_w+\left(R+h_w+\frac{t_f}{2}\right)w_f t_f\right)\right)$$

$$BF = \frac{W_H}{W_w}$$

Equation (24) shows the calculation for W_H, the weight of the hull structure, W_w, the weight of the displaced water, and BF, the buoyancy factor, using variables and parameters previously defined and the radius of the pressure hull, R. The thickness of the end plate is calculated using the pressure, p, at maximum depth and Equation (27), which is a restatement of a calculation for the thickness of hemispherical pressure vessel endcaps taken from the sources mentioned at the beginning of this section.

$$t_{ec} = \frac{(pR)}{2\sigma_y} \tag{27}$$

The thickness of the bulkheads and the decks is assumed to be the same as the thickness of the endcaps, t_{ec}.

The structures discipline is constrained by a limit on five modes of failure. The relationships that define these failure modes—i.e. shell yielding, lobar buckling, general instability, frame yielding, and frame instability—were taken from several sources [91, 98-100]. As with the displacement constraint that works with the other discipline level objective functions, there are no new design variables introduced in the constraints for the structures problem. There are several new parameters however. These new parameters are summarized in Table 11 below.

The full formulation of the constraints defined in Table 11 is summarized well in the sources listed above and will not be discussed in depth here. The interested reader is referred to the listed works for a detailed derivation.

Table 11: Constraint Parameter Definitions

Parameter Definitions		
Param.	Definition	Value
SF_{sy}	Safety factor in shell yielding	1.5
SF_{lb}	Safety factor in lobar buckling	2.25
SF_{fy}	Safety factor in frame yielding	1.5
SF_{fi}	Safety factor in frame instability	1.8
E	Young's modulus	29.7e6 psi
υ_p	Poisson's ratio	0.3

3.1.4: Maneuvering

The model for the maneuvering discipline is adapted from a Naval Postgraduate School thesis [134]. The remainder of this section restates the highlights of Tsamilis' work as they apply directly to the new concepts discussed in this chapter. The theoretical derivation of the model that comprises the maneuvering discipline introduces several new parameters. These new parameters are summarized in Table 12.

Table 12: Maneuvering Discipline Parameter Definition

Param.	Definition	Param.	Definition
$b(x)$	Local beam of the hull	(ϕ, θ, ψ)	Euler angles
C_D	Quadratic drag coef.	U	Constant vehicle speed
δ_r	Rudder deflection	(u, v, w)	Translational velocities
$h(x)$	Local height of the hull	(x, y, z)	Distances along body axes
(I_{xx}, I_{yy}, I_{zz})	Veh. mass mmts of inert.	(X, Y, Z)	Force components
(I_{xy}, I_{yz}, I_{zx})	Cross products of inertia	(x_G, y_G, z_G)	Coordinates of the CG
(K, M, N)	Moment components	(x_B, y_B, z_B)	Coordinates of the CB
m	Vehicle mass	x_{nose}	Fore coordinate of body
(p, q, r)	Rot. vel. componentss	x_{tail}	Aft coordinate of vehicle

The derivation which applies directly to this work begins with a linearization of the simplified equations of motion show in Equation (28).

$$\mathbf{A}\dot{\mathbf{x}} = \mathbf{B}\mathbf{x} + \mathbf{g}(\mathbf{x}) \tag{28}$$

The state vector $\mathbf{x}$, and the state matrices $\mathbf{A}$ and $\mathbf{B}$ are defined as

$$\mathbf{x} = \begin{bmatrix} v \\ r \\ p \\ \phi \end{bmatrix},$$

$$\mathbf{A} = \begin{bmatrix} m - Y_{\dot{v}} & mx_G - Y_{\dot{r}} & -mz_G - Y_{\dot{p}} & 0 \\ mx_G - N_{\dot{v}} & I_{zz} - N_{\dot{r}} & -I_{xz} - N_{\dot{p}} & 0 \\ -mz_G - K_{\dot{v}} & I_{xz} - K_{\dot{r}} & I_{xx} - K_{\dot{p}} & 0 \\ 0 & 0 & 0 & 1 \end{bmatrix},$$

and

$$\mathbf{B} = \begin{bmatrix} Y_v U & Y_r U - mU & Y_p U & 0 \\ N_v U & -mx_G U + N_r U & N_p U & 0 \\ K_v U & mz_G U + K_r U & K_p U & 0 \\ 0 & 0 & 1 & 0 \end{bmatrix}.$$

All nonlinear terms of the equations of motion are contained in the $\mathbf{g}(\mathbf{x})$ term:

$$g_1 = y_G p^2 + y_G r^2 + (W - B)\sin\phi + Y_{\delta_r} U^2 \delta_r - C_{D_y} \int_{x_{tail}}^{x_{nose}} h(x)(v + xr)|v + xr|\, dx,$$

$$g_2 = I_{xy} p^2 + I_{yz} pr + y_G vr + (x_G W - x_B B)\sin\phi + N_{\delta_r} U^2 \delta_r - C_{D_y} \int_{x_{tail}}^{x_{nose}} h(x)(v + xr)|v + x$$

$$g_3 = -I_{xy} pr - I_{yz} r^2 - my_G vp + U^2 K_{prop} + (y_G W - y_B B)\cos\phi - (z_G W - z_B B)\sin\phi,$$

$$g_4 = 0$$

Since this analysis is only interested in the linear approach, the nonlinearities expressed in the $\mathbf{g}(\mathbf{x})$ term must be linearized using a Taylor series expansion about an initial starting point $\mathbf{x}_0$.

$$\mathbf{x}_0 = \begin{bmatrix} v_0 \\ r_0 \\ p_0 \\ \phi_0 \end{bmatrix} = 0$$

The linearized equations of motion can now be written in matrix form

$$\mathbf{A}'\dot{\mathbf{x}} = \mathbf{B}'\mathbf{x} \tag{29}$$

where $\mathbf{A}'$ and $\mathbf{B}'$ are defined as follows:

$$\mathbf{A}' = \mathbf{A},$$

$$\mathbf{B}' = \begin{bmatrix} Y_v U & Y_r U - mU & Y_p U & W - B \\ N_v U & -mx_G U + N_r U & N_p U & x_G W - x_B B \\ K_v U & mz_G U + K_r U & K_p U & -z_G W + z_B B \\ 0 & 0 & 1 & 0 \end{bmatrix}.$$

The next step is to conduct an eigenvalue analysis of the linearized system expressed in Equation (29) in order to assess the dynamic stability of the submarine. The polynomial form of the characteristic equation of the linearized system is given by:

$$A\lambda^4 + B\lambda^3 + C\lambda^2 + D\lambda + E = 0. \tag{30}$$

The coefficients of the characteristic equation are developed using algebra and will not be discussed in this concise summary of the derivation.

Once the coefficients of the characteristic equation are known, the stability of the system can be examined using Routh's criterion, which states that two inequality criteria must be met in order for the vessel to be stable. Since the purpose of the maneuvering discipline is to determine the limiting case of a loss of dynamic stability, the first criterion is set equal to zero, as is shown in Equation (31).

$$BCD - AD_2 - EB^2 = 0. \tag{31}$$

The coefficients of this equation can be rewritten using algebra to be in the form

$$
\begin{aligned}
A &= A_1 z_G{}^2 + A_2 z_G + A_3, \\
B &= B_1 z_G{}^2 + B_2 z_G + B_3, \\
C &= C_1 z_G{}^2 + C_2 z_G + C_3, \\
D &= D_1 z_G + D_2, \\
E &= E_1 z_G + E_2.
\end{aligned}
\tag{32}
$$

For a complete definition of the coefficients, $A_1, A_2, A_3, B_1, B_2, B_3, C_1, C_2, C_3, D_1, D_2, E_1$, and E_2, the author refers the interested reader to pages 14-16 in the Tsamilis thesis. The lines of Equation (32) can be substituted into Equation (31), and the result can be rewritten as follows,

$$
F_5 z_G^5 + F_4 z_G^4 + F_3 z_G^3 + F_2 z_G^2 + F_1 z_G + F_0 = 0, \tag{33}
$$

where F_0 through F_5 are functions of the coefficients A_1 through E_1. Using Equation (33), and several values of the longitudinal location of the center of gravity, x_G, a corresponding value for the vertical center of gravity, z_G, can be determined. The objective of the maneuvering discipline in this work is to maximize the number of these x_G values that produce a stable, that is positive, value for z_G subject to a constraint on the displacement.

3.2: Creation of the System-Level Objective Function

SEER is a commercially available cost estimation software package that is capable of producing a sophisticated approximation of the financial burden of fabricating a particular product. The version used for this research is SEER-DFM, taking its name from the popular industry concept of “design for manufacturing”. SEER-DFM

allows for the modeling of the manufacturing costs of a product, in this case a submarine pressure hull. In order to use SEER, the following steps are necessary:

1. Develop the Work Breakdown Structure (WBS) of the product to be developed;
2. Define all the types of production operations that are needed;
3. Define the geometry of each component;
4. Gather data about the production operations; and
5. Input the data in the code (can be accomplished remotely).

As is mentioned in the final step above, the SEER products enable remote operation via a text-based command file. This fact is instrumental in incorporating the existing code into the larger MDO framework used in this research. The costs for the components of the product are determined in the lower levels of the WBS and are basically divided into:

1. Labor costs/unit – calculated using the time needed to do the work and the hourly labor cost. Includes the setup costs for the machines needed to do the work;
2. Material costs/unit – calculated using the material selected for the components;
3. Tooling costs/unit – calculated using the machines/tools needed for the components.

Based on these costs, the SEER-DFM code determines the total cost/unit, using a bottom-up strategy, adding all the costs until the top level of the WBS is reached.

For this particular work, the five steps necessary to use the SEER code are all accomplished through the use of a MATLAB program. This information is then written and saved to a text-based command file, the MATLAB code calls the SEER code and uses the command file for input. The SEER code processes the information in the command file and outputs a file with results which are read by the MATLAB code and integrated into the MDO routine. The details of these operations are discussed below.

As is illustrated in the WBS for the submarine pressure hull in the "System-Level Optimization" box on the left side of Figure 4 of this chapter, the first step in the process is to fabricate the hull itself. Industrial knowledge [89] indicates that submarines are constructed in a series of modules or hoops, which are then joined together. In order to accomplish this, the pressure hull must be further broken down from the $L_{ph,a}$, $L_{ph,pmb}$, and $L_{ph,f}$ measurements, which were calculated in the deck area discipline, into hoops. These hoops must then be formed and populated with decks and a limited outfit before they are joined together to form the pressure hull itself.

The process of breaking the hull down further into hoops is accomplished in two steps. First, the pressure hull is segmented using bulkheads. The aftmost section is assumed to be 11.583 meters long and the foremost section to be 9.144 m long—values which were brought from the literature [91]—and the remaining length of the hull is considered to be a uniform cylinder interrupted only periodically by kingposts for

stiffness. These three sections are then split up further into actual hoops in the following manner.

In the affordability discipline code, the dimensions of each hoop are determined automatically. The standard hoop width is set to four times the frame spacing. This hoop width is then used to divide the three lengths of the pressure hull into the number of hoops that will make up each of these sections. The result of this breakdown is a certain number of standard hoops, and one "leftover" hoop of some nonstandard width, for each section. The diameter of the pressure hull is then used to determine the length of the piece of material that will be formed into these hoops. The thickness of the plate is a design variable, and therefore it is easily passed to the affordability discipline. Finally, since the hoop widths are not uniform along the length of the hull, an array of all hoop widths is generated to be used later in the code.

Creating values that define the dimensions of the endcaps is not as involved as creating the dimensions of the hoops. Since each endcap is modeled as a hemisphere, the radii of these hemispheres serve as the main dimension necessary to define their construction. The fabrication process for the endcaps is assumed to include the dual-axis bending of four plates into the shape of ¼ of each hemispherical endcap. The dimensions of these plates are easily obtained from the geometry of a hemisphere, and therefore the input dimensions for the code are also readily available. The thickness of the endcap was calculated in the structures discipline and is passed to the affordability discipline accordingly.

Once the dimensions for the hoops and endcaps have been created and stored, the next step is to populate the matrix which contains the dimensions for the decks of the vessel. The necessary dimensions of the decks have already been calculated in the deck area discipline. These values are passed to the affordability code at this stage. It is during this stage of the affordability code that the bulkheads are also manufactured.

The dimensions of the material that makes up each section of the pressure hull, are not the only inputs into the SEER-DFM program which must be entered. There are also several additional inputs, most of which are specified in the input data file for the SEER code, that provide specifics to the program concerning the manufacturing process being modeled. These additional inputs include such things as material used (low carbon steel), the material yield for each part (varies), the type of procedure being performed (plate roll bending on several), and specific information about the details of the procedure (the form diameter and number of passes for the plate roll bending procedure).

After every major piece of the pressure hull has been fabricated, it must then be assembled into the complete hull. In order to accomplish this task, the affordability discipline counts the total number of parts that must be assembled and measures the total length of the weld that must be run in order to complete the pressure hull. A general weight category is assigned to each part type, i.e. hoops, decks, endcaps, bulkheads, structure for each of them, etc., along with a general distance traveled.

All of this manufacturing data is saved by MATLAB into one matrix and passed to a text-based file. MATLAB then calls the SEER-DFM package to take the data and

process it as a command file input. Once SEER-DFM has completed its simulation, it sends its output file to be read by MATLAB. The output file contains per unit cost information for each level of the WBS, as well as summary for each type of cost, i.e. labor, material, and tooling, and total cost for the entire manufacturing process.

3.3: Benchmarking and Single Discipline Optimization Results

Before the single discipline optimization results are discussed, a note must be made regarding the normalization of the design variable and objective function values used in this work. The design variables have been normalized between 0.5 and 1.5 using their maximum and minimum values. The objective function values are multiplied by 100, a measure shown through experience with the MDO algorithm to improve performance, and then normalized using the objective function value given when all design variables are at the midpoint of their range. Lastly, the displacement constraint was set to the value that results when all design variables are at their midpoint. The objective functions are defined as in Equation (34).

$$\begin{aligned}
&\max\ f_1(\mathbf{x}) = \text{ Deck Area} \\
&\min\ f_2(\mathbf{x}) = \text{ Effective Power} \\
&\min\ f_3(\mathbf{x}) = \text{ Structures} \\
&\max\ f_4(\mathbf{x}) = \text{ Maneuvering} \\
&\min\ f_5(\mathbf{x}) = \text{Affordability}
\end{aligned} \tag{34}$$

In Equation (34), the subscripts "$_1$" through "$_5$" denote the different objective functions that were optimized in this section. Single discipline optimization of the discipline level and system level objective functions was completed using a straight Monte Carlo simulation, coupled with engineering logic and experience. The author

chose a Monte Carlo over other non-gradient-based methods, such as a Particle Swarm Optimizer, or Genetic Algorithm, since the disciplines were relatively inexpensive in terms of computational time. In addition, based on previous experience, a PSO algorithm is not necessarily less computationally expensive, nor does it produce appreciable improvement in the results, when compared to a Monte Carlo solution. The Monte Carlo simulation was allowed to progress until 2500 points were found that satisfied all constraints. Table 13 lists the minimum values for each discipline that were found during the exploration of these five objective functions using the Monte Carlo simulation.

In addition to using the Monte Carlo results as a method of finding the single discipline optimization results—in actuality, in keeping with the original motivation for using a Monte Carlo algorithm—the results were also used to create plots relating affordability to each of the other discipline level objective function results. These plots are discussed later in the chapter.

3.4: Background for Multidisciplinary Design Optimization (MDO)

The basic framework for the MDO analyses conducted in this phase of the research was outlined in detail in section 2.3 of this dissertation.

3.5: Multidiscipline Optimization and Results

Once the ranges for each design variable were selected, the values that correspond to a normalized value of 1.0 were considered to comprise the nominal design and the starting point for the optimization.

The objective functions involved in the multidiscipline optimization are defined similarly as those involved in the single discipline optimization. The only change is that the affordability objective function is no longer $f_5(\mathbf{x})$, but is now the top-level objective function, or $f_T(\mathbf{x})$, where the subscript "$_T$" denotes "top". Table 13 compares the MDO results to those from the single discipline optimizations as discussed previously.

It can be seen from Table 13 that, although the MDO results posted significant losses when compared to the benchmark single discipline optimization results, it indeed improved in every single one of the disciplines compared to the affordability-based single discipline results.

Table 13: Comparison of MDO Results

Value	Starting Point	Deck Area	Effective Power	Structures	Maneuvering	Cost	MDO
$x(1)$	1.0	1.5	0.52	1.0	1.5	1.40	1.50
$x(2)$	1.0	1.5	1.3	1.2	1.2	0.86	0.75
$x(3)$	1.0	1.5	1.1	1.0	0.56	0.81	1.02
$x(4)$	1.0	1.5	0.89	1.0	1.51	1.37	1.50
$x(5)$	1.0	1.0	1.0	0.96	1.0	0.92	1.37
$x(6)$	1.0	1.0	1.0	0.53	1.0	1.04	0.74
$x(7)$	1.0	1.0	1.0	0.5	1.0	1.32	1.12
$x(8)$	1.0	1.0	1.0	0.5	1.0	0.83	1.49
$x(9)$	1.0	1.0	1.0	0.5	1.0	1.07	0.99
$x(10)$	1.0	1.0	1.0	0.5	1.0	1.42	0.68
$f_1(\mathbf{x})$	100	39.9	104	84.4	81.4	133	131.12
$f_2(\mathbf{x})$	100	162	99.0	115	129	105	103.03
$f_3(\mathbf{x})$	100	80.3	90.8	68.5	89.5	115	101.63
$f_4(\mathbf{x})$	100	100	130	108	72.2	81.3	81.27
$f_T(\mathbf{x})$	100	256	128	133	139	80.4	72.56

Table 14 highlights the percent change associated with each of these differences. Italicized and bolded values indicate a worsening of the performance criteria.

Table 14: Percent Improvement of MDO values

Value	% change (from best in discipline)	% change (from starting point)	% change (from best-cost)
$f_1(\mathbf{x})$	***229***	***31.1***	1.15
$f_2(\mathbf{x})$	***4.07***	***3.03***	1.96
$f_3(\mathbf{x})$	***48.4***	***1.63***	11.5
$f_4(\mathbf{x})$	***12.6***	18.7	0.00
$f_5(\mathbf{x})$	9.8	27.4	9.8

To summarize the contents of Table 14 in practical terms, the MDO submarine will be 229% smaller than the submarine designed just for the maximization of deck area. It will require 4% more power to propel it through the water at a given speed than the hull designed with just this parameter as a goal. Its structure will be 48% less efficient than the most structurally efficient design, and it will be 13% less dynamically stable than the most dynamically stable design. Perhaps more telling is the fact that the MDO submarine will cost 9.8% less than the least expensive design if just cost is taken into consideration and nearly 30% less than the starting design.

In addition to a tabular representation of the results, it is helpful to see where the MDO design falls in the design space using graphical means. Figures 5 through 9 highlight the location of the MDO point, and the path the algorithm followed to get from the starting point to that MDO-optimum point, compared to the points determined by the Monte Carlo simulation using plots of each discipline objective

function versus the affordability objective function. All results in these figures are unitless and the affordability is always plotted horizontally.

From the normalized deck area vs. affordability plot, it is obvious that the MDO algorithm has arrived at a very good point. Not only is the point at a minimum cost, as will be seen throughout the remaining three plots as well, but it is also at a comparatively high deck area, i.e. the elbow in the front at approximately 80 on the affordability axis was avoided. It is also worth noting that the algorithm chose the correct direction to progress from this elbow, that is to the higher deck area, but lower cost, point. Finally, it can be seen from Figure 5 that the MDO algorithm did not simply select the lowest cost design. It explored these points, but pulled itself back due to the interaction between the top-level and the discipline-level objective functions. Similar conclusions can be drawn when examining the points in Figures 6, 7, and 8. The MDO solution identified the configuration with the lowest system level objective while at the same time improving each discipline objective to the largest possible extent.

In addition to those contained in Figures 5 through 8, one additional summary plot is presented in Figure 9. The purpose of this plot is to show how the MDO algorithm performed compared to a more traditional multi-objective type of formulation. It can be seen from this figure that the MDO algorithm out-performed this simple weighted sum (all weights are equal) approach.

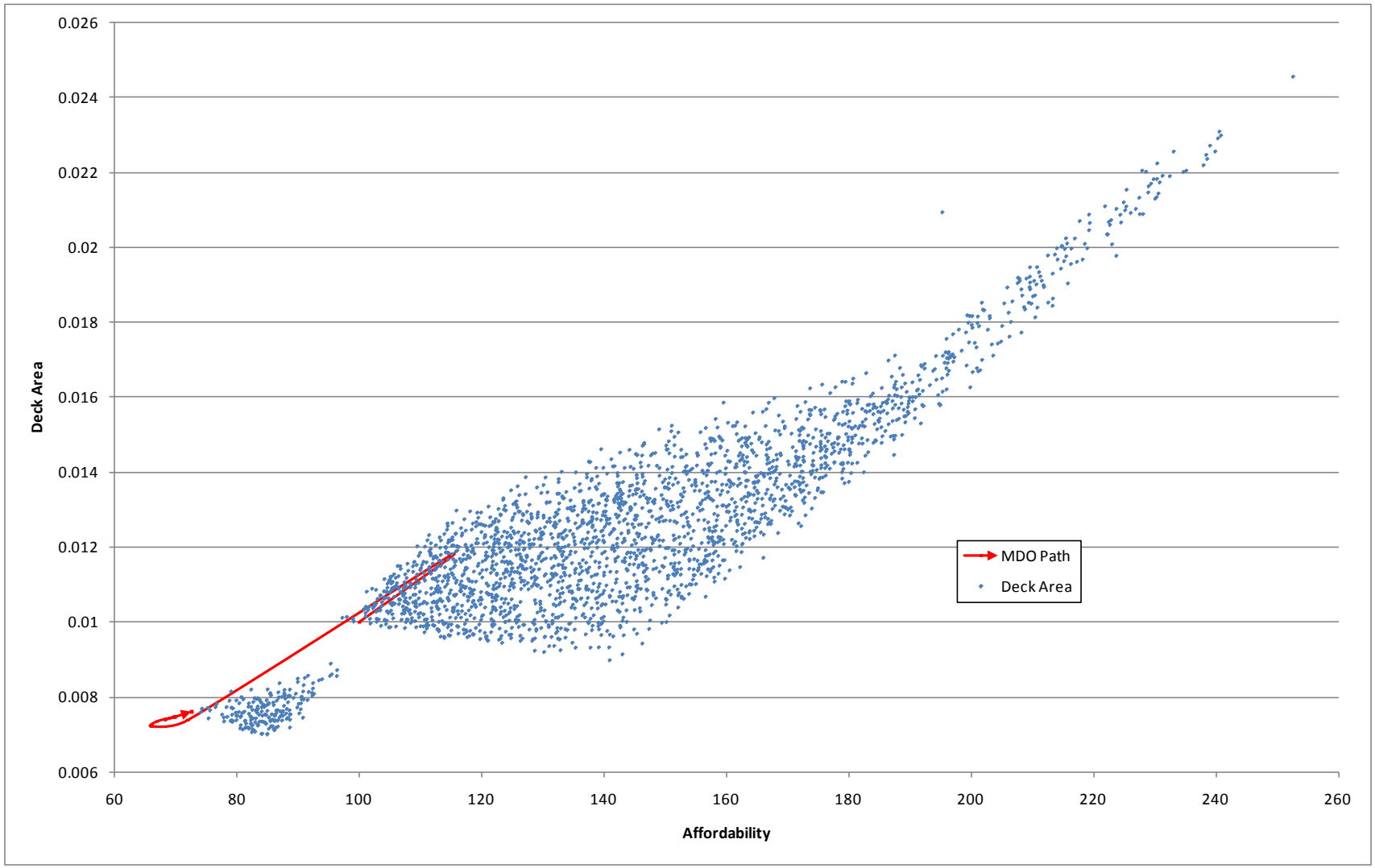

Figure 5: Normalized Deck Area vs. Affordability

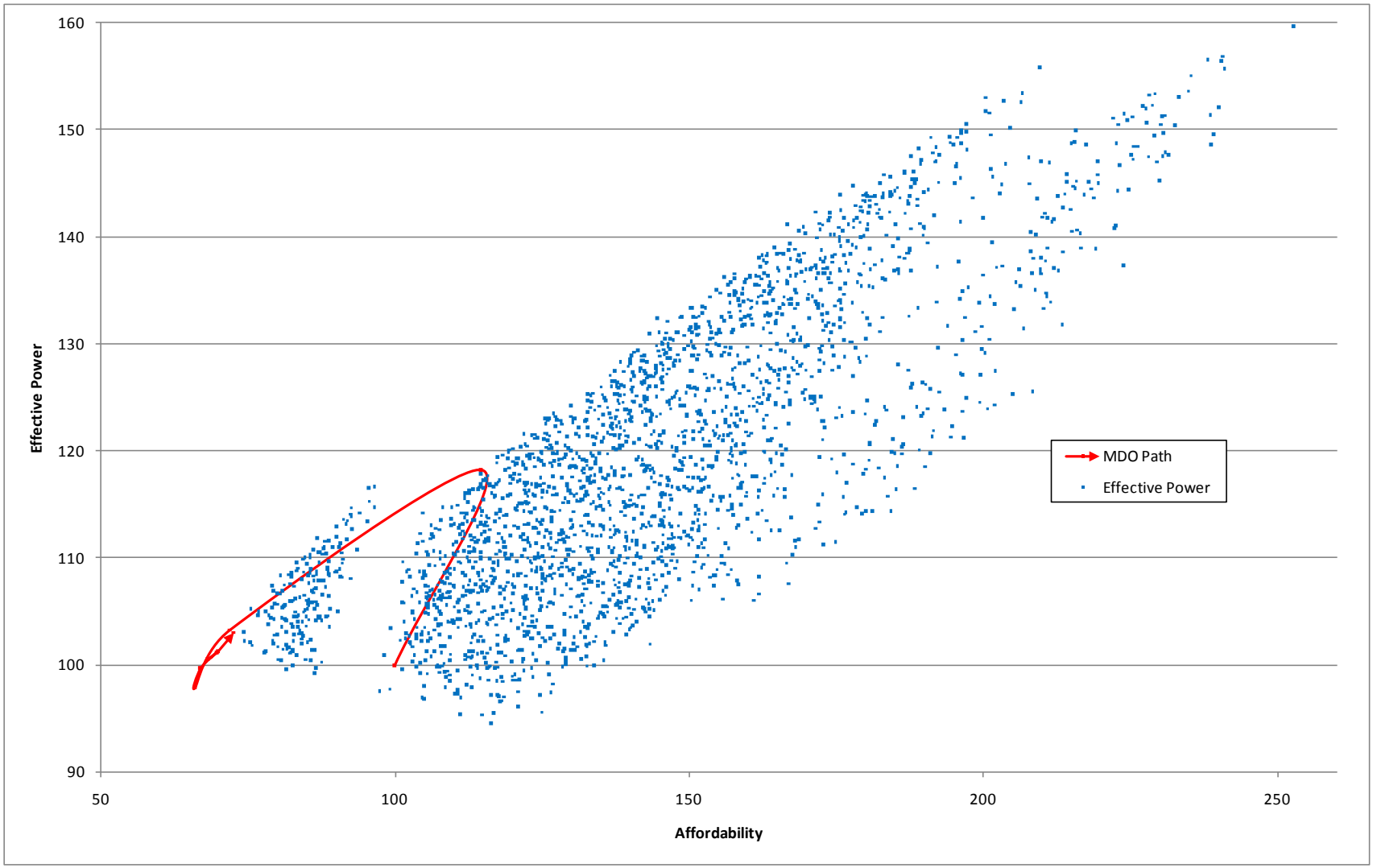

Figure 6: Normalized Effective Power vs. Affordability

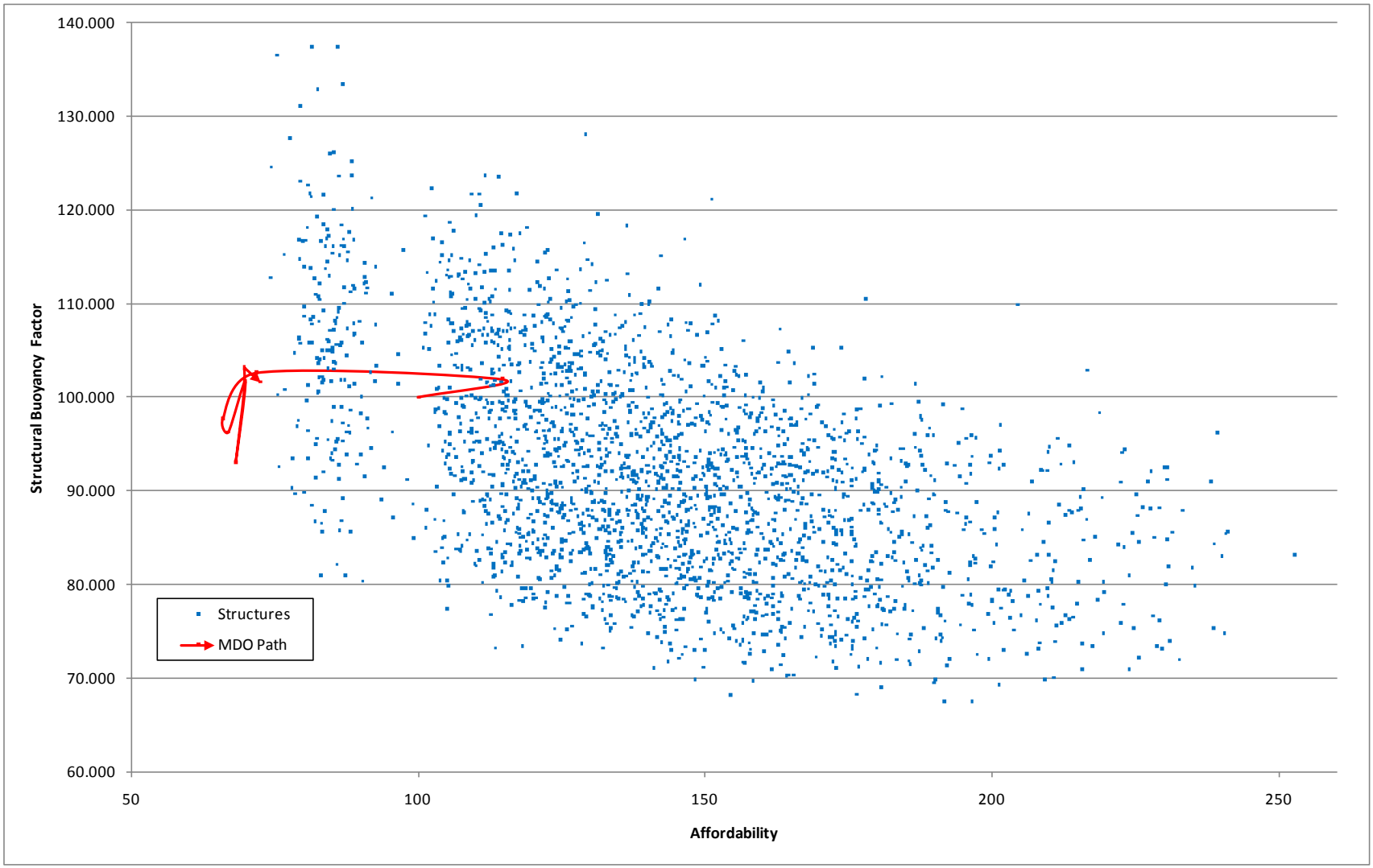

Figure 7: Normalized Structural Buoyancy Factor vs. Affordability

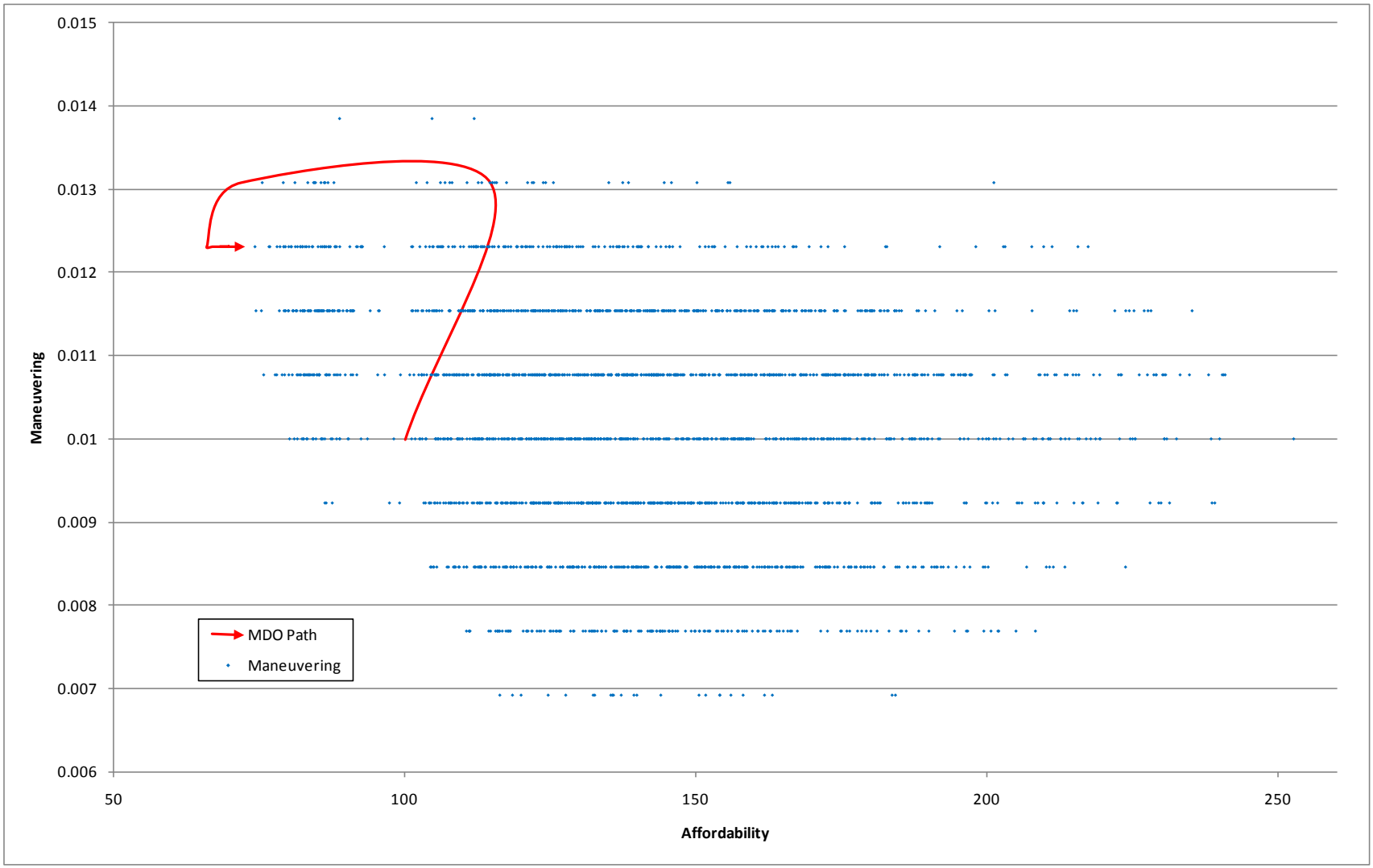

Figure 8: Normalized Dynamic Stability vs. Affordability

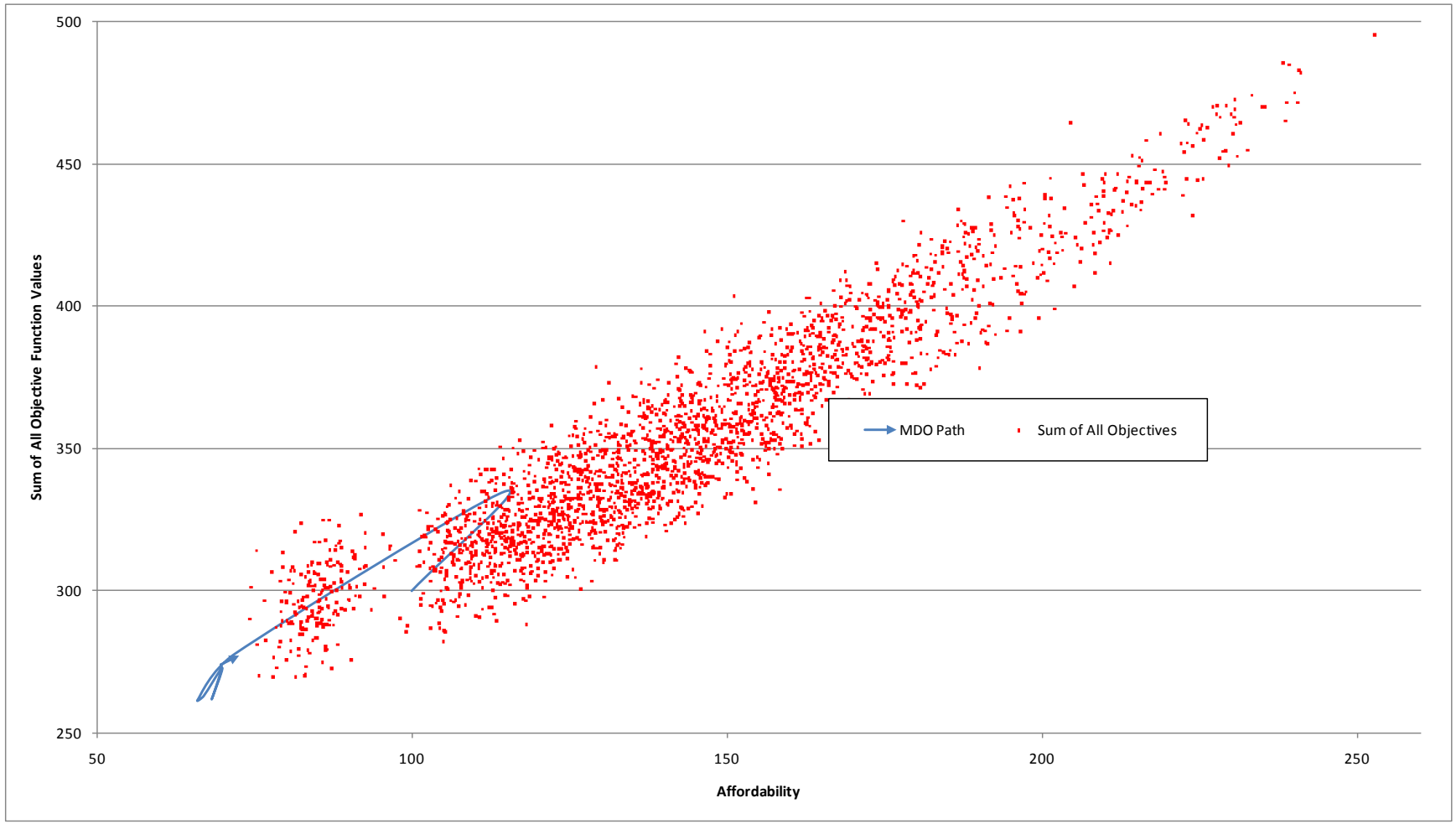

Figure 9: Sum of Top- and Discipline-level Objective Function Values vs. Affordability

CHAPTER 4:
AN IMPROVED COST ESTIMATION METHODOLOGY FOR THE DESIGN OF COMPLEX ENGINEERING SYSTEMS

The main objective of this chapter is the creation of a higher fidelity cost model for the manufacture of a complex engineering system. Secondary objectives include: 1.) the application of methodologies from datamining in order to learn more about a set of cost data and 2.) an investigation of various regression-type methods that allows the lessons from the datamining analysis to be used to improve the predictive capability of a cost estimation model. The use of more sophisticated methods will aid in gaining insight into novel economic drivers in a cost data set derived from physical parameters and historical cost information and in developing a meaningful relationship between predictive (physical parameters) and response (cost) variables. Figure 10 outlines the approach taken in this research to meet these objectives. The steps in Figure 10 are outlined in depth in the next section of this chapter.

The method covered in this chapter introduces principal component analysis (PCA) into the modeling of cost in the design of a complex engineering system. Additionally, the outputs from PCA are used to improve a sophisticated regression model based on an adaptive Kriging method. The result is a cost estimation methodology, the "Method of Improved Cost Estimation for the Design of Complex

Engineering Systems" or MISERLY, which has a much higher fidelity and increased predictive capability when compared to methods currently in use. The next section of this chapter will cover the steps of MISERLY. This section will be followed by three which provide background and theoretical foundation for the algorithms and methods used by the MISERLY process. The background and theoretical foundation for the process will be followed by a section framing the case study used to apply the MISERLY process, and the chapter will close with results, closure, and acknowledgements sections.

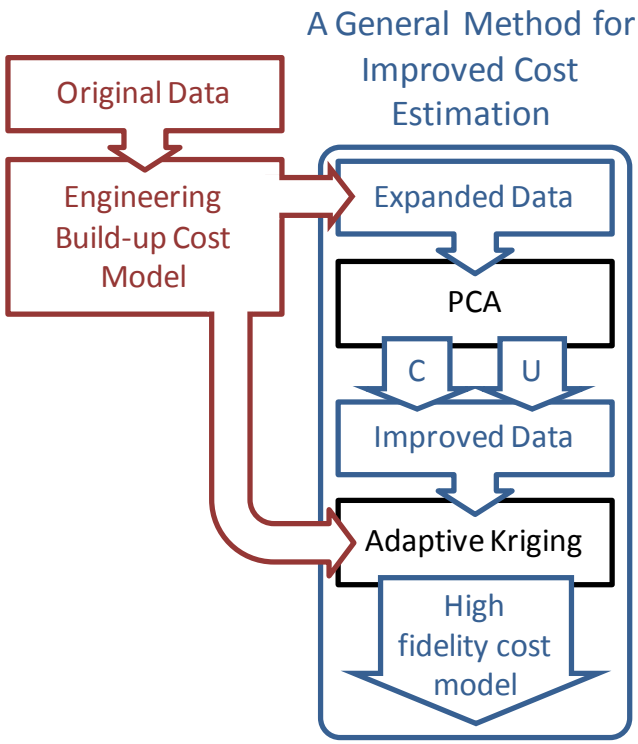

Figure 10. A graphical representation of the steps associated with MISERLY

4.1: MISERLY: Step-by-Step

Figure 10 above provides a graphical representation of the steps taken by MISERLY in the creation of a higher fidelity cost model. These steps are described in further detail in this section.

a. **Original Data:** The original data set is made up of physical parameters and historical cost records that are gathered for a given complex engineering system. Examples of a complex engineering system include, but are not limited to: ships, aircraft, spacecraft, advanced ground vehicles, submarines, offshore oil and gas platforms and other energy production facilities, and large land-based structures subjected to a diverse set of dynamic loads. Ideally, several copies and/or versions of this complex engineering system have already been constructed. The original data set consists of the X (physical parameter) and Y (cost parameter) matrices that should be arranged as shown in Equation (35).

$$\mathrm{X}=\begin{pmatrix} x_{11} & \cdots & x_{1p} \\ \vdots & \ddots & \vdots \\ x_{n1} & \cdots & x_{np} \end{pmatrix};\mathrm{Y}=\begin{pmatrix} y_{11} & \cdots & y_{1q} \\ \vdots & \ddots & \vdots \\ y_{n1} & \cdots & y_{nq} \end{pmatrix} \tag{35}$$

In these relationships, the X matrix consists of the $_{p}$ physical parameters of the $_{n}$ different designs upon which data was gathered. Similarly, the Y matrix consists of the $_{q}$ historical cost parameters which were gathered for each of the $_{n}$ designs.

b. **Engineering Build-up Model:** An interim engineering build-up cost model is created from this original data set. This engineering build-up model must be

formulated from a combination of sound engineering judgment and experience in the particular domain of the system in question. It also must be capable of recreating the values contained the original data set.

c. **Expanded Data:** An expanded data set is generated using this engineering build-up cost model. The expanded data set should be considerably larger, by at least an order of magnitude, than the original data set.

$$\mathrm{X_e} = \begin{pmatrix} x_{11} & \cdots & x_{1p} \\ \vdots & \ddots & \vdots \\ x_{m1} & \cdots & x_{mp} \end{pmatrix}; \mathrm{Y_e} = \begin{pmatrix} y_{11} & \cdots & y_{1q} \\ \vdots & \ddots & \vdots \\ y_{m1} & \cdots & y_{mq} \end{pmatrix} \text{where } m >> n \tag{36}$$

Here, $\mathrm{X_e}$ is the expanded matrix of physical parameters and $\mathrm{Y_e}$ is the matrix of expanded cost parameters. The physical parameters chosen to populate the expanded data set should represent a uniform distribution throughout the feasible design space. The expanded data set should include the original data set.

d. **PCA and Component-Influenced Parameters:** The expanded data set of physical parameters $\mathrm{X_e}$ is then analyzed using principal component analysis (PCA). Two outputs from the PCA, the C array and U matrix, are used to identify which of the original p physical parameters, and which of the principal components (PCs) that are output from PCA, account for the greatest amount of variation in the design. Each high-variation PC is composed of values that are treated as weights and are denoted by the variable w. These weights are used to create one component-influenced parameter, or a weighted sum of the original design

variables, for each PC. Component-influenced parameters are denoted by the variable t. When the PCA step is finished, there will be r physical parameters and s PCs identified as high-variation. A more thorough discussion of the concept of component-influenced parameters is undertaken in the next section.

e. **Improved Data:** A set of predictor variables is developed using the r high-variation physical parameters from the original set and s component-influenced parameters which were calculated using a weighted sum of the physical parameters in the original data set. Equation (37) shows the structure of this improved data set, X^*.

$$\mathrm{X}^* = \begin{pmatrix} x_{11} & \cdots & x_{1r} & t_{11} & \cdots & t_{1s} \\ \vdots & \ddots & \vdots & \vdots & \ddots & \vdots \\ x_{n1} & \cdots & x_{nr} & t_{n1} & \cdots & t_{ns} \end{pmatrix} \tag{37}$$

f. **Adaptive Kriging:** This new set of predictor variables is regressed, using the sophisticated adaptive Kriging method, on the historical cost values (response variables), or the Y matrix from Equation (35). The adaptive Kriging method engages the engineering build-up model in order to create additional data in areas of the design space that are covered in a deficient manner by the improved data set.

Once the adaptive Kriging model has identified and corrected problem areas in the model, the high fidelity cost model is ready to be employed in predicting cost information given a new set of physical parameters. Now that the steps of MISERLY

have been outlined in detail, the next three sections will build the theoretical foundation upon which the process was built.

4.2: Principal Component Analysis

PCA is a method for reducing the dimensionality of a set of data while still retaining most of the variation in the data set. This reduction in dimensionality allows a large, complex data set which relates thousands, or even tens of thousands, of variables, to be expressed by a new set, usually much smaller in number, of variables. In most cases, these new variables are linear combinations of the original variables, and identify directions in the data along which variation is the maximum [226]. A specific relationship between these individual components is not defined in PCA. The mechanics of PCA are summarized in [228], and are presented here for completeness.

There are several methods for performing principal component analysis, the most popular being dubbed R-, Q-, and N-analysis. The most general method of these is N-analysis, also known as singular value decomposition (SVD). N-analysis was chosen for this work due to this generality, as well as the method's simplicity. Although N-analysis requires familiarity with a new algorithm (SVD), it is a single-stage procedure that contrasts with the two-stage R- and Q-analyses.

The fundamental identity of SVD:

$$\mathrm{X}=\mathrm{Z}\mathrm{L}^{\frac{1}{2}}\mathrm{U}' \tag{38}$$

decomposes the centered and scaled $n\times p$ data matrix X into the $p\times p$ U and $\mathrm{L}^{\frac{1}{2}}$ matrices and the $n\times p$ Z matrix. The U matrix represents the characteristic vectors of

$X'X$, Z the characteristic vectors of XX', and $L^{\frac{1}{2}}$ is a diagonal matrix that is function of their characteristic roots.

For this work, the matrices of interest from SVD are the U and $L^{\frac{1}{2}}$ matrices. The diagonal elements of the $L^{\frac{1}{2}}$ matrix were converted into an array and then modified in order to facilitate interpretation using the following relationship:

$$C_i = \left(\frac{L_{ij}^{\frac{1}{2}}}{\sqrt{n-1}} \right)^2 \quad \text{where } i = j = 1,2,\ldots,p \tag{39}$$

By performing this modification, the C array, like its source $L^{\frac{1}{2}}$ matrix, contains a ranking of the amount of variance accounted for by each of the p PCs. The benefit of the modification is that the sum of the values in the C array now equals p. This is powerful because it relates each of the PCs to the physical parameters. If one of the PCs has a value in the C array that is greater than one, it accounts for greater variation than any of the design variables.

The U matrix is not modified in this work. The columns of the U matrix correspond to each PC while its rows correspond to each of the original physical parameters. Therefore each PC contains weights for each of the original predictor variables. These weights can also be interpreted as an indication of the importance of each of these predictor variables in each of the PCs.

When the high-variability PCs are engaged in creating the component-influenced parameters, each of their values is treated as a weight for the corresponding physical

parameter. The component-influenced parameters are then a sum of these weighted physical parameters:

$$t_{\mathrm{jk}} = \begin{Bmatrix} w_{1k} \\ \vdots \\ w_{pk} \end{Bmatrix} \times \begin{Bmatrix} x_{j1} & \cdots & x_{jp} \end{Bmatrix} \text{ where j = 1,2,…,n and k = 1,2,…,s} \tag{40}$$

In this relationship, $_j$ refers to the number of designs in the original data set, and $_k$ to the number of principal components determined to be high variation PCs. This analysis follows that contained in section 12.3.1 of [228] except that Adaptive Statistical Kriging, which is covered in the next two sections, takes the place of the regression methods, i.e. latent root regression, partial least-squares regression and maximum redundancy, used in the reference

4.3: Statistical Kriging Models

The Kriging model is based on treating $\mathrm{Z}(\tilde{x})$, the difference between the actual performance variable $\mathrm{y}(\tilde{x})$ and a regression model prediction $\hat{\mathrm{F}}(\tilde{x})$, as a stochastic process:

$$\mathrm{y}(\tilde{x}) = \hat{\mathrm{F}}(\tilde{x}) + \mathrm{Z}(\tilde{x}) \tag{41}$$

Where $\tilde{x}$ is the d-dimensional vector of the variables that defines the point where the performance variable is evaluated, and “d” is the number of variables. A regression model which is a linear combination of “m” selected functions $\mathrm{f}(\tilde{x})$ is used here:

$$\hat{\mathrm{F}}\left(\tilde{x}\right)=\beta_1 \mathrm{f}_1\left(\tilde{x}\right)+\ldots+\beta_m \mathrm{f}_m\left(\tilde{x}\right)=\mathrm{f}^{\mathrm{T}}\left(\tilde{x}\right) \tag{42}$$

where $\beta^{\mathrm{T}}=\left\{\beta_1,\beta_1,\ldots\beta_m\right\}$ are regression parameters. $\mathrm{Z}\left(\tilde{x}\right)$ is considered as a normal process with zero mean and a covariance that can be expressed as:

$$\mathrm{cov}\left(\mathrm{Z}\left(\tilde{x}_i\right),\mathrm{Z}\left(\tilde{x}_j\right),\right)=\sigma^2\mathrm{R}\left(\tilde{x}_i,\tilde{x}_j\right) \tag{43}$$

where σ^2 is the process variance and $\mathrm{R}\left(\tilde{x}_i,\tilde{x}_j\right)$ is the spatial correlation function. The equation used for the spatial correlation function is a Gaussian spatial correlation function:

$$\mathrm{R}\left(\tilde{x}_i,\tilde{x}_j\right)=\prod_{k=1}^{d}\exp\left(-\theta_k\left(\tilde{x}_{i,k}-\tilde{x}_{j,k}\right)^2\right) \tag{44}$$

and it indicates a process with infinitely differentiable paths in the mean square sense. θ_k is the correlation parameter that corresponds to the kth component of the d-dimensional vector of the random variables $\tilde{x}$, i.e. k = 1,2,…,d; and θ represents the vector of the θ_k parameters. For a set $\tilde{x}_s$ comprised of "n" number of sample points

$$\begin{aligned}&\tilde{x}_{si}\\&\tilde{x}_s^T=\left\{\tilde{x}_{s1},\tilde{x}_{s1},\ldots,\tilde{x}_{sn}\right\}\end{aligned}\quad \text{where i = 1,2,…,n} \tag{45}$$

The corresponding performance variable $\tilde{y}_s$ is considered known and its values are defined as:

$$\tilde{y}_s^{\mathrm{T}}=\left\{y\left(\tilde{x}_{s1}\right),y\left(\tilde{x}_{s2}\right),\ldots,y\left(\tilde{x}_{sn}\right)\right\} \tag{46}$$

The vector of correlations between the sample points $\tilde{x}_s$ and the evaluation point $\tilde{x}$ can be expressed as:

$$\tilde{r}^{\mathrm{T}}\left(\tilde{x}\right)=\left\{\mathrm{R}\left(\tilde{x},\tilde{x}_{s1}\right),\mathrm{R}\left(\tilde{x},\tilde{x}_{s2}\right),...,\mathrm{R}\left(\tilde{x},\tilde{x}_{sn}\right)\right\} \tag{47}$$

The correlation matrix [R] is also defined among all the sample points:

$$\left[\mathrm{R}\right]=\left[\mathrm{R}\left(\tilde{\mathrm{x}}_{\mathrm{si}},\tilde{\mathrm{x}}_{\mathrm{sj}}\right)\right]_{nxn} \tag{48}$$

The spatial correlation function in Equations (47) and (48) has been defined by Equation (44). In the Kriging method the value of the performance function evaluated by the metamodel at the evaluation point $\tilde{\mathrm{x}}$ is treated as a random variable. The computation of β and $\mathrm{Z}\left(\tilde{\mathrm{x}}\right)$ in Equations (41) and (42) is based on minimizing the mean square error (MSE) in the response:

$$\mathrm{MSE}\left[\hat{y}\left(\tilde{\mathrm{x}}\right)\right]=\mathrm{E}\left[\hat{y}\left(\tilde{\mathrm{x}}\right)-y\left(\tilde{\mathrm{x}}\right)\right]^{2} \tag{49}$$

subjected to the unbiased constraint:

$$\mathrm{E}\left[\hat{y}\left(\tilde{\mathrm{x}}\right)\right]=\mathrm{E}\left[y\left(\tilde{\mathrm{x}}\right)\right] \tag{50}$$

The matrix R and the parameters β and σ^{2} depend on θ. Once θ is determined, the regression parameter β and the variance σ^{2} can be computed as:

$$\hat{\beta}=\left(\tilde{F}^{\mathrm{T}}R^{-1}\tilde{F}\right)^{-1}\tilde{F}^{\mathrm{T}}R^{-1}\tilde{y}_{s} \tag{51}$$

$$\hat{\sigma}^{2}=\frac{1}{n}\left(\tilde{y}_{s}-\tilde{F}\hat{\beta}\right)^{\mathrm{T}}R^{-1}\left(\tilde{y}_{s}-\tilde{F}\hat{\beta}\right) \tag{52}$$

where the matrix $\tilde{F}$ is defined as $\tilde{F}=\left[\mathrm{f}_{\mathrm{j}}\left(\tilde{x}_{si}\right)\right]_{nxm}$. The value for the response of interest is computed as:

$$\hat{y}\left(\tilde{\mathrm{x}}\right)=\mathrm{f}\left(\tilde{\mathrm{x}}\right)^{\mathrm{T}}\hat{\beta}+\tilde{r}^{\mathrm{T}}\left(\tilde{x}\right)R^{-1}\left(\tilde{y}_{s}-\tilde{F}\hat{\beta}\right) \tag{53}$$

In the traditional Kriging method, the optimal value of θ is computed as the maximum likelihood estimator of the likelihood function:

$$L\left(\theta,\beta,\sigma^2\left|\tilde{y}_s\right.\right)=p\left(\tilde{y}_s\left|\theta,\beta,\sigma^2\right.\right) \tag{54}$$

$$p\left(\tilde{y}_s\left|\theta,\beta,\sigma^2\right.\right)=\frac{1}{\sqrt{2\pi\sigma^2\left(\det\left(\mathrm{R}\right)\right)}}\exp\left(-\frac{\left(\tilde{y}_s-\tilde{F}\hat{\beta}\right)^{\mathrm{T}}R^{-1}\left(\tilde{y}_s-\tilde{F}\hat{\beta}\right)}{2\sigma^2}\right)$$

where $p\left(\tilde{y}_s\left|\theta,\beta,\sigma^2\right.\right)$ is the multivariate normal distribution for the "n" observations $\tilde{y}_s$ given the model parameters θ, β, and σ^2. In the ordinary Kriging method this is accomplished by minimizing the product $\left[\left(\det\left(\mathrm{R}\right)\right)^{1/n}\left(\sigma^2\right)\right]$ while neglecting the variations in the model parameters θ, β, and σ^2.

4.4: Adaptive Kriging Models

This section presents the development of an adaptive metamodel generation code. The code determines a specified number of adaptive sample points that are generated from an initial metamodel in regions of the variable domain defined according to the specified target result of the modeled function.

As mentioned above, a metamodel is a technique used to predict the response of a process and intends to reduce the number of expensive numerical simulations, and hence, reduce the computational cost. In this work, it has been applied as a sophisticated interpolation function with the purpose of increasing the predictive capability of a parametric cost estimation model. The metamodel predictor of a process defined by a relation $Y\left(X\right)$, where $X=\left\{X_1,X_2,...X_m\right\}$ and

$Y = \{Y_1(X), Y_2(X), \ldots Y_n(X)\}$ is constructed based on experiments, which consists in a series of sample points X and their correspondent response Y.

The adaptive metamodel intends to generate more accurate responses Y of the modeled function $Y(X)$ when the responses Y are inside or in the vicinity of a desired target response T. The target T can be defined either as a single value or as a response region with minimum and maximum values, $\{T_{\min}, T_{\max}\}$, as shown in Figure 11. Hence, the adaptive metamodel generated in these regions with response inside or in the vicinity of T will be more accurate due to the presence of a larger number of SP's conveniently distributed than the metamodel created by sampling all SP's with random generators.

The adaptive metamodel is generated from a previous conventional metamodel. The criteria for determining the new adaptive SP's is to reduce the mean square error (MSE) of the metamodel for responses Y inside the target response region T. It is also desirable to consider regions in the vicinity of T, such that responses Y that are outside T due to errors in the initial metamodel evaluation can also be improved.

From the initial conventional metamodel, the mean square error (MSE) is estimated inside the domain of the input variable X. By defining the target region T, a weight function, W, is calculated, such that W is higher when the modeled function result approaches or is inside T. The new adaptive SP's are attracted to the target region based on the values of $W \times MSE$. Hence, if in the variable domain a position has a high value of MSE and is inside T (high value of W), it is a potential candidate to receive a sample point there. Regions with very small MSE inside T or regions with high

MSE with results out of T have a smaller probability of attracting adaptive SP's. Regions outside and far from T (small value of W) and with small MSE will have virtually zero probability of receiving a SP.

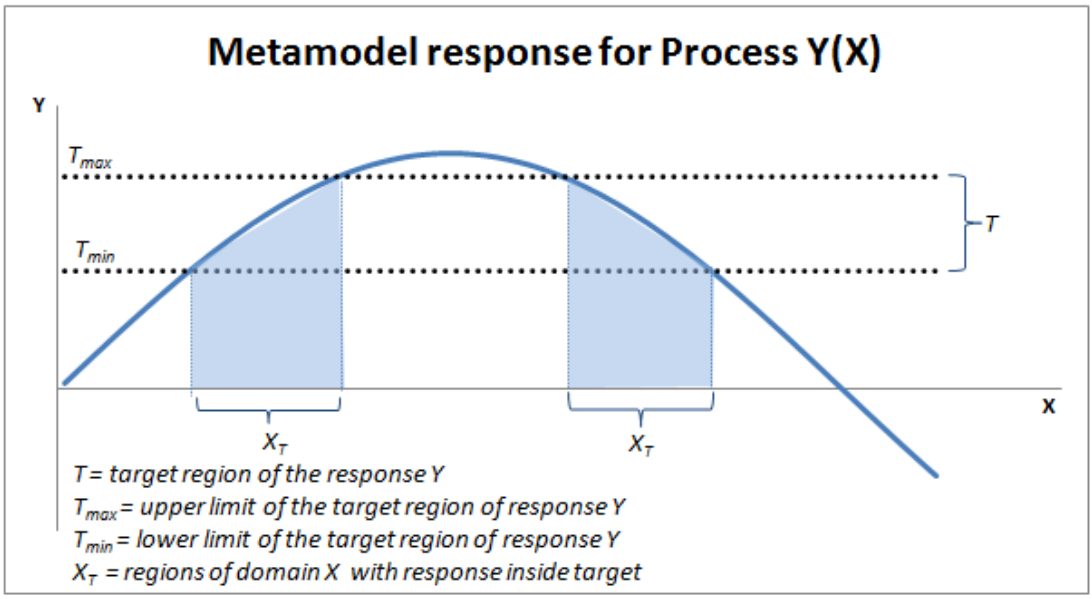

Figure 11. Metamodel response $Y(X)$ and target regions of response T.

The weight function W must be flexible in order to attract adaptive SP's to positions where the MSE is large enough to provoke an error in the estimated function value such that it can take this value out of the target region. Several types of weight functions can be used. These functions are similar to probability density functions, with a higher probability of sampling a SP inside the target region and a smaller probability outside it. A suitable weight function is based on an exponential decay and considers both the MSE and a user defined decay parameter σ_ε^2 for selecting the size of the domain of interest. This function is shown in Equation (55).

$$W(X) = e^{\left(-\frac{(m_k(X)-T)^2}{2\sigma_\varepsilon^2 + s_K^2(X)} \right)} \quad (55)$$

where:

$W(X)$ = weight function at X coordinates;

X = coordinates of the variables (example: for a two dimensional metamodel: $X = x_1, x_2$);

T = target value;

$m_k(X)$ = metamodel prediction of $Y(X)$ at X coordinates;

σ_ε^2 = parameter that defines the size of the domain of interest (works like a variance, which increases or decreases the length of decay of the exponential); and

$s_k^2(X)$ = MSE of the Kriging Metamodel at X coordinates.

If the response target value T is defined as a region delimitated by values $\{T_{\min}, T_{\max}\}$, as shown in Figure 11, Equation (56) is used to determine the weight function in the following way:

$$W(X) = \begin{cases} 1 & \text{if } m_k(X) \text{ is inside } T \\ e^{\left(-\frac{(m_k(X)-T)^2}{2\sigma_\varepsilon^2 + s_K^2(X)} \right)} & \text{if } m_k(X) \text{ is outside } T \end{cases} \quad (56)$$

If the target value T is defined as a single value (not a region), Equation (56) is used directly, presenting a maximum value of $W(X)$ equal to 1 if the metamodel prediction of function $Y(X)$, $m_k(X)$, is equal to the target T. The value of the weight

function $W(X)$ decays exponentially as the value of $m_k(X)$ goes away from the target T.

The relative maxima of the product $W \times MSE$ define the coordinates X where the adaptive SP's must be positioned.

A summary of steps to be performed in the adaptive Kriging model follow.

1. Create an initial metamodel with a specified number of SPs.
2. Create the grid coordinates for determination of $W \times MSE$, according to the domain.
3. Determine the MSE (Mean Square Error) of the original Metamodel at the grid coordinates.
4. Determine W at the grid coordinates, according to the target value, for the Adaptive Metamodel.
5. Calculate $W \times MSE$ at the grid coordinates.

The peak values of the product of W and MSE indicate the positions that are close or inside the target region and that have a large MSE. These positions are the candidates to receive a new adaptive SP.

Generate the new adaptive SP's. (The regions where the peaks of the function $W \times MSE$ occurred are identified and the adaptive SP's are generated in these regions. In order to eliminate very small peaks, a filter is used, which considers only the positions where the values of $W \times MSE$ are larger than the average value of $W \times MSE$ calculated

over the grid. If more adaptive sample points than peaks are needed, the remaining SP's are generated at positions defined according to a probability determined as:

$$\text{Probability} = \frac{W\sqrt{MSE}}{\sum_{i=1}^{G}\left(W\sqrt{MSE}\right)_i} \quad \text{where G = size of the grid} \tag{57}$$

which considers only the filtered regions. Positions with higher value of $W\sqrt{MSE}$ have more chance to receive an adaptive SP.

The results (new adaptive SP's) are passed to the solver.

4.5: Case Study Definition

Since actual cost information is not readily available from open sources, a conceptual submarine design was chosen as a generic and representative case study that highlights the nature of many manufacturing processes. This case study is an extension of the system-level objective function created in Chapter 3 of this dissertation.

A commercially available cost estimation software package was utilized to create the bottom-up cost model. In reality, this bottom-up cost model would be created using the actual cost data and physical parameters from the actual manufacture of several designs.

4.6: Results

The results of the case study are presented in a manner which matches closely the step-by-step discussion of how the MISERLY process is executed.

4.6.1: Original Data

The original data set for the case study consists of physical parameters and historical cost information for a hypothetical set of 50 designs. As has been discussed, it is assumed that this data set would originate from actual cost data in a practical application of this method. For this case study, the SEER-DFM model described in the previous section was used to generate the submarine cost data.

4.6.2: Engineering Build-up Model

The same SEER-DFM model that created the original data set for this case study is also used as a proxy for the engineering build-up model. In a "real-world" application of this process, the engineering build-up model would have been created using the actual design data from the manufacturing of a class, or several classes, of submarines.

4.6.3: Expanded Data

The engineering build-up model creates the expanded data set. The physical parameters modeled in this work are those listed in the "design variables" section of Table 15, and the total cost and the total labor hours were the two pieces of cost information used. The columns of the case study expanded data set are summarized below. Thousands of designs (two orders of magnitude more than the original data set) comprised the expanded data set for this case study.

Table 15: Data Variable definition

Model variable	Description
x_1	Length of the parallel midbody
x_2	Maximum hull diam.
x_3	Aft form factor
x_4	Forward form factor
x_5	Frame spacing
x_6	Plate thickness
y_1	Total labor hours
y_2	Total cost

4.6.4: PCA and Component-Influenced Parameters

PCA can be used in many ways to investigate a data set. For this particular work, PCA was performed on the several subsets of the expanded data. PCA was performed on the top and bottom 10% of the data when sorted from highest to lowest total cost. This analysis was executed in an effort to determine the design variables which had the greatest effect on making a design expensive (or more affordable) to manufacture. A myriad variations on this theme can be imagined by the interested researcher. For this chapter, a more general application of PCA—that is to determine which physical parameters, and the resulting PCs, account for the majority of the variation in the data—is envisioned and discussed in depth here. To realize this goal, PCA is executed on the physical parameters of the expanded data set. The C array and U matrix from these calculations are included in Tables 16 and 17.

Table 16: C Matrix for Conceptual Submarine Design Case Study

C array					
PC1	PC2	PC3	PC4	PC5	PC6
1.36	1.05	1.03	1.00	0.99	0.57

Table 17: U Matrix for Conceptual Submarine Design Case Study

	U matrix					
	PC1	PC2	PC3	PC4	PC5	PC6
L_{pmb}	0.69	-0.30	0.14	0.00	0.02	-0.64
D	-0.72	-0.19	0.09	0.05	-0.02	-0.66
n_a	0.05	0.88	0.19	-0.08	0.28	-0.31
n_f	0.06	0.23	-0.84	-0.03	-0.42	-0.24
L_f	-0.04	-0.05	0.11	-0.98	-0.18	0.00
t_p	-0.02	-0.19	-0.47	-0.19	0.84	-0.02

The C array and U matrix contain a significant amount of information regarding the data set in question. The C array indicates how much of the variation in the model is accounted for by each of the PCs. As was indicated earlier, the numbers in the matrix shown in Table 15 have added value—their importance can be compared directly to the original predictor variables due to a modification procedure followed in this work. For this example, the 1st, 2nd, 3rd, and 4th PCs account for more variation than any single of the original predictor variables. This fact is noted, and the four PCs will be used in the creation of the component-influenced parameters that will make up part of the improved data set.

In addition to identifying which of the PCs account for more variability than any of the physical parameters, the raw numbers contained in the C array show not only that the first PC accounts for the largest amount of the variation, but also, by looking at

the change in the amount of variation accounted for by each PC, that there is a much larger drop in importance between the first and second PCs. In fact, the relative importance of the 2nd, 3rd, 4th, and 5th PCs are very close indeed, and they are much lower than the importance of the 1st PC. It isn't until the last PC that there is another significant drop in importance. This relationship between the PCs aids in the next step of the method—looking at the original predictor variables in an effort to select the most influential.

Like the C array, the U matrix also carries a tremendous amount of information. Most importantly for this application, it relates each of the principal components to the original predictor variables. For this particular example it was determined that the first PC accounts for a large amount of the variation of the data set and that the second, and subsequent, PCs account for a significantly lesser amount of the variation. With this in mind, the first PC will be used to determine the most influential of the original values. It is very obvious, when examining the absolute values in the first column of the U matrix, that the first two variables, the length of the parallel midbody and the diameter, have by far the largest impact on the data. In fact, their influence is so strong that the first PC can be assigned a general physical interpretation as the "Large Dimension Component".

In addition to their absolute values, there is significance in their opposite sign. After careful evaluation of the application of PCA to several instances, the author determined that the absolute signs of the weights do not matter, as has been observed in other applications of PCA as well, but the relative signs of the weights do. The

opposite sign of the two weights in a PC indicates an inverse relationship. In this particular instance, this inverse relationship has an important physical interpretation: there is a strong correlation between large values of the parallel midbody length and small values of the diameter and vice versa.

4.6.5: Improved data

In this case study, the improved data set was composed of the first two original physical parameters, and the first four component-influenced parameters. The matrix for the improved data is identical to that shown in Equation (37) with n = 50, r = 2, and s = 4.

4.6.6: Adaptive Kriging

First, a Kriging model was created for the 50 "sample" points in both the original and the improved data sets. Once these models were created, they were tested against 10 additional points for which the response was known. Additionally, two "advanced" regression tools discussed in the introduction, PLS and CART, were also used to create a model from the 50 "sample" points and tested against the same 10 sample points. Table 18 summarizes these results.

Table 18: Comparison of Regression Results (avg absolute % error)

	PLS	CART	MISERLY
Labor hours	38.6	33.5	2.28
Total cost	303.4	520.7	4.21

Once a normal Kriging model had been created, an adaptive model was engaged in an effort to reduce the error of the cost model further. A minimal amount of grid divisions (10) were chosen in the creation of the model with a low-cost target. As indicated by a user-generated input file, the adaptive Kriging model determined 25 points that were areas which should be examined further. When the adaptive Kriging model had selected the 25 points, two new Kriging models were created. The first was created using the 50 original sample points, and the second using 75 sample points (50 originals plus 25 adaptive). Both of these models were tested with 10 new points whose costs were known, and whose costs fell below the low-cost target value. When these 25 points were included in the creation of the new model, the mean error of the ten test points prediction of the total cost was reduced from 4.1% to 3.6%.

CHAPTER 5:
COST ASSESSMENT UNDER UNCERTAINTY IN MULTIDISCIPLINARY SUBMARINE CONCEPTUAL DESIGN OPTIMIZATION

The main objective of this chapter is the creation of an evidence theory-based algorithm for quantifying uncertainty, integrating the algorithm into an improved methodology for cost assessment and then utilizing this cost assessment under uncertainty model in an MDO framework. Secondary objectives include: demonstrating how multidisciplinary design optimization can increase the understanding of the multifaceted relationship between affordability and performance in the conceptual design of a submarine; employing first-order models for four representative engineering disciplines that are typical of those encountered in conceptual submarine design; and demonstrating the impact of considering cost uncertainties in the MDO decision-making process.

The evidence theory-based algorithm presented in this paper for introducing uncertainty in the cost estimation process is utilized within a MDO analysis of a representative conceptual submarine design. The MDO algorithm discussed throughout this dissertation is utilized for carrying out the optimization analysis. The same conceptual submarine design study is also employed in the discipline-level. The MISERLY cost model that is prescribed in Chapter 4 of this dissertation evaluates the system level objective function in the representative conceptual submarine design.

Finally, the influence of uncertainty on the optimal design and the effect on the cost estimation are also discussed.

5.1: Algorithm for Including Uncertainty in the Cost Estimation

In this section, the new algorithm for integrating elements of the evidence theory in the MISERLY cost estimation model is presented. The MISERLY process is described in detail in Chapter 4 of this dissertation.

Numerical and computational models of physical phenomena, as well as safety, financial performance, and reliability, are finding more and more favor in commercial and government applications. As these models are not capable of capturing the entirety of the systems they represent, various methods have been developed in order to quantify, or estimate, the uncertainty associated with the predictive capacity of this models. Evidence theory, originally known as the Dempster-Schafer theory of evidence after its originators, is one such method. Evidence theory is especially interesting in business and financial applications because it is able to handle both aleatoric (objective or traditional) and epistemic (subjective or lack-of-knowledge-based) uncertainty and presents a range of likelihoods that a certain event will occur. This range of likelihoods is bounded by the two measures associated with evidence theory, belief and plausibility. A summary of the steps used in the integration of evidence theory into the system-level objective function for this study is presented here. In order to illustrate the steps, each step below is tied to the integration of evidence theory into the MISERLY framework. The foundation for this algorithm is contained in [260].

a) **Function Definition:** A function or operation that will serve as an input/output mapping tool for the analysis is defined. In this study, the input parameters are going to be the design variables. The output value is cost, as calculated by MISERLY.

b) **Data Collection:** Data must be collected in order to quantify the uncertainty associated with the input parameters for the function defined in Step 1. This can be done in several ways and can consist of actual, measured uncertainties as well as more subjective sources of uncertainty for relationships that cannot be readily assigned a measured uncertainty, or do not conform to a traditional distribution. The subjective uncertainty from expert opinion regarding the relationship between design variables and cost is considered in this work.

In this study, the "experts" comment on upper and lower values for two cost-influencing parameters, given values of a and b, and likelihoods (called mass function values or Basic Probability Assignments, or BPA, in evidence theory) that the a and b values will fall between these upper and lower values. The data is compiled into a_l, a_u, b_l, and b_u vectors, which contain the lower and upper values of the two variables, and matrices containing the mass function values. In this work, a and b are taken to be coefficients that determine the influence that the two most important design variables, i.e. length and diameter, as determined by MISERLY, have on the cost.

The upper and lower value vectors are created by listing all values mentioned by the experts in ascending order for all (both, in this case) variables.

Thus, the lower value vectors, a_l and b_l, contain all of the listed values except the greatest one and the upper value vectors, a_u and b_u, are all of the listed values except the least one. The matrix of mass function values is of a three-dimensional, lower triangular structure. Each element in the matrix corresponds to a mass function value for a given upper value (row), lower value (column), and expert (third dimension) for a single variable. An example of the structure for the a variable mass function value matrix for the first expert is shown in Equation (58).

$$A(:,:,1)=\begin{bmatrix} m\left(\left[a_{u,1},a_{l,1}\right]\right) & & & \\ m\left(\left[a_{u,2},a_{l,1}\right]\right) & m\left(\left[a_{u,2},a_{l,2}\right]\right) & & \\ \vdots & \vdots & \ddots & \\ m\left(\left[a_{u,n},a_{l,1}\right]\right) & m\left(\left[a_{u,n},a_{l,2}\right]\right) & \cdots & m\left(\left[a_{u,n},a_{l,n}\right]\right) \end{bmatrix} \quad (58)$$

c) **Data Combination:** Once the data has been collected from all of the experts for each of the variables, it must be combined into one, two-dimensional matrix for each of the variables. This is accomplished by averaging each element across the third dimension. All non-zero mass function values for each variable, denoted as m_A and m_B for this study, are then collected, along with their corresponding upper and lower variable values, and form the basis for the calculation of m_C, or collection matrix. The elements of the d dimensional, where d is the number of variables (two in this example) with uncertainty, collection matrix are then calculated as the product of the non-zero mass function values for each variable.

Using this $d = 2$ example, m_A is arranged corresponding to the columns of m_C, and m_B according to the rows. Each element of m_C is then calculated as the product of the mass function values of the associated m_A and m_B. Each element of m_C also has values corresponding to the upper and lower values of each of the variables that resulted in the collection matrix values. In the space defined by axes for each of the design variables, the upper and lower values for each of the variables that correspond to each m_C element create a d dimensional cube wherein the mass function is equal to the value in each element of the collection matrix.

d) **Create Output Range:** A discretized range of outputs from the function defined in Step 1 is calculated in Step 4. There are several methods for doing this. A Monte Carlo simulation is a fairly efficient method.

e) **Test Output Range:** Each entry in the discretized range of outputs created in Step 4, must now be tested against the d dimensional cubes created in Step 3. If all design variable values within a d dimensional cube satisfy the criteria in question (for this example, it is to determine the likelihood that a given design can be manufactured for less than a given cost) for the output value being examined, then the m_C value for that d dimensional cube will be counted in the belief measure sum. If any of the design variable values within a d dimensional cube satisfy the criteria in question for the output value being examined, than

the m_C value for that d dimensional cube will be counted in the plausibility measure sum.

f) **Collect and Plot Bel and Pl:** Once each of the function output values has been tested against each of the d dimensional cubes, a Bel and Pl value can be calculated for each of the function output values. These values can then be plotted against the function output values, and the evidence theory process is complete.

In the representative conceptual submarine design application, the objective function value is the cost with Pl = 0.05, or that with only a 5% likelihood of being exceeded.

5.2: Creation of the Discipline-Level Objective and Constraint Functions

In the conceptual submarine application presented in this chapter, the technical disciplines under consideration are: deck area, resistance (or actually the effective power necessary to overcome this resistance), structures, and maneuvering (or dynamic stability). The same low-fidelity, first-order models explained in Chapter 3 were chosen to model the four engineering performance disciplines. It should be noted that examining each of these disciplines in the manner suggested in this work is not the way in which submarines are actually designed today since this chapter demonstrates the MDO process as applied to a conceptual submarine design based on models take from the open literature. Due to the modularity of the MDO system, arrangements,

volumetrics, weights, and ship balance can be considered instead if representative models are available for each discipline.

5.3: Results

The results of the multidisciplinary conceptual submarine design study are presented in two subsections. The first highlights the results of the MISERLY analysis, including varying levels of uncertainty, for the starting point of the optimization. The second presents the results of the MDO analyses that correspond to each level of uncertainty.

5.3.1: MISERLY Results, with Uncertainty

The cost, without uncertainty, for the starting point of the optimization is normalized to 100 in order to clearly illustrate change.

As is to be expected, the value of the cost no longer takes the deterministic value of 100 when uncertainty is introduced. The following figures plot the Complimentary Cumulative Plausibility and Belief Functions, CCPF and CCBF respectively, against cost.

Figures 12 and 13 provide a clear visualization of the result of the application of evidence theory to the costs associated with a single design point. They also provide a means of understanding the top-level objective function for the MDO analysis performed in this work. The optimization statements for the system and discipline levels are summarized below.

$$\begin{aligned}
&\max\ f_1(\mathbf{x}) = \text{ Deck Area} \\
&\min\ f_2(\mathbf{x}) = \text{ Effective Power} \\
&\min\ f_3(\mathbf{x}) = \text{ Structures} \\
&\max\ f_4(\mathbf{x}) = \text{ Maneuvering} \\
&\min\ f_5(\mathbf{x}) = \text{Cost, as indicated by } \mathrm{Pl}(>Y) = 0.05
\end{aligned} \tag{59}$$

Equation (58) illustrates that the MDO analysis is working to maximize the internal deck area, minimize the effective power, minimize the buoyancy factor, maximize the maneuverability of the submarine and, at the system level, to minimize the cost that has only a 5% likelihood of being exceeded.

5.3.2: MDO Results

Five cases were performed in this multidisciplinary conceptual submarine design optimization study. Each of the cases were identical in structure and execution with the exception of how the uncertainty surrounding the relationship between two design variables and the cost was defined. The five cases are summarized in the table below.

Table 19: MDO Case Definition

Case Title	Case description
Base	Deterministic relationship between variables
Narrow	Low uncertainty on both variables
Wide	High uncertainty on both variables
A_wide	High uncertainty on only the first variable
B_wide	High uncertainty on only the second variable

The results from the five cases are tabulated below.

Table 20: MDO Results

Case Title	Cost	Deck Area	Power	Structures	Maneuvering
Base	39.1	166.3	86.1	87.6	108.4
Narrow	48.0	193.6	85.4	120.8	108.4
Wide	151.5	94.6	108.6	87.8	86.7
A_wide	124.4	100.1	106.7	92.8	100.0
B_wide	66.9	146.8	95.0	134.8	86.7

The emphasis of this paper is the integration of uncertainty into the cost assessment methodology and the impact this integration has on the results of a multidisciplinary design optimization study. As such, the discussion will focus largely on the system level results.

Table 20 shows, as would be expected, that the base case cost, i.e. the one without uncertainty in the relationship between the design variables and cost, is the lowest. It also shows that the remaining costs relate to this base case in a logical manner, that is, added uncertainty raises the cost. It is interesting to note the magnitude of the jump between the narrow bounds on uncertainty and the wide bounds on both variables. To put it in perspective, there is a better than 50% improvement (lowering) in cost over the arbitrarily chosen starting design, even when narrow uncertainty surrounding the relationship between the design variables and the cost is included. When that uncertainty is widened, there is a greater than 50% worsening (raising) of the assessed cost.

To add even more interest to the analysis, it becomes obvious, from the A_wide and B_wide rows, that the two variables effect the cost very differently. There is a general improvement, over the wide uncertainty results, if one of the variables are

returned to the narrow values. The results in Table 20 show that uncertainty in the "B" variable's relationship to cost is much more acceptable than uncertainty in the "A" variable's relationship to cost. To the designer, this indicates that efforts to eliminate uncertainty should be focused on the "A" variable.

In a traditional method for considering uncertainty in design, a "safety factor" is added to the final design. It can be seen from the remaining columns of information in this analysis that this method does not accurately reflect the true extent of the uncertainty's effect on the design as indicated by the available information. The relationship between uncertainty and cost is much more nuanced than can be captured by a simple safety factor, and the various types of uncertainty are also important to capture, and thus the recommended use of a technique such as evidence theory. By incorporating uncertainty into the analysis from the beginning, a much more thorough understanding of how that uncertainty effects the final design can be achieved.

The plots contained in Figures 14 through 17 provide a graphical representation of the final designs corresponding to each uncertainty case on the backdrop of a two-dimensional design space. Each of the black points on the plots represent a feasible design in that design space. The green spot is the starting point of the design, and the various colored "x's" are the final designs for each of the uncertainty cases. Even though, as Equation (58) shows, the algorithm is working to maximize some objective functions and minimize others, all of the plots here are representing the minimization, that is the inverse of the objective function values in the case of the disciplines that are maximized. Therefore the "ideal" design, from the perspective of just the two

dimensions shown, in each of the plots would be a design that is in the lower left corner. Notice that there are few of these ideal designs in the plots shown here. What we see instead is a tradeoff between the various disciplines and the system level objectives. The exact definition of this tradeoff changes as the uncertainty model changes. This is one of the strengths of an MDO analysis.

Figure 18 is included simply to highlight a typical trajectory of a design through the design space. There are several additional plots such as this one which could be created, but Figure 18 is presented here as a sample.

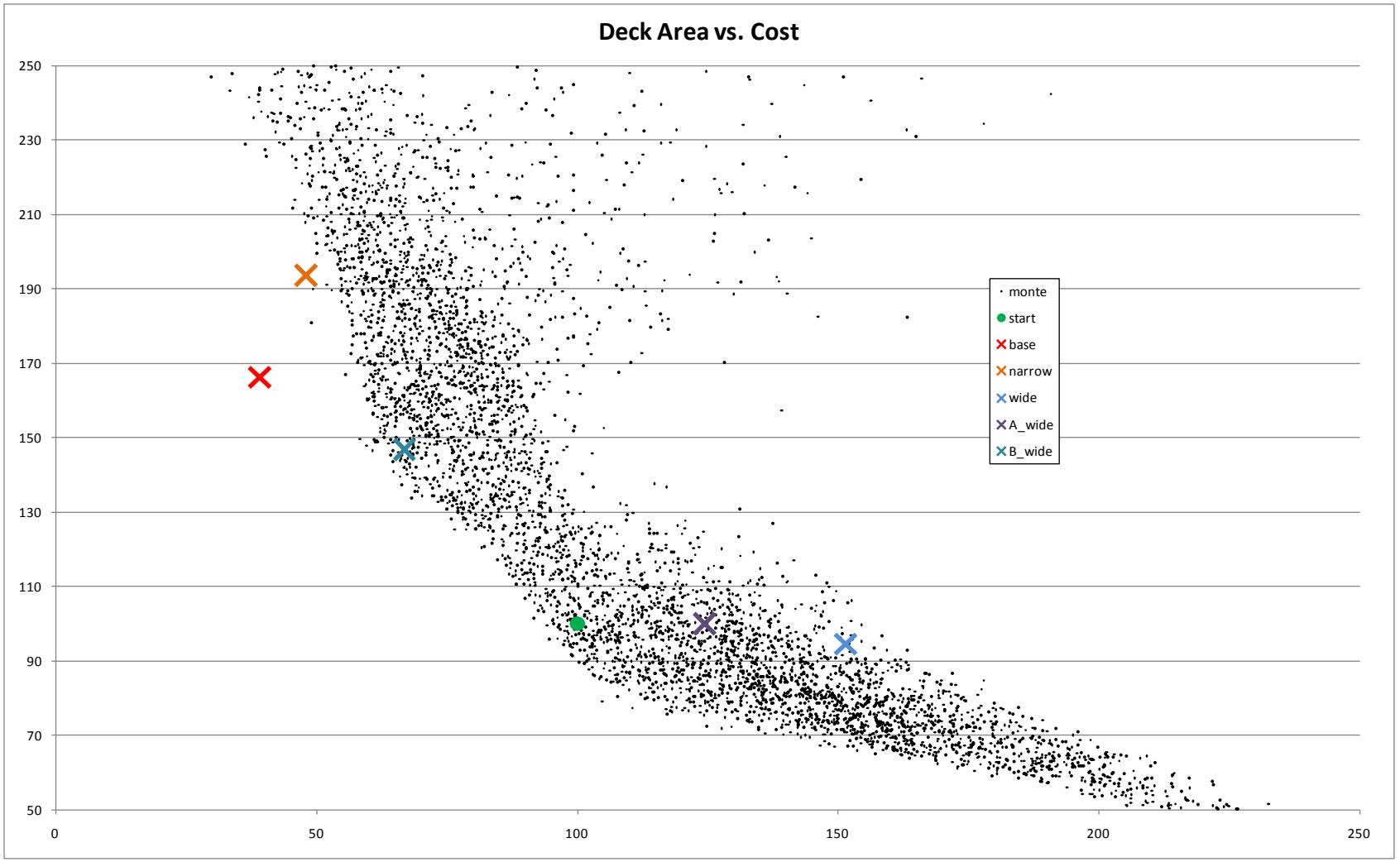

Figure 12: Final Deck Area and Cost design values for all uncertainty cases

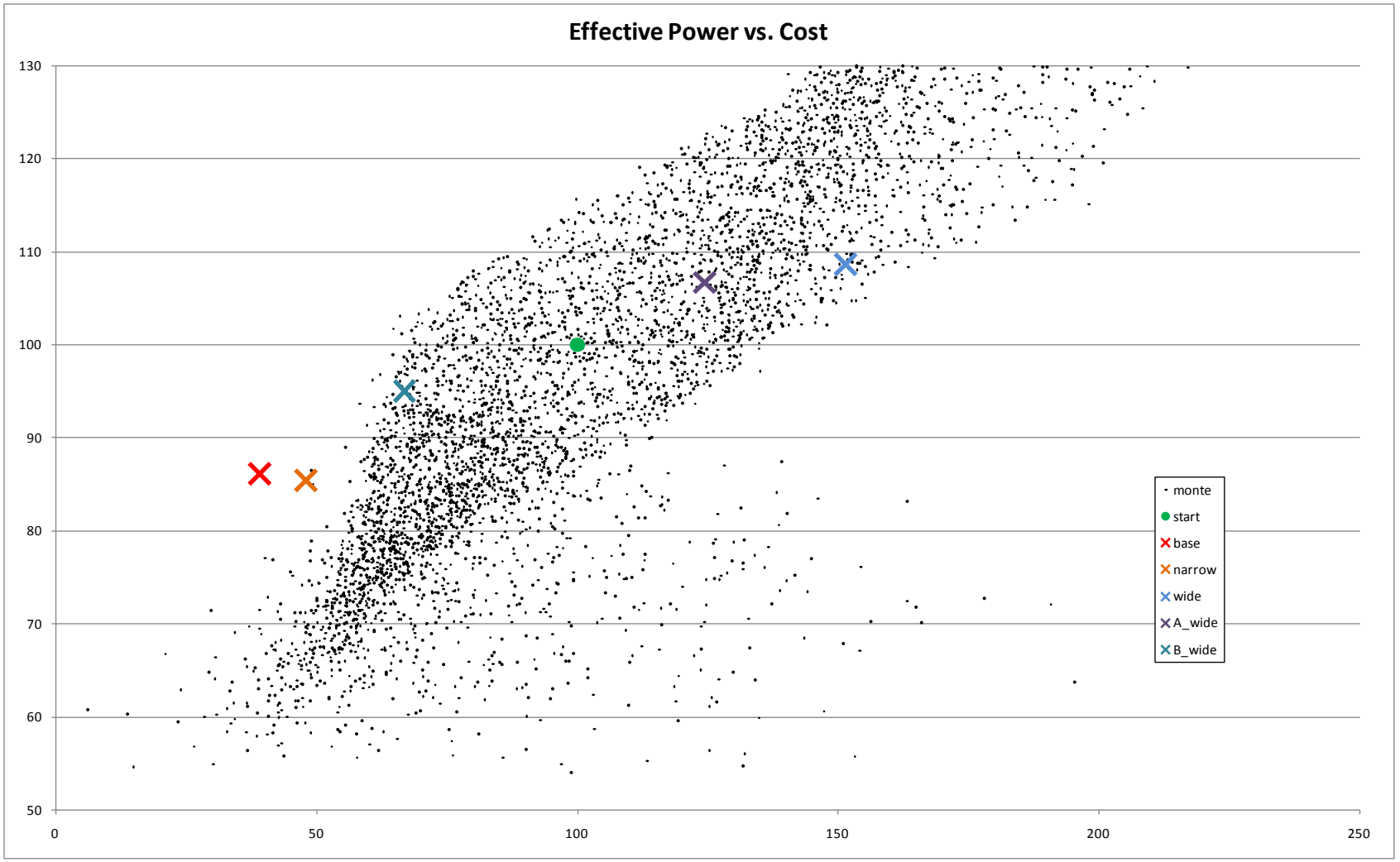

Figure 13: Final Effective Power and Cost design values for all uncertainty cases

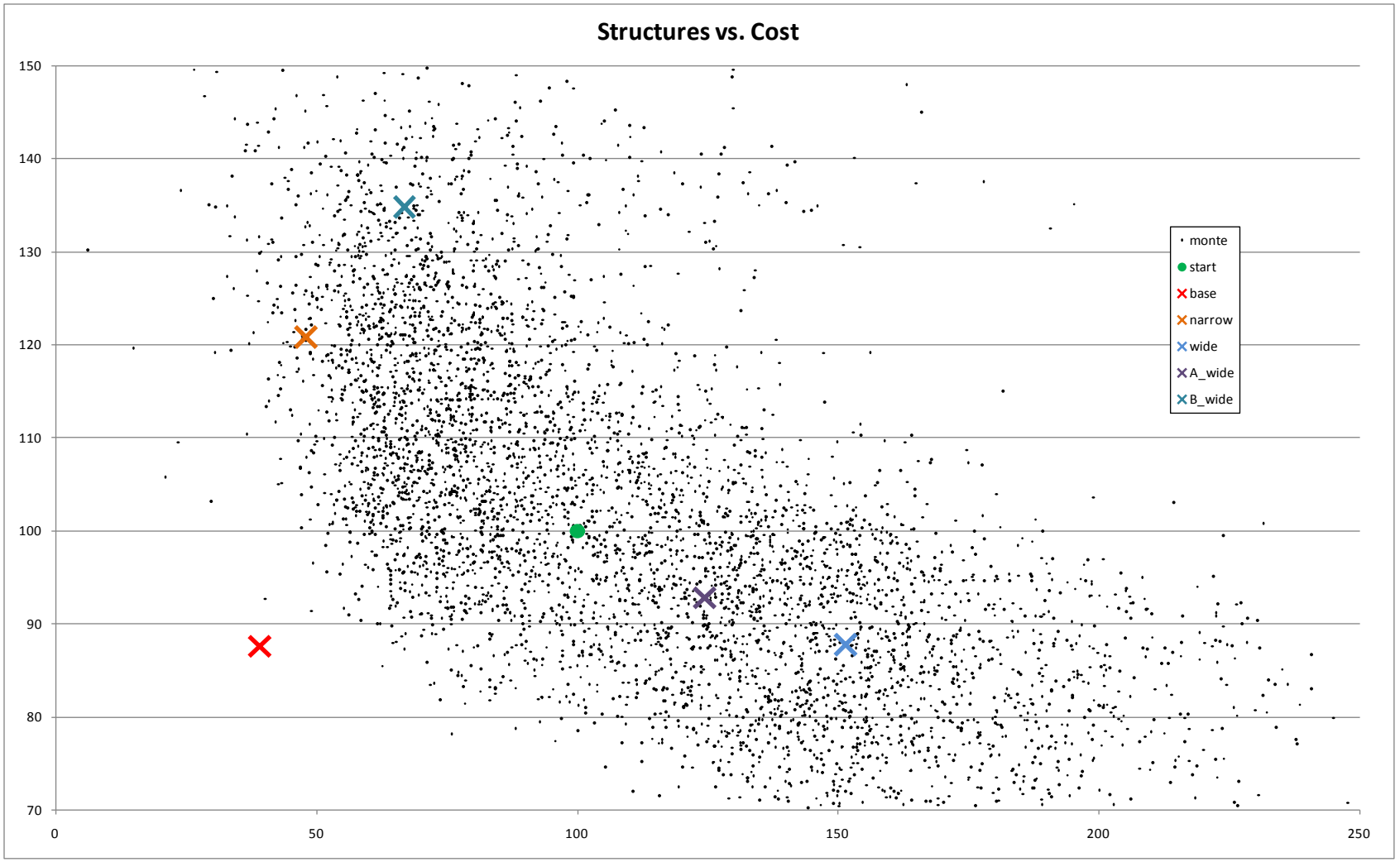

Figure 14: Final Structural Efficiency and Cost design values for all uncertainty cases

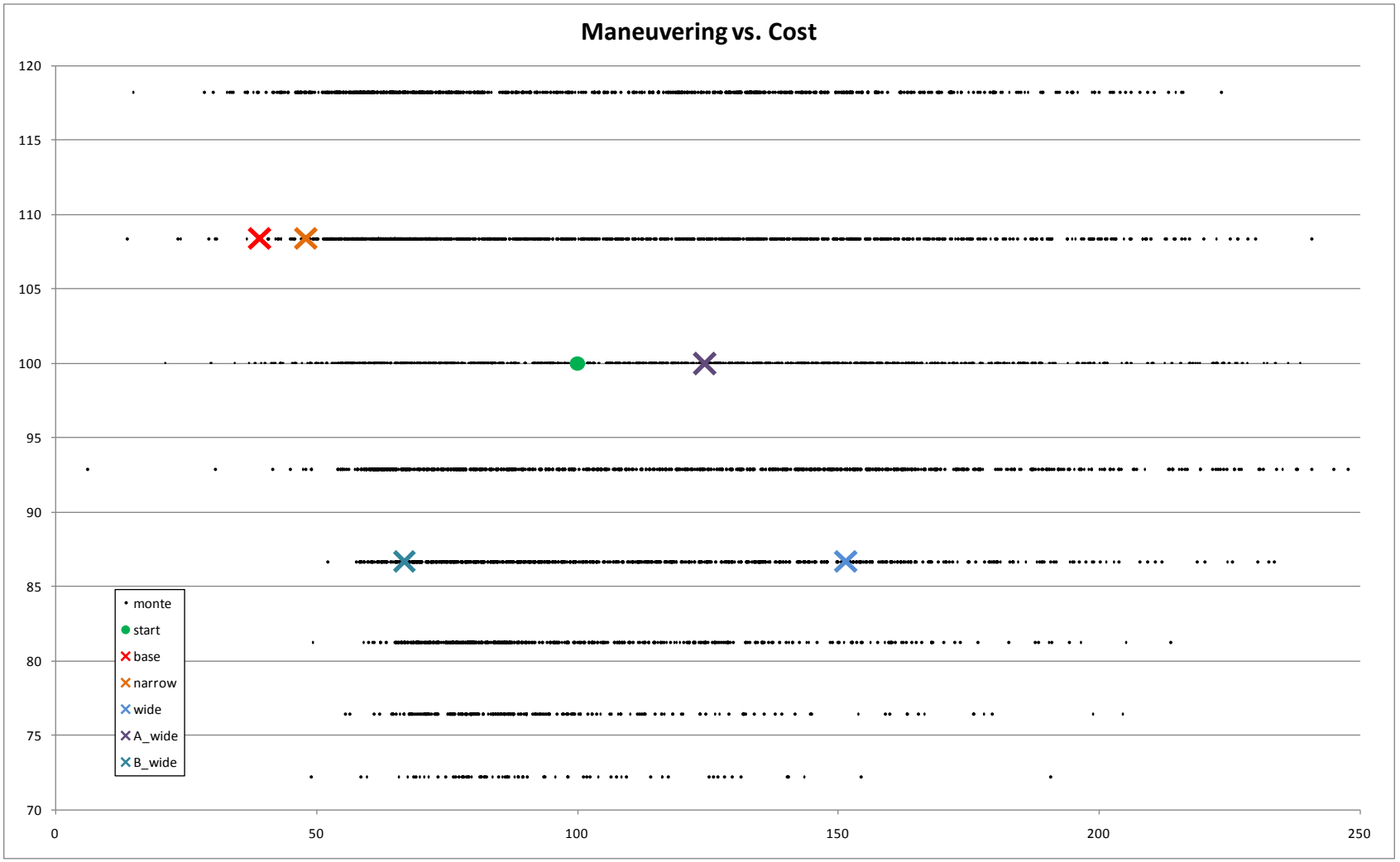

Figure 15: Final Maneuverability and Cost design values for all uncertainty cases

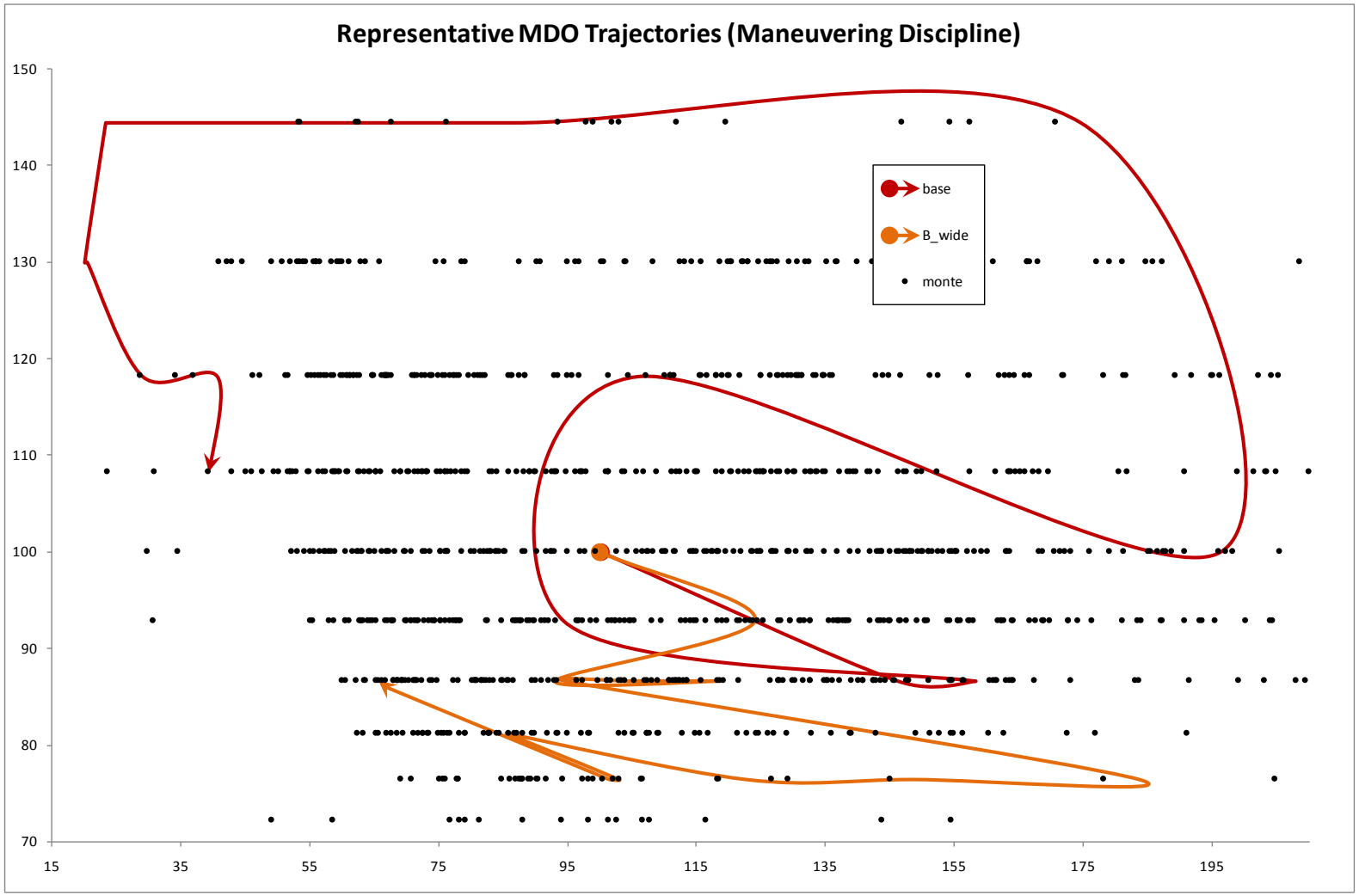

Figure 16: Representative design trajectories for two uncertainty cases in maneuvering discipline

CHAPTER 6:
CONCLUSIONS AND RECOMMENDATIONS

The preceding pages contain an exploration of how dwindling financial resources change the process of creating the complex systems that facilitate mankind's existence on this planet. Specific conclusions that can be taken from this exploration and a set of recommendation on where it can go from here are presented in this last chapter.

6.1: Conclusions

In the first phase of this research, a particle swarm optimization (PSO) algorithm has been created, compared to existing optimization algorithms, and integrated into a multidisciplinary design optimization (MDO) framework which is based on the target cascading method. The integrated MDO/PSO algorithm is applied to a conceptual ship design case study from the literature and the results are presented.

The PSO algorithm is found to produce results of comparable quality to existing algorithms, but at a much higher computational cost. Depending on the objective function and the starting point, the PSO algorithm is observed to find a better optimum than the existing gradient based algorithms. Additionally, PSO is observed to perform worse, both in terms of minimum function value and computational expense, compared to a simple Monte Carlo (MC) model in a single and multicriterion environment.

The extreme computation cost associated with PSO was exacerbated by the multi-level approach to multidisciplinary design optimization (MDO). Thus it is concluded that it is not feasible to obtain high fidelity results using this form of PSO as the driver for an MDO framework.

Next, a geometric model for the internal deck area of a submarine was created, and resistance, structural design, and maneuvering models are adapted from theoretical information available in the literature. Commercial cost estimating software was leveraged to create an automated affordability model for the fabrication of a submarine pressure hull that takes into account the physical dimensions of the submarine and the manufacturing process. These five implementations were synthesized into a multidisciplinary optimization statement reflecting a conceptual submarine design problem. The multidisciplinary design optimization (MDO) framework was used to systematically build a foundation for increasing the understanding of the multifaceted relationship between affordability and performance in the conceptual design of a complex engineering system. The results from this coordinated effort governed by the response of a system-level objective, with special emphasis on defining the complicated relationship between performance and affordability metrics, were presented in both tabular and graphical form and discussed.

Thirdly, a general method for improving the fidelity of cost estimation in the design of complex engineering systems is proposed and a case study addressing the fabrication of a submarine pressure hull is developed in order to illustrate this method. The new general method is known as MISERLY. In the case study, a significant level of

improvement is realized when the results from MISERLY's final regression model are presented and compared to results from the original data set.

Lastly, an evidence theory method for quantifying uncertainty was created and integrated into an improved methodology for cost assessment. The cost assessment under uncertainty methodology was then applied as the top-level driver for the MDO analysis of a conceptual submarine design. This MDO analysis was performed for five cases, each with varying levels of uncertainty associated with the relationship between the design variables and the resulting costs. The results from the five cases showed the benefits of incorporating uncertainty in to a design study from the beginning.

6.2: Recommendations for Future Work

It is recommended that the next step of this work be to replace the classic models for each discipline with higher fidelity models such as CFD, FEA, and internal arrangements optimization codes. Additionally, the affordability model should be expanded to include the entire life-cycle costs associated with the production, sale, use, and disposal of a complex engineering system. Another idea is that optimization algorithms capable of handling nonlinearities and singularities in complex mathematical functions should be brought to bear on these higher-fidelity models in order to ensure that the "best" optimum design results. An effort could also be initiated that replaces the model-generated data in the MISERLY model with actual cost data from the manufacture of a complex engineering system. This would allow the method proposed here to be applied in a real-world scenario and would greatly improve the applicability and validity of the method. Lastly, the MISERLY driven MDO approach should be

applied to any variety of complex engineering systems. Marine renewable energy systems, such as offshore wind and marine hydrokinetic systems, would benefit tremendously from this type of analysis since they, unlike more traditional energy (oil and gas) systems, which are capable of generating revenues that more than offset costs, are cost driven operations.

REFERENCES

1. Kennedy, J. and R. Eberhart (1995). "Particle swarm optimization." Neural Networks,Proceedings of IEEE International Conference on 4.
2. Shi, Y. and R. C. Eberhart (1998). "Parameter selection in particle swarm optimization." Evolutionary Programming 7: 611-616.
3. Shi, Y., R. C. Eberhart, et al. (1999). "Empirical study of particle swarm optimization." Evolutionary Computation, 1999.CEC 99.Proceedings of the 1999 Congress on 3.
4. Shi, Y., R. C. Eberhart, et al. (2001). "Fuzzy adaptive particle swarm optimization." Evolutionary Computation, 2001.Proceedings of the 2001 Congress on 1.
5. Karakasis, M. K. and K. C. Giannakoglou (2006). "On the use of metamodel-assisted, multi-objective evolutionary algorithms." Engineering Optimization 38(8): 941-957.
6. Merkle, D., M. Middendorf, et al. (2002). "Ant colony optimization for resource-constrained project scheduling." Evolutionary Computation, IEEE Transactions on 6(4): 333-346.
7. Serra, M. and P. Venini (2006). "On some applications of ant colony optimization metaheuristic to plane truss optimization." Structural and Multidisciplinary Optimization 32(6): 499-506.
8. Villagra, M. and B. Baran (2007). "Ant Colony Optimization with Adaptive Fitness Function for Satisfiability Testing." LECTURE NOTES IN COMPUTER SCIENCE 4576: 352.
9. Fourie, P. C. and A. A. Groenwold (2002). "The particle swarm optimization algorithm in size and shape optimization." Structural and Multidisciplinary Optimization 23(4): 259-267.
10. Venter, G. and J. Sobieszczanski-Sobieski (2003). "Particle swarm optimization." AIAA Journal 41(8): 1583-1589.
11. Bochenek, B. and P. Forys (2006). "Structural optimization for post-buckling behavior using particle swarms." Structural and Multidisciplinary Optimization 32(6): 521-531.
12. Campana, E., G. Fasano, et al. (2006). Dynamic system analysis and initial particles position in particle swarm optimization.
13. Campana, E. F., G. Fasano, et al. (2006). "Particle swarm optimization: Efficient globally convergent modifications." Proceedings of the III European Conference on Computational Mechanics, Solids, Structures and Coupled Problems in Engineering, Lisbon, Portugal.

14. Pinto, A., D. Peri, et al. (2007). "Multiobjective Optimization of a Containership Using Deterministic Particle Swarm Optimization." Journal of Ship Research 51(3): 217-228.
15. Wang, J. and Z. Yin (2008). "A ranking selection-based particle swarm optimizer for engineering design optimization problems." Structural and Multidisciplinary Optimization: 1-17.
16. Schutte, J., J. Reinbolt, et al. (2004). "Parallel Global Optimization with the Particle Swarm Algorithm." Int. J. Numer. Meth. Engng 61: 2296-2315.
17. Koh, B., A. George, et al. (2006). "Parallel asynchronous particle swarm optimization." Int. J. Numer. Meth. Engng 67: 578-595.
18. Venter, G. and J. Sobieszczanki-Sobieksi (2006). "A parallel particle swarm optimization algorithm accelerated by asynchronous evaluations." Journal of Aerospace Computing, Information, and Communication 3: 123-137.
19. Chiba, K., Y. Makino, et al. (2007). "Multidisciplinary Design Exploration of Wing Shape for Silent Supersonic Technology Demonstrator." AIAA Paper 4167: 2007-6.
20. Chiba, K., Y. Makino, et al. (2008). "PSO/GA Hybrid Method and Its Application to Supersonic-Transport Wing Design." Journal of Computational Science and Technology 2(1): 268-280.
21. Venter, G. and J. Sobieszczanski-Sobieski (2004). "Multidisciplinary optimization of a transport aircraft wing using particle swarm optimization." Structural and Multidisciplinary Optimization 26(1): 121-131.
22. Poli, R., J. Kennedy, et al. (2008). "Editorial: particle swarms: the second decade." Journal of Artificial Evolution and Applications 2008(3).
23. Idahosa, U., V. V. Golubev, et al. (2005). "APPLICATION OF DISTRIBUTED AUTOMATED MDO ENVIRONMENT TO AERO/ACOUSTIC SHAPE OPTIMIZATION OF A FAN BLADE." 11th AIAA/CEAS Aeroacoustics Conference (26th Aeroacoustics Conference): 1-14.
24. Fletcher, R. (1987). Practical methods of optimization, Wiley-Interscience New York, NY, USA.
25. Statnikov, R. B. and J. B. Matusov (1995). Multicriteria Optimization and Engineering, Chapman & Hall.
26. Sen, P. and J. B. Yang (1998). Multiple criteria decision support in engineering design, Springer New York.
27. Papalambros, P. Y. and D. J. Wilde (2000). Principles of Optimal Design.
28. Floudas, C. A. and P. M. Pardalos (2001). Encyclopedia of optimization, Kluwer Academic.
29. Kendall, P. M. H. (1972). "A theory of optimum ship size." Journal of Transport Economics and Policy 6: 128–146.
30. Jansson, J. O. and D. Shneerson (1982). "The optimal ship size." Journal of Transport Economics and Policy 16: 217–238.
31. Lewis, K. (2002). "Multidisciplinary design optimization." Aerospace America 40(12): 42.

32. Berends, J., M. J. L. van Tooren, et al. (2006). "A Distributed Multi-Disciplinary Optimisation of a Blended Wing Body UAV using a Multi-Agent Task Environment." 47th AIAA/ASME/ASCE/AHS/ASC Structures, Structural Dynamics, and Materials Conference: 1-22.
33. Jouhaud, J. C., P. Sagaut, et al. (2007). "A surrogate-model based multidisciplinary shape optimization method with application to a 2D subsonic airfoil." Computers and Fluids 36(3): 520-529.
34. Kim, H. M., M. Kokkolaras, et al. (2002). "Target cascading in vehicle redesign: a class VI truck study." International Journal of Vehicle Design 29(3): 199-225.
35. Sinha, K. (2007). "Reliability-based multiobjective optimization for automotive crashworthiness and occupant safety." Structural and Multidisciplinary Optimization 33(3): 255-268.
36. Venkayya, V. B. (1989). "Optimality criteria: A basis for multidisciplinary design optimization." Computational Mechanics 5(1): 1-21.
37. Kim, I. Y. and O. L. de Weck (2005). "Adaptive weighted-sum method for bi-objective optimization: Pareto front generation." Structural and Multidisciplinary Optimization 29(2): 149-158.
38. Parashar, S. and C. L. Bloebaum (2006). "Multi-Objective Genetic Algorithm Concurrent Subspace Optimization (MOGACSSO) for Multidisciplinary Design." 47th AIAA/ASME/ASCE/AHS/ASC Structures, Structural Dynamics, and Materials Conference: 1-11.
39. Moles, C. G., P. Mendes, et al. (2003). "Parameter Estimation in Biochemical Pathways: A Comparison of Global Optimization Methods." Genome research 13(11): 2467-2474.
40. Cox, S. E., R. T. Haftka, et al. (2001). "A Comparison of Global Optimization Methods for the Design of a High-speed Civil Transport." Journal of Global Optimization 21(4): 415-432.
41. Moraes, H. B., J. M. Vasconcellos, et al. (2007). "Multiple criteria optimization applied to high speed catamaran preliminary design." Ocean Engineering 34(1): 133-147.
42. Craig, K. J. and T. C. Kingsley (2007). "Design optimization of containers for sloshing and impact." Structural and Multidisciplinary Optimization 33(1): 71-87.
43. Peri, D., E. F. Campana, et al. (2001). "Development of CFD-based design optimization architecture." 1st MIT Conference on Fluid and Solid Mechanics, Cambridge.
44. Peri, D., M. Rossetti, et al. (2001). "Design optimization of ship hulls via CFD techniques." Journal of Ship Research 45(2): 140-149.
45. Parsons, M. G., D. J. Singer, et al. (1999). "A hybrid agent approach for set-based conceptual ship design." Proceedings of the International Conference on Computer Applications in Shipbuilding, Cambridge, MA: 7-11.
46. Parsons, M. G. and R. L. Scott (2004). "Formulation of Multicriterion Design Optimization Problems for Solution With Scalar Numerical Optimization Methods." Journal of Ship Research 48(1): 61-76.

47. Peri, D. and E. F. Campana (2004). "High-Fidelity models for Multiobjective Global Optimization in Simulation-Based Design." Journal of Ship Research.
48. Mistree, F., W. F. Smith, et al. (1990). "Decision-Based Design: A Contemporary Paradigm for Ship Design." Transactions, Society of Naval Architects and Marine Engineers 98: 565-597.
49. Ray, T., R. P. Gokarn, et al. (1995). "A global optimization model for ship design." Computers in Industry 26(2): 175-192.
50. Lee, D. (1999). "Hybrid system approach to optimum design of a ship." AI EDAM 13(01): 1-11.
51. Yang, Y. S., C. K. Park, et al. (2007). "A study on the preliminary ship design method using deterministic approach and probabilistic approach including hull form." Structural and Multidisciplinary Optimization 33(6): 529-539.
52. Frank, P. D., A. J. Booker, et al. (1992). "A comparison of optimization and search methods for multidisciplinary design." AIAA Paper: 92-4827.
53. Alexandrov, N. M. and M. Y. Hussaini (1997). Multidisciplinary Design Optimization: State of the Art, Society for Industrial & Applied.
54. Cramer, E. J., J. E. Dennis, et al. (1994). "Problem formulation for multidisciplinary optimization." SIAM Journal on Optimization 4(4): 754-776.
55. Giesing, J. P. and M. B. Jean-Francois (1998). "A Summary of industry MDO applications and Needs." Symposium on Multidisciplinary Analysis and Optimization.
56. Hulme, K. F. and C. L. Bloebaum (2000). "A simulation-based comparison of multidisciplinary design optimization solution strategies using CASCADE." Structural and Multidisciplinary Optimization 19(1): 17-35.
57. Neu, W. L., O. Hughes, et al. (2000). "A Prototype Tool for Multidisciplinary Design Optimization of Ships." Ninth Congress of the International Maritime Association of the Mediterranean, Naples, Italy, April.
58. Peri, D. and E. F. Campana (2003). "High fidelity models in the Multi-disciplinary Optimization of a frigate ship." 2nd MIT Conference on Fluid and Solid Mechanics, Cambridge.
59. Peri, D. and E. F. Campana (2003). "Multidisciplinary Design Optimization of a Naval Surface Combatant." Journal of Ship Research 47(1): 1-12.
60. Demko, D. (2005). Tools for Multi-Objective and Multi-Disciplinary Optimization in Naval Ship Design, Virginia Polytechnic Institute and State University.
61. Tahara, Y., S. Tohyama, et al. (2006). "CFD-based multi-objective optimization method for ship design." INTERNATIONAL JOURNAL FOR NUMERICAL METHODS IN FLUIDS 52(5): 499.
62. Kim, H. M., N. F. Michelena, et al. (2003). "Target cascading in optimal system design." Journal of Mechanical Design(Transactions of the ASME) 125(3): 474-480.
63. Kim, H. M. (2001). Target Cascading in Optimal System Design. Mechanical Engineering. Ann Arbor, University of Michigan. PhD.
64. Kim, H. M., M. Kokkolaras, et al. (2002). "Target cascading in vehicle redesign: a class VI truck study." International Journal of Vehicle Design 29(3): 199-225.

65. Kokkolaras, M., R. Fellini, et al. (2002). "Extension of the target cascading formulation to the design of product families." Structural and Multidisciplinary Optimization 24(4): 293-301.
66. Kim, H., D. Rideout, et al. (2003). "Analytical Target Cascading in Automotive Vehicle Design." TRANSACTIONS-AMERICAN SOCIETY OF MECHANICAL ENGINEERS JOURNAL OF MECHANICAL DESIGN 125(3): 481-489.
67. Kim, H. M., N. F. Michelena, et al. (2003). "Target cascading in optimal system design." Journal of Mechanical Design(Transactions of the ASME) 125(3): 474-480.
68. Michelena, N., H. Park, et al. (2003). "Convergence properties of analytical target cascading." AIAA Journal 41(5): 897-905.
69. Tosserams, S., L. F. P. Etman, et al. (2006). "An augmented Lagrangian relaxation for analytical target cascading using the alternating direction method of multipliers." Structural and Multidisciplinary Optimization 31(3): 176-189.
70. He, J., G. Zhang, et al. (2008). "Uncertainty propogation in Multi-Disciplinary Design Optimization of Undersea Vehicles." SAE Paper: 2008-01-0218.
71. Sun, J., G. Zhang, et al. (2006). "Multi-Disciplinary Design Optimization under Uncertainty for Thermal Protection System Applications." AAIA Paper: 2006-7002-547.
72. He, J., G. Zhang, et al. (2008). "Uncertainty propogation in Multi-Disciplinary Design Optimization of Undersea Vehicles." SAE Paper: 2008-01-0218.
73. Vlahopoulos, N., A. Wang, et al. (2008). Engaging Structural-Acoustic Simulations in Multi-Discipline Optimization. NOISE-CON 2008. Dearborn, MI.
74. Ali, M. and P. Kaelo (2008). "Improved particle swarm algorithms for global optimization." Applied Mathematics and Computation 196(2): 578-593.
75. Arentzen, E. S. and P. Mandel (1960). "Naval Architectural Aspects of Submarine Design." SNAME Trans: 622-692.
76. Perreault, G. L., T. T. Roess, et al. (1972). Submarine Parameter Identification. Buffalo, NY, Bell Aerospace Company: 117.
77. Daniel, R. J. (1983). "Considerations Influencing Submarine Design, Paper 1." Proceedings of the Int. Symp. on Naval Submarines, RINA, London.
78. Richardson, W. (1983). "Modern Submarines- Shipbuilding Aspects." Proceedings of the Int. Symp. on Naval Submarines, RINA, London.
79. Winkler, K. (1983). "Trends in the Design of Conventional Submarines." Proceedings of the Int. Symp. on Naval Submarines, RINA, London.
80. Friedman, N. (1984). Submarine design and development, Naval Institute Press Annapolis, Md.
81. Gabler, U. (1986). "Submarine Design." Bernard & Graefe Verlag.
82. Cederholm, B. (1983). "Swedish Submarine Development." Proceedings of the Int. Symp. on Naval Submarines, RINA, London.
83. Saeger, H. (1983). "Non-Nuclear Submarines and Some Aspects of Their Development in Germany." Proceedings of the Int. Symp. on Naval Submarines, RINA, London.

84. Breemer, J. S. (1989). Soviet Submarines: Design, Development, and Tactics, Jane's Information Group.
85. Raman, R., R. Murphy, et al. (2005). The United Kingdom's Nuclear Submarine Industrial Base, Volume 3: Options for Initial Fuelling, Santa Monica, Calif., USA: RAND Corporation, MG-326/3-MOD.
86. Downs, D. S. (2007). "Type 45: Design For Supportability." WARSHIP 2007-INTERNATIONAL SYMPOSIUM THEN CONFERENCE: 23.
87. Ross, C. T. F. and C. Eng (2007). "Conceptual Design of Submarine to Explore Europa's Oceans." Journal of Aerospace Engineering 20: 200.
88. Allmendinger, E. E. (1990). Submersible Vehicle Systems Design, Society of Naval Architects & Marine Engineers.
89. Burcher, R. and L. Rydill (1994). Concepts in Submarine Design, Cambridge University Press.
90. Zimmerman, S. (2000). Submarine Technology for the 21st Century, Trafford Publishing.
91. Alemayehu, D., R. B. Boyle, et al. (2006). Design Report, Guided Missile Submarine SSG(X). Ocean Engineering, Virginia Tech. BS: 132.
92. Cao, A.-x. Z., Min; Liu, Wei; Cui, Wei-cheng (2007). "Application of Multidisciplinary Design Optimization in the Conceptual Design of a Submarine." Journal of Ship Mechanics 11(3): 1-13.
93. Grunitz, L. and L. Petersen (2007). "First Ever Classification of a Naval Submarine." WARSHIP 2007-INTERNATIONAL SYMPOSIUM THEN CONFERENCE: 89.
94. Schank, J., M. Arena, et al. (2007). Sustaining US Nuclear Submarine Design Capabilities, RAND NATIONAL DEFENSE RESEARCH INST SANTA MONICA CA.
95. Jackson, H. (1992). "Fundamentals of Submarine Concept Design." SNAME Transactions.
96. Jackson, H. A. (1983). "Submarine Parametrics." Proceedings of the Int. Symp. on Naval Submarines, RINA, London.
97. Gertler, M. (1950). "Resistance Experiments on a Systematic Series of Streamlined Bodies of Revolution-For Application to the Design of High-Speed Submarines."
98. Loid, H. P. and L. Bystrom (1983). "Hydrodynamic Aspects of the Design of the Forward and Aft Bodies of the Submarine." Proceedings of the Int. Symp. on Naval Submarines, RINA, London.
99. McGrattan, R. J. and G. A. Peteros (1990). Structural Principles. Submersible Vehicle Systems Design. E. E. Allmendinger, The Society of Naval Architects and Marine Engineers: 271.
100. MacNaught, D. F. (1967). Strength of Ships. Principles of Naval Architecture. J. P. Comstock. New York, NY, The Society of Naval Architects and Marine Engineers: 167-255.
101. Radha, P. and K. Rajagopalan (2006). "Ultimate strength of submarine pressure hulls with failure governed by inelastic buckling." Thin-Walled Structures 44(3): 309-313.

102. (ATTC (1952). Nomenclature for Treating the Motion of a Submerged Body Through a Fluid. Report of the American Towing Tank Conference. T. S. o. N. A. a. M. Engineers. New York, The Society of Naval Architects and Marine Engineers.
103. Abbott, I. H. and A. E. Von Doenhoff (1959). Theory of Wing Sections, Dover Publications.
104. Gertler, M. and G. R. Hagen (1967). Standard Equations of Motion for Submarine Simulation (Report 2510). Washington, DC, Naval Ship Research and Development Center: 29.
105. Abkowitz, M. A. (1969). Stability and Motion Control of Ocean Vehicles, MIT Press.
106. NAVSEA (1971). Fundamentals of Submarine Hydrodynamics, Motion, and Control. NAVSHIPS 0911-003-6010.
107. Glasson, D. P. (1974). Unsteady Hydrodynamics of a Body of Revolution with Fairwater and Rudder (Report 74-7). Cambridge, MA, Massachusetts Institute of Technology, Department of Ocean Engineering.
108. Newman, J. N. (1977). Marine Hydrodynamics, MIT Press.
109. Fossen, T. (1991). Nonlinear modelling and control of underwater vehicles, Norwegian University of Science and Technology, Faculty of Information Technology, Mathematics and Electrical Engineering.
110. Bohlmann, H. J. and I. Lubech "An Analytical Method for the Prediction of Submarine Maneuverability [A]." Warship 91
111. Humphreys, D. and K. Watkinson (1978). Prediction of Acceleration Hydrodynamic Coefficients for Underwater Vehicles from Geometric Parameters, Storming Media.
112. Lloyd, A. R. J. M. (1983). "Progress Towards a Rational Method of Predicting Submarine Manoeuvres." Proceedings of the Int. Symp. on Naval Submarines, RINA, London.
113. Brix, J. (1993). "Manoeuvring Technical Manual." Hamburg: Seehafen: 147.
114. Falzarano, J. and F. Papoulias (1993). "Nonlinear Dynamics of Marine Vehicles: Modeling and Applications, Bound Volume to Sessions." ASME Winter Annual Meeting, OMAE/DSC: 125.
115. Holmes, E. (1995). Prediction of Hydrodynamic Coefficients Utilizing Geometric Considerations, Storming Media.
116. Jones, D., D. Clarke, et al. (2002). The Calculation of Hydrodynamic Coefficients for Underwater Vehicles, DSTO Platforms Sciences Laboratory.
117. Heggstad, K. M. (1984). "Why X-form Rudders for Submarines." Maritime Defence: 3-6.
118. Nosenchuck, D. (1991). "Submarine Sail Trailing Vortex Simulation and Control." Dept. of Mech. & As. Eng., Princeton University, Princeton, NJ 8544.
119. Huang, H., R. Hira, et al. (1993). A submarine maneuvering system demonstration based on the NISTreal-time control system reference model.
120. Anonymous (2001). "US Navy investigates radical submarine sail design." Warship Technology July/August: 16-17.

121. Gorski, J. J. and R. M. Coleman (2002). "Use of RANS Calculations in the Design of a Submarine Sail." Proc., NATO RTO AVT Symp.
122. Bridges, D. H., J. N. Blanton, et al. (2003). "Experimental investigation of the flow past a submarine at angle of drift." AIAA Journal 41(1): 71-81.
123. Rais-Rohani, M., G. Quinn, et al. (2004). "Finite Element Analysis and Sizing Optimization of an Advanced Design Concept for a Composite Sail Structure." Proceedings of the 45 thAIAA/ASME/ASCE/AHS/ASC Structures, Structural Dynamics, and Materials Conference, Palm Springs, CA, April: 19-22.
124. Rais-Rohani, M. and J. Lokits (2006). "Comparison of First- and Zeroth-Order Approaches for Reinforcement Layout Optimization of Composite Submarine Sail Structures." 11 th AIAA/ISSMO Multidisciplinary Analysis and Optimization Conference.
125. Rais-Rohani, M. and J. Lokits (2007). "Reinforcement layout and sizing optimization of composite submarine sail structures." Structural and Multidisciplinary Optimization 34(1): 75-90.
126. Fossen, T. I. (1994). Guidance and Control of Ocean Marine Vehicles, John Wiley and Sons Ltd. New York.
127. Papoulias, F. A. and H. A. Papadimitriou (1995). "Nonlinear studies of dynamic stability of submarines in the dive plane." Journal of ship research 39(4): 347-356.
128. Papanikolaou, S. (1996). Parametrics of Submarine Dynamic Stability in the Vertical Plane, Storming Media.
129. Garga, A., H. Gibeling, et al. (2000). "Investigation of Multi-Dimensional Interpolation Methodologies for Vehicle Maneuvering and Design."
130. Guo, J. and F. Chiu (2001). Maneuverability of a Flat-streamlined Underwater Vehicle, IEEE; 1999.
131. Mackay, M. and R. Defence (2003). The Standard Submarine Model: A Survey of Static Hydrodynamic Experiments and Semiempirical Predictions, Defence R&D Canada-Atlantic.
132. Triantafyllou, M. and F. Hover (2003). "MANEUVERING AND CONTROL OF MARINE VEHICLES." Internet.[Accessed November 20, 2003]< http://ocw. mit. edu/NR/rdonlyres/Ocean-Engineering/13-49Maneuvering-and-Control-of-Surface-and-Underwater-VehiclesFall2000/9902D412-8BF9-4401-874B-850F2FC6267A/0/all. pdf.
133. Minnick, L. (2006). A Parametric Model for Predicting Submarine Dynamic Stability in Early Stage Design. Aerospace and Ocean Engineering, Virginia Tech. Master of Science.
134. Tsamilis, S. (1997). Nonlinear Analysis of Coupled Roll/Sway/Yaw Stability Characteristics of Submersible Vehicles, Storming Media.
135. Fisher, D. (2001). Intermediate Macroeconomics: A Statistical Approach, World Scientific.
136. Leeper, E. M. and T. Zha (2001). "Assessing Simple Policy Rules: A View from a Complete Macroeconomic Model." Federal Reserve Bank of St. Louis Review 83(4): 83-110.

137. Guvenen, F., et al. (2003). A Parsimonious Macroeconomic Model for Asset Pricing: Habit Formation Or Cross-sectional Heterogeneity?, University of Rochester, Rochester Center for Economic Research.
138. Mankiw, N. G. (2004). Brief Principles of Macroeconomics, Thomson/South-Western Mason, Ohio.
139. Arestis, P. (2007). "What is the New Consensus in Macroeconomics?" Is There a New Consensus in Macroeconomics.
140. Cohn, S. (2007). Reintroducing Macroeconomics: A Critical Approach, ME Sharpe.
141. Lubik, T. A. and M. Marzo (2007). "An inventory of simple monetary policy rules in a New Keynesian macroeconomic model." International Review of Economics and Finance 16(1): 15-36.
142. Belsley, D. A. (1994). Computational Techniques for Econometrics and Economic Analysis, Springer.
143. Hendry, D. F. (1995). Dynamic Econometrics, Oxford University Press, USA.
144. Hendry, D. F. (2000). Econometrics: Alchemy Or Science?: Essays in Econometric Methodology, Oxford University Press.
145. Bardsen, G. (2005). The Econometrics of Macroeconomic Modelling, Oxford University Press.
146. Florens, J. P., V. Marimoutou, et al. (2007). Econometric Modeling and Inference, Cambridge University Press.
147. Benford, H. (1956). "Engineering economy in tanker design."
148. Benford, H. (1961). Principles of Engineering Economy in Ship Design, University of Michigan.
149. Thuesen, G. J. and W. J. Fabrycky (1964). Engineering economy, Prentice-Hall Englewood Cliffs, NJ.
150. Buxton, I. L. (1987). "Engineering Economics and Ship Design (Wallsend: British Maritime Technology Limited)."
151. Buxton, I. L. (1997). "Engineering Economics and Shipping , Tyne and wear." British maritime technology ltd.
152. Blank, L. T. and A. Tarquin (2004). Engineering Economy, McGraw-Hill Science/Engineering/Math.
153. Roy, R. (2003). Cost engineering: why, what and how? Decision Engineering Report Series. C. Kerr. Bedfordshire, UK, Cranfield University: 1-45.
154. Hollman, J. K. (2007). "What is Cost Engineering and How is Cost and Schedule Management an "Engineering" Function?" Cost Engineering 49(11): 8.
155. Blanchard, B. S. (1998). Logistics engineering and management, Prentice Hall Upper Saddle River, NJ.
156. Mileham, A. R., G. C. Currie, et al. (1993). "A Parametric Approach to Cost Estimating at the Conceptual Stage of Design." Journal of Engineering Design 4(2): 117-125.
157. Dean, E. B. (1995). "Parametric Cost Deployment."
158. Fabrycky, W. J. and G. J. Thuesen (1974). Economic Decision Analysis, Prentice Hall.

159. Hicks, D. T. (1999). Activity-Based Costing: Making It Work for Small and Mid-Sized Companies, Wiley.
160. Lowe, D. J., M. W. Emsley, et al. (2006). "Predicting Construction Cost Using Multiple Regression Techniques." Journal of Construction Engineering and Management 132: 750.
161. Curran, R., P. Watson, et al. (2003). "Development of an Aircraft Cost Estimating Model for Program Cost Rationalisation." Proceedings of the Canadian Aeronautics and Space institute (CASI), April, Montreal.
162. Curran, R., J. Early, et al. (2005). "Economics Modelling for Systems Engineering in Aircraft." AIAA 5 th Aviation, Technology, Integration, and Operations Conference(ATIO): 1-19.
163. Curran, R., M. Price, et al. (2005). "Integrating Aircraft Cost Modeling into Conceptual Design." Concurrent Engineering 13(4): 321.
164. Curran, R., S. Castagne, et al. (2007). "Aircraft cost modelling using the genetic causal technique within a systems engineering approach." AERONAUTICAL JOURNAL-NEW SERIES- 111(1121): 409.
165. Curran, R., A. K. Kundu, et al. (2001). "Costing Tools for Decision Making within Integrated Aerospace Design." Concurrent Engineering 9(4): 327.
166. Hamaker, J. W. C., Paul J (2005). "Improving Space Project Cost Estimating with Engineering Management Variables." Engineering Management 17(2): 28.
167. Benford, H. (1966). Economics in Ship Design and Operation. Ann Arbor, MI, The University of Michigan Engineering Summer Conferences.
168. Sato, S. (1967). "Effects of Principal Dimensions on Weight and Cost of Large Ships." SNAME, New York Metropolitan Section, February.
169. Benford, H. (1968). "General cargo ship economics and design."
170. Fetchko, J., A. (1968). Methods of Estimating Investment Costs of Ships, University of Michigan, Engineering Summer Conferences.
171. Benford, H. (1969). "The Practical Application of Economics to Merchant Ship Design."
172. Benford, H. (1981). "Fundamentals of ship design economics."
173. Benford, H. (1984). Ships' Capital Costs: The Approaches of Economists, Naval Architects, and Business Managers. Paper for presentation at the September 10-14, 1984 Ships' Costs Conference, University of Wales Institute of Science and Technology, Cardiff. UMTRI 70523: i-iii, 1-35.
174. Beenstock, M. (1985). "A theory of ship prices." Maritime Policy & Management 12(3): 215-225.
175. Hughes, C. N. (1987). Ship Performance: Some Technical and Commercial Aspects, Lloyd's of London Press.
176. Talley, W. K. and J. Pope (1988). "Inventory costs and optimal ship size." The Logistics and Transportation Review 24: 107–120.
177. Evans, J. J. and P. B. Marlow (1990). Quantitative methods in maritime economics, Fairplay.

178. Benford, H. (1991). A Naval Architect's Guide to Practical Economics. Department of Naval Architecture and Marine Engineering. Ann Arbor, MI, University of Michigan: i-iv, 1-123.
179. Wijnolst, N. (1995). Design Innovation in Shipping, Delft University Press.
180. Kavussanos, M. G. (1997). "The dynamics of time-varying volatilities in different size second-hand ship prices of the dry-cargo sector." Applied Economics 29(4): 433-443.
181. Stopford, M. (1997). Maritime Economics, Routledge.
182. Schneekluth, H. and V. Bertram (1998). Ship Design for Efficiency and Economy, Butterworth-Heinemann.
183. Bruce, G. J. and I. Garrard (1999). The Business of Shipbuilding, LLP.
184. Veenstra, A. W. and M. W. Ludema (2006). "The relationship between design and economic performance of ships." Maritime Policy & Management 33(2): 159-171.
185. Lambert, J. and D. W. Chalmers (1996). "Towards More Cost Effective Submarine Hulls." WARSHIP-INTERNATIONAL SYMPOSIUM THEN CONFERENCE: 18-18.
186. Bailey, A. D. and J. T. Wickenden (2007). "Affordable Yet Capable Warship? Science and Technology Squares The Circle." WARSHIP 2007-INTERNATIONAL SYMPOSIUM THEN CONFERENCE-: 43.
187. Bricknell, D. J. and P. Vedlog (2007). "Capturing the Commercial Cost Base in Delivering Naval Auxiliaries." WARSHIP 2007-INTERNATIONAL SYMPOSIUM THEN CONFERENCE-: 111.
188. Courts, M., B. Durant, et al. (2007). "Affordable Warships-Understanding The Possible." WARSHIP 2007-INTERNATIONAL SYMPOSIUM THEN CONFERENCE: 1.
189. Giles, D. and J. Harris (2007). "Less Bang For Your Buck." WARSHIP 2007-INTERNATIONAL SYMPOSIUM THEN CONFERENCE: 65.
190. Lamerton, R. F. (2007). "The Affordable Warship-A Design To Cost Approach Based in the Concept Phase." WARSHIP 2007-INTERNATIONAL SYMPOSIUM THEN CONFERENCE: 33.
191. Linegar, A. (2007). "Cost Effective Support Solutions for Naval Auxiliary Ships." WARSHIP 2007-INTERNATIONAL SYMPOSIUM THEN CONFERENCE: 121.
192. Martin, A. A. (2007). "Survivability and the Affordable Warship." WARSHIP 2007-INTERNATIONAL SYMPOSIUM THEN CONFERENCE-: 51.
193. Noel-Johnson, N. and R. Kattan (2007). "Warship Design Complexity-Measurement and Valuation." WARSHIP 2007-INTERNATIONAL SYMPOSIUM THEN CONFERENCE: 15.
194. Sloan, G. W. (2007). "Optimal Naval Warship Design for Fabrication and Maintenance." WARSHIP 2007-INTERNATIONAL SYMPOSIUM THEN CONFERENCE: 89.
195. Thornton, J. S., M. D. Courts, et al. (2007). "Making Warship Survivability Affordable." WARSHIP 2007-INTERNATIONAL SYMPOSIUM THEN CONFERENCE: 59.
196. Schank, J., M. Arena, et al. (2007). Sustaining US Nuclear Submarine Design Capabilities, RAND NATIONAL DEFENSE RESEARCH INST SANTA MONICA CA.

197. Sterman, J. D. (2000). Business dynamics: systems thinking and modeling for a complex world, Irwin/McGraw-Hill.
198. Cooper, K. G. (1980). "Naval Ship Production: A Claim Settled and a Framework Built." Interfaces 10(6): 20-36.
199. Bao, H. P. (2002). Process Cost Modeling for Multi-Disciplinary Design Optimization, Old Dominion University Research Foundation: 1-104.
200. Bao, H. P. and J. A. Samareh (2000). "AFFORDABLE DESIGN: A METHODOLOGY TO IMPLEMENT PROCESS-BASED MANUFACTURING COST MODELS INTO THE TRADITIONAL PERFORMANCE-FOCUSED MULTIDISCIPLINARY DESIGN OPTIMIZATION." Proceedings of the Eighth AIAA/NASA/USAF/ISSMO Symposium on Multidisciplinary analysis and optimization, Long Beach, California, USA: 2000–4839.
201. Gantois, K. and A. J. Morris (2004). "The multi-disciplinary design of a large-scale civil aircraft wing taking account of manufacturing costs." Structural and Multidisciplinary Optimization 28(1): 31-46.
202. Peoples, R. and K. Willcox (2006). "Value-Based Multidisciplinary Optimization for Commercial Aircraft Design and Business Risk Assessment." Journal of Aircraft 43(4): 913-921.
203. Fayyad, U., G. Piatetsky-Shapiro, and P. Smyth, From data mining to knowledge discovery in databases. Communications of the ACM, 1996. 39(11): p. 24-26.
204. Wu, X., et al., Top 10 algorithms in data mining. Knowledge and Information Systems, 2008. 14(1): p. 1-37.
205. Han, J. and M. Kamber, Data mining: concepts and techniques. 2006: Morgan Kaufmann.
206. Pawlak, Z., Rough sets: Theoretical aspects of reasoning about data. 1991: Kluwer Academic Print on Demand.
207. Srikant, R. and R. Agrawal. Mining sequential patterns: Generalizations and performance improvements. in 5th International Conference on Extending Database Technology: Advances in Database Technology. 1996: Springer.
208. Tan, P., M. Steinbach, and V. Kumar, Introduction to data mining. 2005: Addison-Wesley Longman Publishing Co., Inc. Boston, MA, USA.
209. Yan, X. and J. Han. gSpan: Graph-based substructure pattern mining. in 2002 IEEE International Conference on Dama Mining (ICDM '02). 2002: Citeseer.
210. Zhang, T., R. Ramakrishnan, and M. Livny. BIRCH: an efficient data clustering method for very large databases. in ACM SIGMOD International Conference on Management of Data. 1996. Montreal, Quebec, Canada: ACM Press, NY, NY.
211. Hand, D. and K. Yu, Idiot's Bayes: Not So Stupid after All? International Statistical Review/Revue Internationale de Statistique, 2001. Rev. 69: p. 385-398.
212. Agrawal, R. and R. Srikant. Fast algorithms for mining association rules. in 20th International Conference on Very Large Databases (VLDB '94). 1994. Santiago, Chile.
213. Breiman, L., Classification and regression trees. 1998: Chapman & Hall/CRC.
214. Brin, S. and L. Page, The anatomy of a large-scale hypertextual Web search engine. Computer networks and ISDN systems, 1998. 30(1-7): p. 107-117.

215. Han, E., et al., Text categorization using weight adjusted k-nearest neighbor classification. 2001: Springer.
216. Hastie, T. and R. Tibshirani, Discriminant adaptive nearest neighbor classification. IEEE Transactions on Pattern Analysis and Machine Intelligence, 1996. 18(6): p. 607-616.
217. McLachlan, G. and D. Peel, Finite mixture models. 2004: Wiley-Interscience.
218. Quinlan, J., C4. 5: programs for machine learning. 1993: Morgan Kaufmann.
219. Vapnik, V., The nature of statistical learning theory. 1995: Springer.
220. Vapnik, V., Statistical learning theory. . NY Wiley, 1998.
221. MacQueen, J. Some methods for classification and analysis of multivariate observations. in 5th Berkeley Symposium Mathematical Statistics and Probability. 1967.
222. Gifi, A., Nonlinear multivariate analysis. 1990: Wiley.
223. Sun, J., J. He, N. Vlahopoulos, P. van Ast, "Model update and statistical correlations metrics for automotive crash simulations," 2007 SAE Congress, SAE Paper No. 2007-01-1744.
224. Sun, J., N. Vlahopoulos, K. Hu, "Model update under uncertainty and error estimation in shock applications," SAE Paper No. 2005-01-2373, 2005 SAE Noise and Vibration Conference, Traverse City, MI.
225. Wall, M., A. Rechtsteiner, and L. Rocha, Singular value decomposition and principal component analysis. A practical approach to microarray data analysis, 2003: p. 91-109.
226. Ringnér, M., What is principal component analysis? Nature Biotechnology, 2008. 26(3): p. 303-304.
227. Adler, N. and B. Golany, Evaluation of deregulated airline networks using data envelopment analysis combined with principal component analysis with an application to Western Europe. European Journal of Operational Research, 2001. 132(2): p. 260-273.
228. Jackson, J., A user's guide to principal components. 2005: Wiley-Interscience.
229. Jolliffe, I., Principal component analysis. 2002: Springer.
230. Scholkopf, B., A. Smola, and K. Muller, Kernel principal component analysis. Lecture Notes in Computer Science, 1997. 1327: p. 583-588.
231. Bingham, E., Advances in independent component analysis with applications to data mining. 2003: Helsinki University of Technology.
232. Apte, C., et al., Business applications of data mining. 2002.
233. Berson, A., S. Smith, and K. Thearling, Building data mining applications for CRM. 1999: McGraw-Hill Professional.
234. David, M., Quantum computing explained.
235. Meglicki, Z., Quantum Computing Without Magic: Devices. 2008: The MIT Press.
236. Williams, C. and S. Clearwater, Explorations in quantum computing. 1997: Springer-Verlag TELOS Santa Clara, CA, USA.
237. Williams, C. and S. Clearwater, Ultimate zero and one: computing at the quantum frontier. 2000: Springer.

238. Craven, P., Wahba, G., “Smoothing Noisy Data with Spline Functions: Estimating the Correct Degree of Smoothing by the Methods of Generating Cross-Validation,” Numerical Mathematics, Vol.31, pp. 377-403, (1978).
239. Hajela, P. and Berke, L., “Neural Networks inStructural Analysis and Design: An Overview”, 4th AIAA/USAF/NASA/OAI Symposium on Multidisciplinary Analysis and Optimization, Cleveland, OH, AIAA 2, pp 901-914, AIAA-92-4805-CP, (1993).
240. Rumelhart, D. E., Widrow, B. and Lehr, M. A., “The Basic Ideas in Neural Networks”, Communications of the ACM, Vol.37, n3, pp. 87- 92, (1994).
241. Cheng B. and Titterington D. M., “Neural Networks: A Review from a Statistical Perspective”, Statistical Science, Vol.9, n1, pp. 2-54, (1994).
242. Ellacott, S.W., Mason, J.C., and Anderson, I.J., “Mathematics of Neural Networks: Models, Algorithms, and Applications,” Kluver Academic Publishers, Boston, MA, (1997).
243. Dyn, N., Levin, D., and Rippa, S., “Numerical Procedures for Surface Fitting of Scattered Data by Radial Functions,” SIAM Journal of Scientific and Statistical Computing, Vol.7, n2, pp. 639- 659, (1986).
244. Jansen, M., Maifait, M., and Bultheel, A., “Generalized Cross Validation for Wavelet Thresholding,” Signal Processing, Elsevier, n56, pp. 33-44, (1996).
245. Cressie, N., “Spatial Prediction and Ordinary Kriging,” Mathematical Geology, Vol.20, n4, pp. 405-421, (1988).
246. Sacks, J., Welch, W.J., Mitchell, T.J., and Wynn, H.P., “Design and Analysis of Computer Experiments,” Statistical Science, Vol.4, n4, pp.409-435,(1989).
247. Sacks, J., Welch, W.J., and Schiller, S.B., “Designs for Computer Experiments,” Technometrics, Vol.31, n1, pp.41-47,(1989).
248. Z. Qian, C. C. Seepersad, V. R. Joseph, J. K. Allen, C. F. J. Wu, “Building Surrogate Models based on Detailed and Approximate Simulations,” Transactions of ASME, Journal of Mechanical Design, Vol. 128, July 2006.
249. M. Shin, R. G. Sargent, A. L. Goel, “Gaussian Radial based Functions for Simulation Metamodeling,” Proceedings of the 2002 Winter Simulation Conference.
250. J-S Park, J. Jeon, “Estimation of Input Parameters in Complex Simulation Using a Gaussian Process Metamodel,” Probabilistic Engineering Mechanics, Vol. 17, 2002, pp. 219 – 225.
251. M. T. M. Emmerich, K. C. Giannakoglou, and B. Naujoks, “Single and Multi-Objective Evolutianary Optimization Assisted by Gaussian Random Field Metamodels,” IEEE Transactions on Evolutionary Computation, Vol. 10, No. 4, August 2006.
252. Cressie, N., “Spatial Prediction and Ordinary Kriging,” Mathematical Geology, Vol.20, n4, pp. 405-421, (1988).
253. He, Z., N. Vlahopoulos, “Utilization of Response Surface Methodologies in the Multi-discipline Design Optimization of an Aircraft Wing,” SAE Paper 2009-01-0344, 2009 SAE Congress.
254. J. D. Martin, T. W. Simpson, “Use of Kriging Models to Approximate Deterministic Computer Models,” AIAA Journal, Vol. 43, No. 4, April 2005, pp. 853 – 863.

255. He, Z., G. Zhang, N. Vlahopoulos, “Uncertainty propagation in Multi-Disciplinary Design Optimization of Undersea Vehicles,” 2008 SAE Congress, SAE Int. J. Mater. Manuf. Vol1, No.1, pp. 70 – 79, 2008.
256. Yager, R., J. Kacprzyk, and M. Fedrizzi, *Advances in the Dempster-Shafer theory of evidence*. 1994: John Wiley & Sons, Inc. New York, NY, USA.
257. Dubois, D. and H. Prade, *Possibility theory*. 1988: Plenum Press New York.
258. Moore, R., *Interval analysis*. 1966: Prentice-Hall Englewood Cliffs, NJ.
259. Zhou, J., Z. Mourelatos, and C. Ellis, Design under uncertainty using a combination of evidence theory and a Bayesian approach. SAE SP, 2008. 2170: p. 157.
260. Nikolaidis, E., D.M. Ghoicel, et al, *Engineering design and reliability handbook*. 2005: CRC Press, LLC.